Hydrothermal synthesis and optimisation of zeolite Na-P1 from South African coal fly ash

By

Nicholas Mulei Musyoka

BSc Chemistry (honours) - University of Nairobi

A thesis submitted in fulfilment of the requirements for the degree of Magister Scientiae in the Department of Chemistry, University of the Western Cape.

Supervisor: Dr. Leslie F. Petrik

May 2009

Hydrothermal synthesis and optimisation of zeolite Na-P1 from South African coal fly ash

Nicholas Mulei Musyoka

KEYWORDS

Fly ash

Hydrothermal synthesis

Ageing process

Gismondine zeolite type

Zeolite Na-P1

Cation exchange capacity

Statistical design of experiments

Response parameter

Major and interaction effects

Major and trace elements

ABSTRACT

Millions of tonnes of fly ash are generated worldwide every year to satisfy the large demand for energy. Management of this fly ash has been a concern and various approaches for its beneficial use have been investigated. Over the last two decades, there has been intensive research internationally that has focused on the use of different sources of fly ash for zeolite synthesis. However, most of the studies have concentrated on class C fly ash and very few have reported the use of South African class F fly ash as feedstock for zeolite synthesis.

Class F fly ash from South Africa has been confirmed to be a good substrate for zeolite synthesis due to its compositional dominance of aluminosilicate and silicate phases. However, because differences in quartz-mullite/glass proportions of fly ash from different sources produces impure phases or different zeolite mineral phases under the same activation conditions, the present study focused on optimization of synthesis conditions to obtain pure phase zeolite Na-P1 from class F South African coal fly ash. Synthesis variables evaluated in this study were; hydrothermal treatment time (12 - 48 hours), temperature (100 – 160 °C) and addition of varying molar quantities of water during the hydrothermal treatment step (H_2O:SiO_2 molar ratio ranged between 0 - 0.49).

Once the most suitable conditions for the synthesis of pure phase zeolite Na-P1 from fly ash were identified, a statistical approach was adopted to refine the experiments, that was designed to evaluate the interactive effects of some of the most important synthesis variables. In this case, the four synthesis variables; NaOH concentration (NaOH: SiO_2 molar ratio ranged between 0.35 – 0.71), ageing temperature (35 °C – 55 °C), hydrothermal treatment time (36 - 60 hours) and temperature (130 °C – 150 °C) were studied. The response was determined by evaluating the improvement in the cation exchange capacity of the product zeolite.

The starting materials (fly ashes from Arnot, Hendrina and Duvha power stations) and the synthesized zeolite product were characterized chemically, mineralogically and morphologically by X-Ray fluorescence spectrometry, X-ray powder diffraction, scanning electron microscopy, and transmission electron microscopy. Other characterization technique used in the study were

Fourier transform infrared spectroscopy to provide structural information and also monitor evolution of crystallinity during synthesis, as well as cation exchange capacity to determine the amount of exchangeable positively charged ions. Nitrogen adsorption was used to determine the surface area and porosity, and inductively coupled mass spectrometry for multi-elemental analysis of the post-synthesis supernatants.

The results from the X-ray diffraction spectroscopy showed that the most pure zeolite Na-P1 phase was achieved when the molar regime was 1 SiO_2 : 0.36 Al_2O_3 : 0.59 NaOH : 0.49 H_2O and at synthesis conditions such that ageing was done at 47 °C for 48 hours while the hydrothermal treatment time and temperature was held at 48 hours and 140 °C, respectively. Results from statistically designed experiments show that there was a distinct variation of phase purity with synthesis conditions. From the analysis of linear and non linear interactions, it was found that the main effects were ageing temperature and hydrothermal treatment time and temperature, which also showed some interactions. This experimental approach enabled a clearer understanding of the relationship between the synthesis conditions and the purity of the zeolite Na-P1 obtained.

The quality of zeolites is a major determinant in the efficiency of toxic element removal from waste water. Preliminary experiments conducted using optimised zeolite Na-P1 obtained in this study with a cation exchange capacity of 4.11 meq/g showed a high percentage removal of Pb, Cd, Ni, Mn, V, As, B, Fe, Se, Mo Sr, Ba and Zn from process brine obtained from Emalahleni water reclamation plant.

In summary, a pure phase of zeolite Na-P1 was obtained from South African class F fly ash feedstock at relatively mild temperature. The systematic approach, incorporating statistical design of experiments, developed in this study resulted in a better understanding regarding the relationships of synthesis parameters in the formation of zeolites from fly ash. The zeolite Na-P1 synthesized with a high cation exchange capacity was effective for removal of toxic elements from brine.

DECLARATION

I declare that "*Hydrothermal synthesis and optimisation of zeolite Na-P1 from South African coal fly ash*" is my own work, that it has not been submitted for any degree or examination in any other university, and that all the resources I have used or quoted have been indicated and acknowledged by complete references.

Nicholas Mulei Musyoka May 2009

Signed.....

ACKNOWLEDGEMENTS

I would like to thank the Almighty God for the blessing of life and for seeing me through up to this point of my life.

Sincere deepest gratitude goes to my supervisor, Dr. Leslie Petrik, for the guidance, encouragement, good advices and for the opportunities that I have got through the Environmental and NanoSciences research group (ENS).

Thank you, Dr. Gillian Balfour, for helpful suggestions, also Dr. Wilson Gitari, Dr. J. E. Hums and Dr. Patrick Ndungu for all the help and advice you accorded me.

Thanks to my colleagues at the ENS group for all the valuable discussions and companionship.

Many thanks to Averil Abbot and Ilse Wells for making life comfortable while doing the research work.

Special thanks go to my parents for their love, care and also for imparting on me the virtue of hard work which has made me achieve this. Thanks to the Hargrave's family and more specifically Meredith Higgins and also not forgetting Beth and Jason Gierch, Betty Hopkins and Brian Sann for the friendship, encouragement and help.

TABLE OF CONTENTS

CHAPTER 3

CHAPTER 4

LIST OF FIGURES

LIST OF TABLES

LIST OF ABBREVIATION

FTIR = Fourier transform infrared spectroscopy

XRD = X-ray diffraction Spectroscopy

XRF = X-ray Fluorescent Spectroscopy

SEM = Scanning electron microscopy

HRTEM = High resolution transmission electron microscopy

BET = Brunauer Emmett Teller

CEC = Cation exchange capacity

TGA = Thermogravimetric analysis

SAED = Selected area electron diffraction

NMR = Nuclear magnetic Resonance

ICP-AES = Inductively coupled plasma atomic emission spectrometry

ICP-MS = Inductively coupled plasma mass spectrometry

BJH = Barrett-Joiner-Halenda method

H = Hematite

IZA = International Zeolite Association

M = mullite

Mag = Magnetite

P = Zeolite Na-P1

T – atoms = Si and Al (Silicon and Aluminium)

Wt = weight

Q = Quartz

Mt/y = Million tonnes per year

JCPDS = Joint Committee on Powder Diffraction Standards

Std = standard

g/cc = grams / centimetre cubed

ZSM = Zeolite Socony Mobil

Stdev = Standard deviation

Stderror = Standard error

Df = Degrees of freedom

VIF = Variance inflation factor

CI = Confidence interval

ANOVA = Analysis of variance

se = standard error

N = the total number of runs in the experiment

P = the number of model parameters

SS = Sum of squares

MSe = Mean Square error

RSM = Response Surface Methods

MS = Mean square

PRESS = Predicted Error Sum of Squares

Meq = Milliequivalents

Cca - Concentration of cationic specie

SBU = Secondary building blocks

EC = Electrical Conductivity

TDS = Total dissolved solids

LO = Loss on ignition

HS = Hydroxy-sodalite

C.V = Coefficient of Variation

R^2 Adj = Adjusted R - squared

R^2_{Pred} = Predicted R - squared

Ci = initial concentration

Ce = final concentration

ENS = Environmental and NanoSciences research group

SOx = sulphur oxides

NOx = nitrogen oxides

CONFERENCE CONTRIBUTIONS

The following conference presentations and publications in preparation are based on work done from different sections of this thesis.

Oral presentation:

N. M. Musyoka, L.F.Petrik, G.Balfour and W.M.Gitari. "Optimization of phase purity of zeolite Na-P1 made from South African coal fly ash." Geoanalysis 2009 Conference, Champagne Sports Resort, Kwazulu Natal, South Africa, 6-12 September, 2009.

Poster presentations:

Petrik L. F., Musyoka N. M., Balfour G., Gitari W. and Mabovu B. "Optimized alkaline hydrothermal conversion of South African coal fly ash to zeolite Na-p1." British zeolite association 2009, University of Cumbria, Ambleside, United Kingdom, 23 - 28 August, 2009.

Musyoka N. M., Petrik L. F., Balfour G., Natasha Misheer., Gitari W. and Mabovu B. "Removal of toxic elements from brine using zeolite Na-P1 made from a South African coal fly ash." International mine water conference, CSIR, Pretoria, South Africa, 19 - 23 October, 2009.

Musyoka N. M., Petrik L. F., Balfour G., Gitari W. and Mabovu B. "Synthesis and optimization of zeolite Na-P1 from a South African coal fly ash." International Symposium on Zeolites and Microporous Crystals, Waseda University, Tokyo, Japan, 3 – 7 August, 2009.

Musyoka N. M., Petrik L. F., Balfour G., Gitari W. and Mabovu B. "Statistical approach to optimization of hydrothermal synthesis of zeolite Na-P1 from a South African coal fly ash" NanoAfrica International conference, CSIR, Pretoria, South Africa, 1 - 4 February, 2009.

Musyoka N. M., Petrik L. F., Balfour G., Gitari W. and Mabovu B. "Optimization of hydrothermal synthesis of zeolites from coal fly ash" 39th National Convention of South African Chemical Institute (SACI), Stellenbosch University, 30th November - 5th December 2008.

Poster paper:

Musyoka N. M., Petrik L. F., Balfour G., Natasha Misheer., Gitari W. and Mabovu B. "Removal of toxic elements from brine using zeolite Na-P1 made from a South African coal fly ash" Peer reviewed by members of the International Scientific Committee (International mine water conference).

Publications in preparation:

Musyoka N. M., Petrik L. F., Balfour G., Natasha Misheer., Gitari W. and Mabovu B. "Synthesis and optimization of zeolite Na-P1 from South African coal fly ash" To be submitted to FUEL journal.

Musyoka N. M., Petrik L. F., Balfour G., Natasha Misheer., Gitari W. and Mabovu B. "Hydrothermal synthesis of hydroxyl sodalite from coal fly ash using brine solution" To be submitted to FUEL journal.

"One man's trash is another man's treasure"

Waste coal fly ash is nowadays becoming a material that has beneficial applications. A time will come when all the fly ash produced in the coal fired power stations will have beneficial applications and many countries will move in the direction of total fly ash usage.
(Barnwell and Tapp, 2001)

CHAPTER 1

1 INTRODUCTION

The aim of this chapter is to present the background and also provide an outline of the focus of this study. The first section presents brief background information on coal in South Africa, fly ash and zeolite synthesis procedures. The synthesis processes of zeolites from fly ash are briefly explored in the second half of the chapter.

The problem statement is outlined later in the chapter and the motivation and objectives of the study are stated. In order to highlight the focus of this study, the scope and structure of the thesis are defined. The delimitations of the thesis are also presented towards the end of the chapter.

1.1 Background

South Africa is largely dependent on the combustion of coal for electricity production. Significant coal deposits in South Africa occur within the Great Karoo basin. This basin extends about 200 km from west to east across the northern Free State Province and in south and east of Mpumalanga Province, and about 400 km from southern Mpumalanga Province in the north to the centre of Kwazulu-Natal in the south. The recent energy crisis, largely driven by factors of economic growth and social integration, has lead to construction of new coal power plants in South Africa.

Fly ash, which is a waste by-product of burning coal to generate electricity, is being produced in large quantities by coal-fired power plants throughout the world. It is estimated that around 300 billion tonnes per year of fly ash is produced world wide and the amount is expected to increase in future due to the pressing need for generation of sufficient energy (Ciccu *et al.*, 1999). Worldwide, China is the largest producer of fly ash producing about 160-185 Mt/y (Koukouzas *et al.*, 2006). South Africa produces around 20-30 Mt/y (Gitari, 2006).

The disposal and management of the huge quantities of fly ash generated worldwide has been a concern to the policy advisers, industrial and the scientific community. Some of the adopted

strategies for the utilisation of fly ash include: (i) applications as an additive in the manufacturing of cement, concrete, construction materials and road pavements (Molina and Poole 2004; Yaping *et al.*, 2008); (ii) utilisation of fly ash in zeolite synthesis for wastewater treatment (Holler and Wirsching, 1985; Shigemoto *et al.,* 1993; Querol *et al.,* 1997, Hollman *et al.,* 1999, Woolard *et al.,* 2000; Querol *et al.*, 2001; Somerset *et al.,* 2004); and (iii) use of fly ash in the neutralisation of acid mine drainage (Petrik *et al.,* 2005; Gitari, 2006). Most of these approaches are either geared to utilize the ash beneficially in order to reduce the cost of disposal, or to minimize their environmental impact.

The discovery of the compositional similarity of fly ash to some volcanic materials, the precursors of natural zeolites, prompted the initial synthesis of zeolites from this waste material (Holler and Wirshching, 1985; Querol *et al.*, 2001). Owing to the high content of aluminosilicate glass, mullite ($Al_6Si_2O_{13}$) and quartz (SiO_2) in fly ash, these combustion wastes are well suited as starting materials for the synthesis of zeolites.

The utilization of fly ash as feedstock in zeolites synthesis is of major interest due to the many industrial applications of zeolites in catalysis, as sorbents for the removal of heavy metal ions and organic contaminants from waste waters, the encapsulation of radioactive wastes, gas separation, and as replacements for phosphates in detergents (Somerset *et al.,* 2004). The conversion of these low-cost waste products into products of higher value such as zeolites would allow beneficiation of fly ash in an environmentally friendly way which is also more economically viable.

Natural zeolites have been found to occur in volcanogenic sedimentary rocks formed by the transformation of volcanic ash in lake and marine waters. Zeolites have unique characteristics such as high specific surface area and cation exchange capacity as well as the ability to store heat between hydration and dehydration cycles (Frederick *et al.*, 1999). On the contrary, due to the lack of purity of natural zeolites, catalysis and various other potential uses that are based on the adsorption properties of high purity zeolite phases are in general precluded (Caputo and Pepe, 2007).

1.1.1 Characteristics of zeolites

Zeolites are natural or synthetic aluminosilicates comprising of ordered arrangements of SiO_4 and AlO_4 tetrahedra. The isomorphic substitution of silicon (Si) by aluminium (Al) creates an overall negative charge (Brönsted acid site) that is compensated by cations such as Na^+, K^+, Ca^{2+} and Mg^{2+}, providing zeolites with the property of cationic exchange (Bailey *et al.,* 1999).

Synthetic zeolites hold interesting key advantages over their natural analogs since they can be manufactured in a uniform, pure-phase state. It is also possible to manufacture desirable zeolite structures which do not appear in nature, and this has lead scientists to classify approximately 50 natural and more than 200 synthetic zeolite structures (Rayalu *et. al,* 2001). Many societies and organisations have been set up to promote and encourage the development of aspects of zeolite science and technology (Baerlocher and McCusker, 2008).

Synthetic zeolites are widely used in separation and refinery industries as catalysts, adsorbents and ion exchangers due to their meso and microporous structures. The significant catalytic activity and selectivity of zeolite materials are attributed to their large internal surface area and highly distributed active Brönsted acid sites that are accessible through their uniform pore sizes, high thermal resistance, chemical inertness and high mechanical strength (Bayati *et al.,* 2008).

1.1.2 Preparation of zeolites

By applying different synthesis methods, many researchers have synthesized various types of zeolites from fly ash, such as zeolite Na–P1 (Inada *et al.,* 2005), zeolite A (Murayama *et al.,* 2002, Rayalu *et al.,* 2001), and zeolite ZSM-5 (Chareonpanich *et al.,* 2004). Querol and co workers (2002) reported that zeolite formation proceeds in various stages, during which the Al- and Si- bearing phases of the fly ash are sequentially dissolved, the aluminosilicate glass phase is activated first, followed by dissolution of the quartz phase and lastly digestion of the mullite phase.

Different proposals for zeolite synthesis routes from fly ash have been published and can be summarised as follows:

i. Classical alkaline conversion of fly ash which is based on the combination of different activation solution/fly ash ratios, with specific conditions of temperature, pressure and reaction time applied to obtain different zeolite types (Querol *et al.*, 2001 and Querol *et al.*, 2002).

ii. Introduction of an alkaline fusion stage to monomerize the Si feedstock prior to conventional zeolite synthesis procedures (Shigemoto *et al.*, 1993).

iii. The application of microwave heating conditions to the synthesis procedure which resulted in the reduction of the overall reaction time to around 30 minutes under the specified conditions (Querol *et al.,* 1997; Kim *et al.*, 2004).

iv. Introduction of a two way stage synthesis procedure to produce pure zeolite products from high Silicon containing solutions (Hollman *et al.,* 1999).

v. The use of a dry or molten-salt method (Park *et al.,* 2000), which has been developed in order to achieve high synthesis efficiency and/or zeolite content.

vi. Introduction of a desilification step after an alkali fusion step during the conventional synthesis which improved the solubility of the Al and Si content of the fly ash (Yaping *et al.*, 2008).

1.2 Problem statement

Presently, there are several low end strategies for the utilisation of fly ash which mostly lead to low uses of fly ash in South Africa. The cost implications, especially those associated with transportation, make it logistically difficult for fly ash to compete with other traditional raw materials. The situation calls for a more value-added high technology utilisation of fly ash such as zeolite synthesis to overcome this barrier.

In order to take advantage of the abundant fly ash produced by the South African coal-fired power stations, there is a need to investigate the optimum procedure to synthesize economically

viable zeolites and explore their potential applications. Querol *et al* (2001) investigated synthesis of zeolites from fly ash at pilot scale using various Spanish fly ashes. They concluded that the optimization of the synthesis yields have to be determined for each type of fly ash due to differences in the mineralogical and chemical compositions (Querol *et al.*, 2001). These findings were the motivation for this study since the same case can be applied to South African fly ashes, which differ considerably in composition and have not previously been used as feedstocks to make pure phase zeolites.

1.3 Motivation and objectives of the study

The synthesis of zeolites from fly ash is still a research area of interest and is receiving increasing attention in academia and industry. Over the past years, various investigations have reported hydrothermal conversion of fly ash to different types of zeolites but few studies have been successful in conversion of fly ash into pure zeolites (Walek *et al.*, 2008).

More investigations are required to improve the quality of zeolites produced from waste fly ash. This is because there has been insufficient experimentation on the optimization of the zeolite synthesis methods to enhance purity of the zeolites formed. Very limited research has been conducted on the different South African fly ashes under laboratory conditions which would lay a basis for large scale conversion of the fly ash to zeolites with specific commercial applications.

Certain impure zeolite phases result because of the inconsistent quality of the fly ash feedstock. For example, two fly ashes with similar SiO_2/Al_2O_3 bulk ratios, but different quartz-mullite/glass proportions, can results in different zeolites under the same activation conditions (Querol *et al.*, 2002).

The zeolite Na-P1 phase was chosen as a synthesis goal and subject of study because it belongs to an important group of zeolites which can be synthesized under mild hydrothermal synthesis conditions without using templates, making them potentially economically viable. The narrow particle size distribution coupled with the micron sized crystallites and the unusual framework flexibility gives this zeolite type unique, favourable ion-exchange and water sorption properties.

This study endeavours to redesign the zeolite synthesis process in order to take maximum advantage of the fly ash properties and hydrothermal chemistry so as to improve on purity and increase yields to enhance productivity and reduce cost. It is also intended that the experiments conducted would contribute to the understanding of the synthesis of zeolites from fly ash. The study also forms a basis to understand the requirements for future large scale synthesis conditions and also looks at potential areas for future research in the progress of successful synthesis of zeolites. The focus in this study was mainly on Arnot fly ash although from other South African fly ashes (Duhva and Hendrina) were also investigated.

The overall objectives of this study can be summarised as:

i. To produce pure, single phase and high crystalline zeolite Na-P1 from fly ash sourced from one of South African coal-fired power stations (Arnot). This was to be achieved by restricting the formation of a hydroxy-sodalite impurity phase and also enhancing the complete dissolution of fly ash components such as quartz, mullite, magnetite and hematite.

ii. To apply the conditions identified for production of pure phase zeolite Na-P1 (identified from objective i) to fly ash sourced from other South African coal-fired power stations (Duvha and Hendrina) and determine whether they would give the same quality of zeolite Na-P1.

iii. To understand the major significant synthesis parameters and investigate the linear and non-linear interactions of these parameters. This study would lay a good foundation for identification of the most important parameters during the scale up of the zeolite Na-P1 synthesis process.

iv. To carry out preliminary trials on the removal of toxic elements from brine using the synthesized zeolites.

1.4 Research approach

In the interest of achieving the above mentioned objectives and selecting the right strategy for synthesizing and optimizing zeolite Na-P1 from fly ash, the following approaches were considered:

i. Explore the type of synthesis procedure to adopt by carrying out literature review.
ii. Choose the parameters to optimise and understand the effects of different variables on product purities based on literature review.
iii. Investigate whether different South African fly ash sources result in the same product purity.
iv. Understand and quantify the effects of the varying synthesis parameters.
v. Investigate whether it would be possible to synthesize zeolite Na-P1 using waste brine solution instead of ultra pure water.
vi. Investigate the removal of toxic elements from waste brine using the zeolite synthesized.

Extensive review on zeolite synthesis techniques was carried out and aspects of the appropriate synthesis methodology were adopted. The variables most likely to affect product purity were identified. These variables were then optimised and the products characterised. The results obtained were also compared with those obtained in other studies since there are significant differences in elemental composition of different sources of fly ash.

The experimental programme was divided into three stages. The first stage involved the search for the necessary conditions for synthesis of pure phase zeolite Na-P1 by adopting and slightly modifying the two-step process of synthesizing zeolites from fly ash published by Hollman *et al.*, 1999. The second stage involved the application of a statistical design of the experiments in order to understand the relationships between product properties and four synthesis parameters which took into account individual effects as well as linear and nonlinear interactions of these parameters.

The final stage comprised of preliminary application experiments where synthesized zeolites were used in the treatment of brine solutions obtained from Emalahleni water reclamation plant. The effect of using brine solution instead of ultra pure water during synthesis was also

investigated to establish whether it would be possible to replace ultra pure water with brine during synthesis. This section of the study was motivated by results reported by Lee et al (2001) and Hiraj and Yoshizuka (2008) who used sea water during the synthesis of zeolites and found that they could get almost similar zeolites as when pure water was used.

For the first stage, fly ash which is discharged from a coal fired power plant (Eskom's Arnot fly ash) in South Africa was used as a starting material for optimization. The reason for the choice of this fly ash source was based on the previous studies that had been conducted at the Environmental and NanoSciences research group (ENS), University of the Western Cape. It had been proved possible to synthesize zeolites from raw fly ash and also from solid residues which are the products of acid mine drainage neutralization (Petrik *et al.*, 2003; Hendricks, 2005).

A mixture of fly ash and alkaline solution was subjected to a pre-treatment step (ageing process) whereby the slurry was vigorously stirred. After ageing, the slurry was then hydrothermally treated under static conditions. In this context the variation of parameters such as hydrothermal treatment time and temperature and addition of varying volumes of water during synthesis were investigated.

The above experiments were done sequentially whereby, at each step, a single factor was changed while other factors remained constant. Once the effect of one factor had been determined, the effect of the next parameter was investigated whilst keeping all the other factors constant. The sequential nature of the experiments created an opportunity for adapting the new results that emerged meaning that an alternative that brings improvement was retained in studying the effect of the next factor.

The disadvantage of this approach is that the minimum number of trials needed grows exponentially with the number of factors to be studied. Because every time an additional factor is added, the minimum number of trials increases. In order to deal with this challenge, a statistical design of experiments was adopted once the pure zeolite phase was achieved. Duplication of some experiments was conducted to check the reproducibility of the synthesis procedure.

After establishing conditions for synthesis of pure phase zeolite Na-P1 using Arnot fly ash, other fly ash sources (Hendrina and Duhva) were used under identical conditions to check whether these materials would result in the same zeolite product giving the same purity.

In the second stage of the study, a statistical experimental design was applied to optimize the synthesis conditions to prepare zeolites from fly ash. The parameters that showed a significant experimental influence in the first part and also those parameters of importance as identified from the literature were investigated in more detail. It was important to make sure that the range of variation from the condition for formation of the pure phase was small so that it would not lead to the change of zeolite type. These first two stages of the study were all geared towards obtaining higher crystallinity of the pure zeolite phase, high yield and higher cation exchange capacity. In section three, the preliminary application of synthesized zeolites was investigated to remove toxic elements from brines obtained from Emalahleni water reclamation plant.

1.5 Scope and delimitations of the thesis

The extensive work done by the Environmental and NanoScience research group (ENS) at the University of the Western Cape created a good foundation for this study. Owing to the wide scope of the science of coal and fly ash, those aspects that seem important to the conversion of fly ash to zeolites were identified and highlighted. However, most of the information which is of less relevance to the study has been left out or briefly described. Out of more than 300 known zeolite types, the study focuses prominently on zeolite Na-P1 and only refers to some other zeolite types that have been successfully synthesized from fly ash.

In the choice of the study parameters during the search of pure phase zeolite Na-P1, the variables that had shown some significant influence in the studies done previously at ENS group were chosen. Owing to the time consuming nature of synthesis of zeolites, only four synthesis parameters were investigated during the statistically designed experiments. The choice of these variables was motivated by the results of the studies for the search of pure phase and also from relevant literature.

In the application experiments, the sorption of toxic metals from brine was studied on a batch wise mode due to the small quantity of zeolite obtained as a result of the limited size of the Parr synthesis vessels used. Calculations of mass balances to determine the mobility and fate of trace elements during the synthesis process were not done in this study due some experimental constraints arising from the small sample sizes of the synthesized zeolitic products. Only the most important concepts used in the statistical philosophy of the experimental design based on mathematical theory are highlighted in this study. The reader is referred to the book by Mead (1991) for a more comprehensive assessment.

1.6 Thesis structure

This thesis is organized into five chapters (including this one) and is structured as follows:

Chapter one, which is the introduction, presents the aims of the study, provides an outline of the research framework and contextualizes the study by presenting a brief overview of the background, problem statement and general literature of zeolites.

Chapter two presents the literature review which covers relevant aspects of coal and fly ash; provides an overview of zeolites with focus on key natural and synthetic zeolites, their characteristics and applications and discusses the different zeolite types, modification of zeolite structures, types of synthetic zeolites, analytical methods for identifying zeolites and characterizing their compositions.

Chapter three gives an account of the research design and methodology and gives the rationale behind the selection of the procedure for zeolite synthesis, details of the actual methodology and research instruments used; the motivation behind the choice of these techniques of analysis.

Chapter four presents the results and discussion with relevant references to literature. The results are summarized followed by a discussion of the main trends, and connecting it with the literature survey and highlights any correlations that have emerged in the data.

Chapter five concludes this thesis by summarising the main points highlights the novelty of the research and provides conclusions and recommendations. An outline of aspects that need further research is presented and also details the relevance of the study of zeolites synthesis.

CHAPTER 2

2 LITERATURE REVIEW

It is important to discuss fly ash with respect to its origin since it is the starting material for the zeolite synthesized in this study. Therefore, this chapter deals with a brief background to the source of fly ash, namely coal, its classification and mineralogy. This is then followed by an introduction to fly ash formation, properties, and applications. Thereafter, an in depth discussion concerning general zeolites, the mechanisms of synthesis, and general applications which is later followed by a more detailed description of the properties and characteristics of specifically zeolite P with emphasis on type Na-P1.

2.1 COAL

Coal is mineralized carbon formed during natural geological processes over millennia and is composed of combustible and noncombustible components. The non-combustible substances of coal are made up of inorganic ions which are bound organically and also mineral matter present as crystals or fragments of true minerals (McLennan *et al.,* 2000). Coal properties can vary widely, depending mainly on the origin of the coal (Goodarzi, 2002). For example a typical bituminous coal on a dry basis might contain 80 wt % carbon, 5 % hydrogen, 10 % mineral matter, and 5 % oxygen (Lawrence, 1998).

Coal is an important energy source especially in the generation of electricity and it has also been used as fuel in the steel and the cement producing industries. Currently, the world coal reserves are estimated to last for another two centuries while gas and oil reserves are estimated to last between 40 to 60 years (World Coal Institute, 2009). Many countries in the world, South Africa included, rely on coal as the major source of energy and have signalled intentions to continue the use of coal as a viable long term and sustainable energy source.

2.1.1 Formation of coal

Organic debris that form coal either occur through allochthonous or autochonous depositions. The allochthonous deposition occurs when materials are transported by either wind or moving

water while autochonous depositon is due to the growth and death of the materials without movements (Scheetz and Earle, 1998). It takes millions of years for such organic depositions to be transformed to coal and be available for mining.

2.1.2 Coal classification criteria

The nature of the coal matrix determines its unique physical and chemical properties and this in turn directs the overall behaviour of a given coal sample (Krevelen, 1993). Classification of coal is important for its commercial use and is based upon the following aspects;

i. Petrographic composition; this can also be referred to as the coal type and is based on the original composition of plant or the microscopically identifiable constituents of organic matter.
ii. Coal rank; this often refers to the degree of coalification because it represents the degree of maturity and metamorphism.
iii. Coal grade; this refers to the amount of impurities in the coal such as ash and sulphur.
iv. Other industrial properties such as coking or agglomeration.

Coals are classified by ATSM standard D388 and divided into four classes;

i. Anthracite coal
ii. Bituminous coal
iii. Subbituminous coal
iv. Lignite coal

South Africa's coal is classified as Bituminuos and Anthracite. South Africa is the fifth largest coal producer in the world, and coal accounts for 77% of South Africa's primary energy supply (Eskom, 2009). Coal burnt in South Africa is of high ash content since it exports its high quality coal (Woodlard et al., 2000; Somerset et al., 2008).

2.1.3 Minerals and trace elements in coal

The inorganic portion of coal which remains behind as ash may consist of many different minerals and the most abundant are clay minerals; illite ($[OH]_4K_2[Si_6Al_2]Al_4O_{20}$), and kaolite ($Si_4Al_4O_{10}[OH]_8$), sulfides, such as pyrite (FeS_2) and marcasite (FeS_2); carbonates like dolomite ($CaCO_3MgCO_3$), ankerite ($2CaCO_3MgCO_3FeCO_3$), calcite ($CaCO_3$), and siderite ($FeCO_3$) and quartz (SiO_2). It has also been noted that the clay minerals make up between 60 – 90 % of the total inorganic mineral matter and quartz is found in almost all coals and can comprise anywhere from 1 – 20 % of the inorganic compounds present in coal (Scheetz and Earle, 1998).

The fate of these inorganic constituents during coal combustion is directed by its nature and occurrence in the coal matrix. For example, in high rank coals, the inorganic constituents are mainly present as discrete minerals while in the low rank coals, higher inorganic element such as Na, Cl and S may be organically associated or occur in solutions in pore water (Vathaluru, 2008).

Studies on the occurrences and distribution of trace elements in coal have shown that their affinities differ from one coal deposit to another (Querol *et al.,* 1995). These elements range from a few percent of the total composition of the coal to a fraction of a part of a million (ppm).

2.1.4 Coal combustion and combustion by products

The nature of the coal, namely its composition, size, and variability, affect both the choice of combustion equipment and the nature of the combustion process. There are three types of combustion systems used to burn solid fuels: fixed-bed, suspension fired, and fluidized bed (Lawrence, 1998).The combustion rates can be influenced by the rates of any of the several steps in the combustion process, heat transfer to the fuel from the furnace environment, mass transport of oxygen to the fuel and transport of gaseous combustion products away from the fuel, and the intrinsic chemical kinetics of the combustion reactions or by combinations of the rates of the individual steps. Combustion rates may be increased by increasing mixing rates, increasing the available oxygen levels, or reducing the particle size (Lawrence, 1998).

South Africa's national power utility (Eskom) uses pulverised coal. Burning the pulverized (powdered) coal produces what is commonly referred to as coal combustion by-products (CCPs) or a combination of non-combustible inorganic residue and incomplete combusted organics (Querol *et al.*, 2002). Some of the resultant combustion by-products are; wet bottom boiler slag, dry bottom ash, economizer ash and fly ash (Scheetz and Earle, 1998).

2.2 FLY ASH

Fly ash, a waste product of coal combustion, is a fine-grained inorganic powdery residue, made up of tiny sphere-shaped glassy particles which are derived from minerals included in coal during the combustion process. Fly ash differs in characteristics depending on the type of coal burned, the process undergone by coal before combustion and the operating conditions of the boiler (Eary *et al.*, 1990).

Fly ash is carried off in the flue gas as it leaves the combustion chamber and is usually collected from the flue gas by means of electrostatic precipitators, bag houses, or mechanical collection devices such as cyclones. The fly ash particle size normally ranges from 0.5 to 200 microns (Scheetz and Earle, 1998) and is composed of a complex mixture of various amorphous and crystalline constituents and the primary components include silica (SiO_2), alumina (Al_2O_3) iron oxides together with other elements such as carbon, calcium, sulphur and magnesium that occur in varying amounts (Wang *et al.,* 2006). Fly ash in South Africa is found to contain a relatively high concentration of SiO_2, Al_2O_3 and CaO (Somerest *et al.,* 2004).

It is estimated that the coal combustion activity in South Africa generate about 27.7 million tonnes of fly ash annually (Gitari, 2006) and this volume continues to grow in direct proportion to the increased consumer and industry energy demands. The prospects of continued use of coal as a viable sustainable long term energy source have created the challenge of finding beneficial ways of utilizing the fly ash and in recent years, utilization of fly ash has gained much attention in public and industry (Wang *et al.,* 2006).

2.2.1 Mechanism of fly ash formation

For a better understanding of the transformation of the inorganic components of the coal to ash particles, studies have involved sampling, analysis, and characterization through the entire process of combustion (Hurley and Schobert, 1991). Studies have shown that during coal combustion, the materials making up coal undergo a variety of complex physical and chemical changes (Helble *et al.,* 1994) that depend on their original mode of occurrence, their time-temperature history, and interactions among the constituents (Gutierrez *et al.*, 1993; Hurley and Schobert, 1991).

Tracing the reactions that lead to the formation of the different species in the ash is not easy but studies by Hurley and Schobert (1991) led to the proposal of two main reaction paths: those that are encountered by the inorganics present in the coal as discrete mineral particles, and those that are followed by the organically associated inorganics.

It is generally agreed that several types of changes such as decomposition, fragmentation, coalescence, vaporization, and condensation can occur in the discrete mineral matter in coal during combustion. For example, the transforming reaction path of some of the main minerals has been suggested to occur as follows: Kaolinite ($Al_4[Si_4O_{10}](OH)_8$) changes into metakaolinite ($Al_4[Si_4O_{10}]O_4$) at a temperature of 450–550 °C, and this converts into pseutmullite ($Al_2[SiO_4]O$) and cristobalite or vitreous body at temperatures of 950–1000 °C (Liu *et al.,* 2004).

Fly ash particles have a layered structure resulting from successive deposition of various chemical species, as the temperature decreases along the particle trajectory through the furnace. For example, the crystalline phases such as quartz and mullite remain in the core, whereas the glass phase of aluminosilicate covers the surface of the particle. The extent of enrichment of specific elements in the fine particles varies with coal type, which is attributed to the differences in the mineral matter distribution in the parent coal (Smith *et al.,* 1998).

2.2.2 Physical and chemical properties of fly ash

Fly ash is composed of several fundamental components such as quartz, which includes the silicate minerals that remain unchanged during the combustion process; glass, which includes the non-crystalline material; and mullite, which includes the crystalline components derived from aluminosilicate minerals associated with the coal and other species like the spinel forms that include magnetite. The carbon residues remaining in the fly ash comprise both those that are carried over as unburnt inertinite and char or coke resulting from the incomplete combustion of thermoplastic, which are mostly vitrinite-derived phases (Hower *et al.*, 1996).

Several authors have described the partitioning of trace elements in coal combustion by-products and classified them into three groups based on volatilisation (Figure 1).

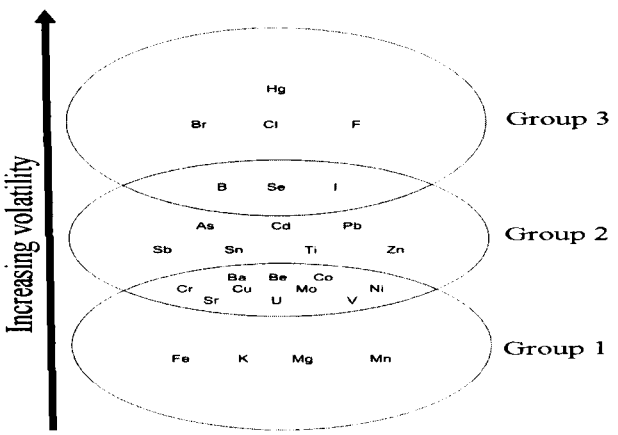

Figure 2-1: Classification of trace elements in coal combustion by-products by their relative volatility (Vories and Thogmorton, 2002).

Studies by Bhanarkar and co-workers (2008) have indicated that the trace elements are preferentially concentrated in fly ash because of its small particles size and large specific surface. This was explained by the fact that the larger surface areas of the smaller particles allows deposition or absorption of volatile elements on the surface of the fly ash, and eventually resulting in an enrichment of certain element in the smaller particles.

Table 2.1 gives a comparison of elements available in fly ash and soil. Certain minor elements, notably Pb, Cd, and As, are more strongly associated with the fly ash collection system, being higher in electrostatic precipitator ash than in mechanically collected ash, than with the sulphur (pyrite) content of the feed coal (Hower *et al.*, 1996).

Table 2-1: Comparison of elements of concern in fly ash and soil and their typical concentrations in ppm (Fansuri *et al.*, 2008).

Element	**Soil**	**Fly ash**
Elements of greatest concern		
Arsenic (As)	7	180
Boron (B)	30	220
Cadmium (Cd)	0.6	230
Mercury (Hg)	0.1	-
Molybdenum (Mo)	1	-
Lead (Pb)	20	530
Selenium (Se)	0.4	20
Elements of moderate concern		
Chromium (Cr)	55	250
Copper (Cu)	25	250
Nickel (Ni)	20	250
Vanadium (V)	80	350
Zinc (Zn)	70	600
Radioactive elements		
Thorium (Th)	9	25
Uranium (U)	2.7	24
Elements of concern but present in low concentrations		
Beryllium (Be)	1	8
Thallium (TI)	0.2	23

2.2.3 Classification of fly ashes

Significant qualities of fly ash may be dictated by its chemical composition, and this may differ widely depending on the coal type (Murphy *et al.,* 1984). Based on the ASTM standards, fly ash is classified according to the content of its major elements (Si, Al, Fe and Ca) as can be seen in Table 2.2.

Table 2-2: Fly ash classification according to chemical composition (ASTM C 618 – 95) (Scheetz and Earle, 1998).

Chemical components	**Class F fly ash**	**Class C fly ash**
Silicon dioxide (SiO_2) + Aluminium oxide (Al_2O_3) + Iron oxide (Fe_2O_3), min. %	70	50
Sulphur trioxide (SiO_3), max. %	5	5
Moisture content, max. %	3	3
Loss of Ignition, max, %	6	6
Available alkali (as Na_2O), max %	1.5	1.5

It has also been highlighted that class F fly ashes are produced from anthracite or bituminous coal combustion while Class C is from lignite or subbituminous coal combustion (Adriano *et al,* 1980). In addition to the above table, Class F fly ashes have also been reported to contain about 5 % CaO, while fly ashes belonging to class C contain a large proportion of CaO which is in the rage of 10–35% (Koukouzas *et al.,* 2007).

2.2.4 Applications of fly ash based on classification properties

Fly ash can either be considered to be an ecological nuisance due to the environmental and economic concerns during disposal or can be treated as a valuable raw material when it is utilized in an economical and beneficial way. Increasing demand for energy throughout the

world has led to an increase in the utilization of coal and, subsequently, in the production of large quantities of fly ash as a waste product (Hui *et al.,* 2005).

Only about 20–30% of the generated fly ash in the world is used, mainly as additive in cement and concrete and as filling material, the rest is disposed of and landfilling is currently the most widely disposal technique used (A'lvarez-Ayuso *et al.,* 2008). Ciccu and co-authors (1999) are quoted as saying that the value of fly ash as a resource is probably still underestimated. Other avenues for fly ash utilization are in concrete related applications (Kruger, 1997; Gitari, 2006).

The characteristics of fly ash such as type of particles, particle size distribution and chemical composition are of paramount importance with a view to their potential applications. Wang (2006) classified the applications of fly ash based on their different properties as follows:

i. Pozzolanic nature

Fly ash has pozzolanic properties, which means that it contains glassy silica and alumina that will, in the presence of water and free lime, react with the calcium in the lime to produce calcium silicate hydrates which is a cementitious compounds. F-type fly ash of South Africa has pozzolanic properties and this causes it to react with various cementitious materials hence it is currently used to enhance the properties of concrete and other building materials and also used with road base binders and asphalt binders (Kruger, 1997).

Fly ash has also found applications in waste stabilization. In this process, it is used to encase the waste in a solid block which assists in transformation of semi-liquid waste to solid matter. Studies have confirmed that fly ash can be used to pasteurize toxic waste like sewage sludge. The resulting product "SLASH" is devoid of pathogens and can either be safely disposed in landfills or preferably used as a soil ameliorant (Reynolds *et al.*, 1999).

ii. Size range and light weight

Uses of fly ash in the building industry especially in the manufacture of light weight concrete make it a good choice due to its economics (Nisnevich *et al.*, 2008). It has also found

applications as fillers for asphalt, paper and plastics and acts as abrasives for scourers and as polisher.

iii. Abundant reserves

The large amounts of fly ash produced in the coal powered power plants find applications in land reclamation as backfill for mines. This is due to its advantages over soil such as high internal angle of friction, low compressibility, reduced settlement and ease of compaction. It has also found applications as underground mine support material especially in the gold mines where it replaces wood packs that were used to keep the stopes open in order to allow the extraction of the ore and by doing this, it helps to conserve the forests (Scheetz and Earle, 1998).

iv. Chemical composition

The great variety of elements in the fly ash creates an interest in recovery of precious metals and other commercial minerals such as alumina. Recovery of trace elements can be accomplished by leaching them from the surface of the fly ash particles. It has been noted that leachability from the smallest particles is easier as they are more reactive, and in addition trace elements tend to concentrate in the finest particles fly ash since they have larger surface areas, which allow for deposition / absorption of volatile elements (refer to section 2.2.2, Table 2.1) on the surface of the fly ash (Liu *et al.*, 2004). Studies report that during combustion, trace elements in fly ash can be enriched up to 30 times relative to the feed coal (Reto *et al.*, 2003).

Many studies have demonstrated that fly ash could be used as source of K, P, Ca, Mg, S and many of the micronutrients needed for agriculture (Truter *et al.*, 2001). However, it has been demonstrated that certain crops growing under fly ash-amended soil conditions may bioaccumulate heavy metals at concentrations greater than normal ranges (Adriano *et al.*, 1980).

It has also been proven that fly ash can be applied in beneficiation of acid mine drainage (Petrik *et al.*, 2005). Acid mine drainage occurs in areas that have previously been mined of coal and is due to the reaction of pyritic minerals associated with coal, with oxygen and water. The reaction is accelerated by the action of thiobacillus bacteria (Gitari, 2006).

v. Modified fly ash

Many studies have shown that fly ash can be used as a raw material in the synthesis of zeolites. This application has an enormous economic benefit because fly ash acts as an inexpensive feedstock of silicon and aluminium during zeolite synthesis and has created much interest due to the many uses of zeolites. This thesis is focussed on the transformation of South African coal waste to form zeolites. More information is presented in the forthcoming section 2.3.8.

2.2.5 Environmental concerns of fly ash

Studies have shown that most trace elements in coal are first vaporized during combustion, then re-condensed to form submicron particles, or adsorbed on the surface of fly ash particles when the flue gas cools down (Liu *et al.*, 2004). The presence of these toxic elements might lead to unwarranted build-up of heavy metals, salts and alkalinity in the fly ash dump sites.

The presence of these toxic elements such as selenium, chromium, boron, and in some instances, mercury and barium have a potential for leaching out from fly ash in ponds or landfills and may end up contaminating ground water and this creates an environmental concern. The ash dumps also cover large tracks of land which makes them unproductive agriculturally, and mars the landscape by being a source of corrosive airborne particles (Petrik *et al.*, 2003).

Toxic element pollution is a serious problem in agriculture and on health of human beings and animals when these elements concentrations are high. Crops such as wheat, soy beans and peanuts can highly accumulate the heavy metals in their shoots especially if they are planted in former ash dumps (Fansuri *et al*, 2008). Classification according to environmental concern as presented by Clarke and Sloss shows that the elements of greatest concern are arsenic, boron, cadmium, mercury, molybdenum, lead and selenium while elements of moderate concern are chromium, copper, nickel, vanadium and zinc (Sloss *et al.*, 1996).

To summarise the environmental concern of fly ash, it is important to stress that the inclusion of toxic elements in the ash and their solubility are the primary determinants of toxicity. Concentration is not the only factor; volatility and toxicity also determine the potential for health and environmental effects (Voriers and Throgmorton, 2002).

2.3 ZEOLITES

2.3.1 General introduction to zeolites

Overall, zeolites can be of either natural or synthetic origin. The term zeolite was first coined by a Swedish mineralogist, Axel F. Cronsted in 1756. The name stemmed from the Greek word "zeo" which means to boil and "lithos" which means a stone and this is due to the fact that the hydrated mineral showed unique frothing features when heated.

The chemical composition of zeolites can be represented by the empirical formula (Breck, 1974);

$$M_{x/n}O[(AlO_2)x.(SiO_2)y].wH_2O$$

Where M = Exchangeable cation with the valence of n

w = Number of water molecules

y/x = Stoichiometric factor between 1-5 depending upon the structure

(x+y) = Total number of tetrahedra in the unit cell

The first analysis of the crystal structure of a zeolite, analcime, was reported by Tayler in 1930 (cited in Breck, 1974). Structurally, zeolites are framework aluminosilicates that are based on an infinitely extension of a three dimensional network of AlO_4 and SiO_4 tetrahedra linked to each other by sharing all oxygen atoms. Cations are introduced as extra framework species in to voids, acting as charge compensating ions to preserve the electronic neutrality since the replacement of tetravalent silicon atoms by trivalent aluminum atoms results in the formation of ionic sites in the vicinity of the aluminum atoms. The cations introduced are usually readily exchangeable and are not part of the lattice framework structure.

Zeolites exhibit some common properties such as porosity, size-selective inclusion and sieving, reversible hydration, and ion exchanging ability. Within the pores, the alkali metal cations and the water molecules are free to move around. It is this feature that allows zeolites to act as a hydrating and dehydrating agent, and also to take up other liquids such as ammonia or alcohol, and to exchange charge compensating cations with ease. The pore size, generally between 3 and

10 Å in diameter, is unique and thus zeolites can act as molecular sieves which are able to sieve ions and molecules below a given size, excluding larger molecules. This shape-dependent or size-dependent selection also enables zeolites to absorb molecules like ammonia, benzene, and others selectively.

These special features are well understood when one looks at the atomic arrangements of the zeolite lattice which is made up of SiO_4 and AlO_4 units which are arranged so that the four corners of the tetrahedron are occupied by oxygen atoms surrounding a silicon or an aluminum atom (Figure 2.2). Each of these oxygen atoms is shared among the tetrahedra building blocks (Szostak, 1989; Weitkamp and Puppe, 1999; Nagy *et al.*, 1998). The silicon and aluminium tetrahedra are combined to form more complicated secondary building units (SBUs). These SBUs join to form structurally and chemically important zeolite pores or channels which are known as oxygen windows that pass though the zeolite (Figure 2.3). The interesting properties of zeolites are brought about by the pore system which penetrates the zeolite in one, two or three directions and the pores vary in size and shape as discussed in section 2.3.3.

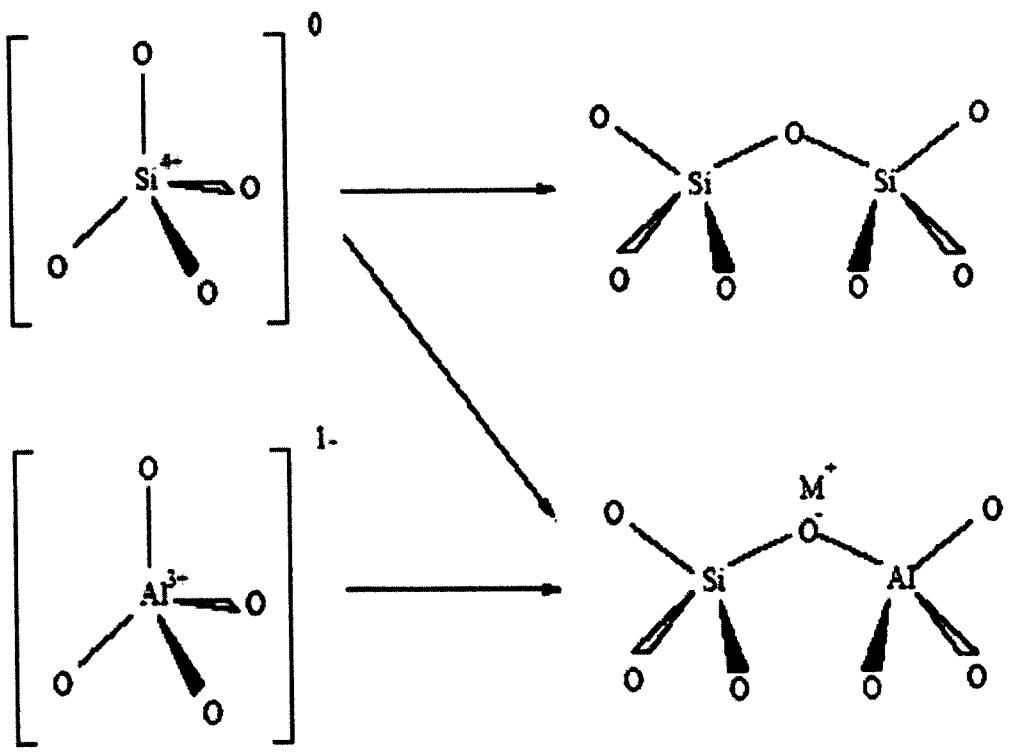

Figure 2-2: Primary building blocks of zeolites.

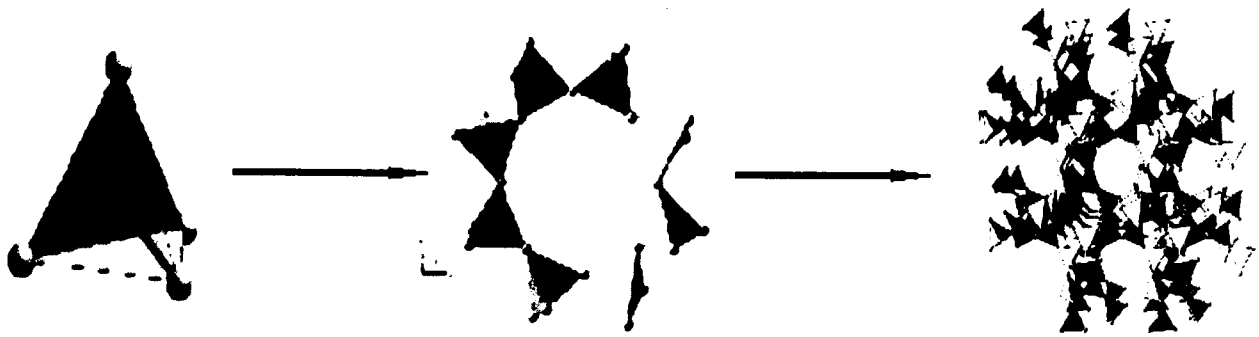

Figure 2-3: Illustration of SiO_4 and AlO_4^- tetrahedra and orientation of tetrahedra to form framework structures (Fansuri *et al.*, 2008).

2.3.2 Physical properties of crystalline zeolites

i. Colour

Pure state natural zeolites are colourless but small amount of impurities account for the colour of these minerals. In the synthetic zeolites, the presence of alkali or alkaline earth cations also impacts on colour. This colour varies with the degree of hydration (Breck, 1974).

ii. Hardness

The crystal hardness of zeolites is found to range from 4 - 5 on the mohr scale.

iii. Density

The density of zeolites ranges from about 2 to 2.3 g/cc (Breck, 1974). The exchange with other heavy ions may increase the density, for example barium zeolite has a density of 2.8 g/cc.

iv. Electrical conductivity and electrochemistry

Zeolites can exhibit electrical conductivity which arises from the movement of ions through the framework. Studies by Breck (1974) showed that the conductivity was strongly dependent on the cation size and size of the channels within the zeolite structure. This property contributes to the ionic conductivity in batteries (Nagy *et al.*, 1998).

v. Ion-exchange capacity

The ion exchange capacity of zeolites arises due to the loosely-bound nature of charge balancing extra-framework cationic species which can be readily exchanged for other types of metal cations when in an aqueous solution. The cation exchange behaviour in zeolites depends upon the (Szostak, 1989; Nagy *et al.,* 1998; Weitkamp and Puppe, 1999):

a. Concentration of the cation species in the solution
b. Type of the anion species associated with the cation in the solution
c. Solvent, that is whether it is an aqueous or an organic solvent
d. Structural characteristics of the particular zeolite
e. Nature of the cation species i.e cation size and charge and whether they are anhydrous or hydrated

In some circumstances, it has been noted that the measured exchange capacity values deviate from the theoretical value due to impurities or variation in the chemical composition. The exchange of cations in zeolites is accompanied by dramatic change in the stability, adsorption and selectivity, catalytic activity and other important physical properties.

Some applications of zeolites based on the ion exchange properties include:

a. Treatment of radioactive waste where zeolites may be used to remove long lived – cesium and strontium isotopes. For the removal to be effective in this case, zeolites have to be be stable in the presence of high levels of radiation and also resistant to chemical attack.

b. Ammonia removal from waste water. Ammonia is toxic to aquatic life and causes accelerated growth of algae which may lead to eutrophic conditions in lakes. Ammonium ions can be removed from municipal, agricultural and industrial waste water using zeolites.

c. Use of zeolites as detergent builders – this enhances the cleaning efficiency of the detergents by removing Ca^{2+} and Mg^{2+} ions from the washing water to prevent their precipitation by surfactants.

vi. Adsorption

Zeolites can adsorb molecules in particular those with a permanent dipole moment, and have other interaction effects with a selectivity not found in other adsorbents. The surface area of zeolites, which is determined experimentally by Brunauer-Emmett-Teller technique (BET) which is based on the relation of adsorption of a given adsorbate under a certain set of specific conditions, plays a key role in adsoption. This is facilitated by the presence of void volume, which is nearly 50% of the zeolite volume, and represents a space where the adsorption field exists.

Some applications of this property include; separation of gases and liquid mixtures and also molecular sieving of water especially in the removal of water from gases and liquids and also for general drying.

2.3.3 Classification of zeolites and related structures

Zeolites are often classified on the basis of their framework structures (Nagy *et al.,* 1998). The International Zeolite Association (IZA) recommends the use of a three letter code for zeolites with various structures (see Table 2.3). This coding style consists of three capital letters that are derived from the names of the type of zeolite mineral. The table below gives examples of the three letter coding (the entire alphabetic list can be found in "Atlas of zeolite framework types" by Baerlocker *et al* (2007) and also on the IZA website (Baerlocher and McCusker, 2008).

Table 2-3: Examples of the three letter coding used by IZA.

	Zeolite name
FAU	Faujasite
GIS	Gismondine
GME	Gmelinite
BOG	Boggsite
MOR	Mordenite

The above framework types can be described by classifying zeolites based on criteria cited in Baerlocker *et al.*, 2007:

i. Framework density (FD)

This is based on the number of T-atoms per per 1000 $Å^3$. In order to distinguish zeolites and other zeolite-like materials from dense tectosilicates, a simple criterion based on the framework density has been developed. The maximum FD for a zeolite ranges from 19 to over 21 T-atoms per 1000$Å^3$ depending on the type of smallest ring present whereas the minimum of the dense structures range from 20 to 22 (Baerlocker *et al.*, 2007). It is important to note that for non-zeolitic framework structures, these values tend to be least 20 to 21 T/1000$Å^3$.

ii. Secondary building blocks (SBU)

As unit cells of zeolites are often complex, lattice structures have been classified according to smaller subunits, usually common to a family of frameworks, called secondary building units (see Figure 2.4). These secondary building units are needed for the construction of a zeolite framework. The zeolites can be thought to consist of finite or infinite secondary building units (the primary building units are the TO_4 tetrahedra) which contains up to 16 T atoms (Baerlocker *et al.*, 2007).

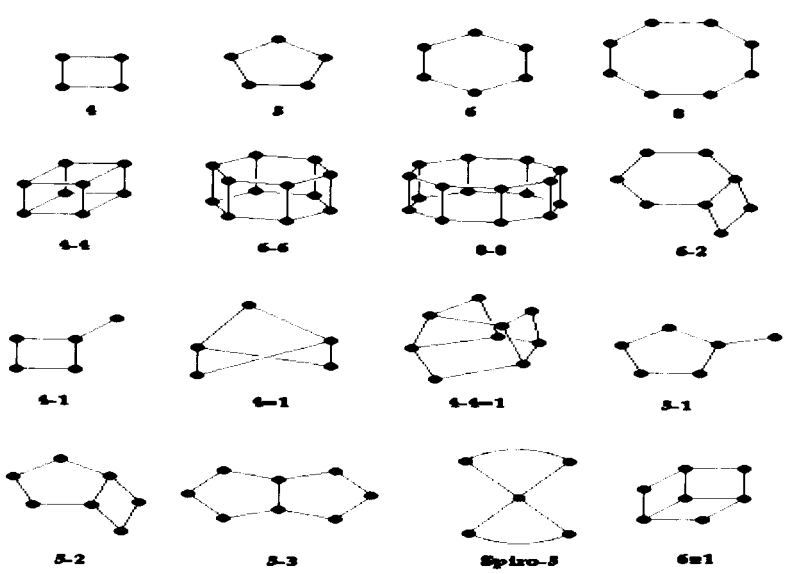

Figure 2-4: Secondary building units; the corner of the polyhedra represent tetrahedral atoms (Nagy *et al.*, 1998).

iii. Pore structure

The arrangement of structural units in the zeolite framework results in the generation of pores and cavities of different dimensions. Zeolites have channels that can be characterized by channel direction. The short hand notation that has been developed to aid in the description of the channel system is, for example, the Gismondine channel system

$$\{[100]\ 8\ 3.1\ *\ 4.5 \leftrightarrow [010]\ 8\ 2.8\ *\ 4.8]\ ***$$

Where $\leftrightarrow$ denotes interconnectivity while the number of asterisks in the notation indicate the channel system as one, two or three dimensional. In the above case, the channels are parallel to the [100] plane together with those parallel to [010] plane results in a three dimensional channel system which can be pictured as an array of partially overlapping tubes. The crystallographic free diameter given in the notation is based on the atomic coordinates of the type of material and oxygen radius of 1.35 Å and may depend upon the hydration state of the zeolite and can also be affected by the non-framework cation and also the temperature (Baerlocker *et al.,* 2007). Porosity can be further sub-grouped as:

i. Small pore materials; pore apertures consist of six, eight or nine membered rings such as zeolite A (~3.5 Å in pore size)
ii. Medium pore materials; have ten membered rings such as ZSM-5 (~5.6 Å in pore size)
iii. Large pore materials; have 12 membered rings such as faujasite (~7.0 Å in pore size)

About 170 framework topologies are known with pore systems differing by their dimensionality or the channel aperture dimensions (Baerlocher and McCusker, 2008). The dimensions of pores in zeolites allow these materials to be used as molecular sieves.

2.3.3.1 Natural zeolites

The most important natural zeolite is clinoptilolite (Wang *et al.*, 2008). Other common natural zeolites are analcime, chabazite, erionite, ferrierite, heulandite, laumontite, mordenite and phillipsite. Initially, zeolites were thought to be rare minerals but various geological studies have confirmed that they are one of the most abundant minerals species on earth (Nagy *et al.,* 1998).

The time required for zeolite formation in nature may be a few hundred years to tens of millions of years depending on the chemical environment (Breck, 1974). Many geological studies have shown that the different origins of natural zeolites can be classified based on the generic types shown in Table 2.4.

Table 2-4: Different generic types of natural zeolites (generated from Nagy *et al.*, 1998).

Hydrothermal-geothermal deposit	Alteration of basaltic lava as a result of hydrothermal or hotspring activity.
Saline, alkaline lake type deposits	Zeolites formed by alteration of volcanic sediments deposited in saline lakes.
Deposits from open hydrological systems	Formed when water with high pH and salt content flows through vitric volcanic ash causing crystal growth
Saline, alkaline soils deposits	Formed at land surface in saline soils as a result of evapotransporation in arid and semi-arid regions.
Zeolite in marine deposits	They result from alterations of volcanic or non-volcanic material in sea-beds due to low temperature or hydrothermal alteration of marine sediments.
Burial diagenesis	This is a low grade metamorphism involving reactions pathways influenced by circulation of ground water and transportation of reactants

The major applications of natural zeolites include use as building materials, agriculture, as animal supplements and in waste water treatment (Nagy *et al.*, 1998). Due to lack of purity, applications such as in catalysis and other potential uses based on the adsorption properties of natural zeolites are in general limited (Colella *et al,* 1999). Due to the lower quality of natural zeolites, the properties of adsorption and ion exchange are exploited in applications such as pet litter, odour removal, fertilizer aids, soil amendment, animal feed supplement, water treatment, aquaculture, removal of radioactive species and heavy metals from waste streams, heat storage and solar refrigeration, pollution control, and many other uses (Nagy *et al.*, 1998).

Studies done by Frost & Sullivan (2001) have indicated that the global consumption of natural zeolites is projected to grow by 5.5 million metric tons per annum by 2010 while consumption of synthetic zeolites is estimated to grow by 1.86 million metric tons per annum by 2010.

2.3.3.2 Synthetic zeolites

As discussed in section (2.3.3.1), it has been understood that natural zeolites originate during the formation of igneous, metamorphic or sedimentary rocks and it is principally through hydrothermal processes over geological time scales. The mechanism of formation of natural zeolites prompted scientists to study the process. During the 1930s they began to produce zeolites artificially in the laboratory and this was done successfully by attempting to mimic the natural conditions required to form natural zeolites. Typical synthetic zeolites are formed by the crystallization of sodium alumino-silicate gels prepared from pure sodium aluminate, sodium silicate, and sodium hydroxide solutions. Predominant types of synthetic zeolites are type A, type X, type Y, and ZSM-5. Table 2.5 show examples of zeolites with commercial interest.

Table 2-5: Examples of zeolites with commercial interest (Mosca, 2006).

Framework code	Zeolite type	Si/Al ratio	Application
FAU	Zeolite X	1 – 1.5	Gas drying in industries Removal of CO2 from industrial flue gases
	Zeolite Y	1.5 – 5.6	As an acid catalyst in fluid catalytic cracking
LTA	Zeolite A	1 – 1.7	Softeners in detergent industrial gas drying
MFI	ZSM-5	> 10	As acid catalyst for fluid catalytic cracking Use in $DeSO_x$ and $DeNO_x$ processes
GIS	Zeolite P	2-8	Waste water treatment Softeners in detergent industrial

All the synthetic zeolites are distinguishable from each other and from natural zeolites on the basis of composition, crystal structure, and sorption properties. The first zeolite synthesis with reliable characterization by chemical analysis, optical properties and XRD were reported by R. M. Barrer in 1940s (cited in Breck, 1974). The positive results triggered enormous interest in systematic studies of zeolite synthesis that have resulted in the production of many zeolite structures. Computer predictions by A. Dyer have shown that there can be around six million conceivable zeolite structures (Dyer, 1988).

Since this work is concerned with synthesis of zeolite P from fly ash, the following discussion will first concentrate on the general properties of synthetic zeolites and then narrow down to the zeolite of interest.

2.3.4 General mechanism of zeolites formation

Various studies investigating different zeolite synthesis procedures have been conducted in an attempt to understand how zeolites are formed from complex mixtures. The synthesis corresponds to the conversion of a mixture of silicate and aluminium compounds, alkaline metal cations and water via an alkaline solution (Barrer, 1982). The dissolution of the silicate and

aluminium compounds which is mediated by the mineralizing agents provides the solution with silicate and aluminate monomers and oligomers, which condense into specific precursor structures and are then organised in more extended structures and finally into the crystalline phase.

The mechanism of formation of zeolites is complex due to the diversity of chemical reactions, including various polymerization equilibria, nucleation and crystal growth processes (Weitkamp and Puppe, 1999). The application of UV Raman spectra of the liquid phase of the synthesis system indicates that the polymeric silicate species are depolymerized into monomeric silicate species during the early stage of zeolite formation and $Al(OH)^{4-}$ species are incorporated into silicate species, (Guang et al., 2001). This leads to the formation of an infinitely extended three dimensional network of AlO_4 and SiO_4 tetrahedra linked to each other by sharing of oxygen atoms.

One of the most favoured synthesis routes has been through sol-gel processing. Sol-gel processing comprises a type of solid materials synthesis procedure, performed in a liquid and at low temperature (Alain and Gérard, 2002). The synthesis via sol-gel process is carried out in alkaline pH (> 10). In this case, a sol of a given precursor is prepared, undergoes some chemical and physical changes, grows in size and forms a gel. The gel is then processed under high temperature conditions to yield the product. It is important to understand the chemical nature of aqueous species as a function of pH, temperature, and concentration since they aid in the formation of the desired products (Jansen et al., 1994).

The zeolite synthesis has been proposed to take place via two steps: nucleation and crystallization. Nucleation is a process where small aggregates of precursors give rise to germ nuclei (embryos), which become larger with time. These small entities can be recognized as having the crystalline atomic structure. In the initial stages of the formation of precursor species, the reaction is thought to be initiated via hydrolysis in order to get reactive M-OH groups (Jansen *et al.,* 1994). Condensation then occurs and leads to the formation of Metal – Oxygen- Metal bonds. The problem is then to make the Si-O-Al bonds in the molecular precursoer and keep them during the whole hydrolysis process (Jansen *et al.,* 1994). This is because a large number of

oligomeric species are formed simultaneously and they are in rapid exchange equilibria and it is not obvious to predict which one would nucleate the solid phase.

The two main mechanisms of condensation are known as olation and oxolation (Jansen *et al.*, 1994). These processes lead to the formation of polynuclear species via the elimination of water molecules from the precursors containing at least one M-OH group. Olation corresponds to the nucleophilic addition of a negatively charged OH group onto a positively charged hydrated metal cation as shown below.

$$M\text{-}OH^{\partial-} + M^{\partial+}\text{-}OH_2 \rightarrow M\text{-}OH\text{-}M^{\partial+}\text{-}OH_2^{\partial+} \rightarrow M\text{-}OH\text{-}M + H_2O$$

The formation of a bridging $H_3O_2^-$ ligand is thought to play a fundamental role in the structure of these primary hydrolysis products. Oxolation involves the condensation of two OH groups to form one water molecule which is then removed to give rise to an 'oxo' bridge as shown below

$$M\text{-}OH + HO\text{-}M \rightarrow M\text{-}O\text{-}M + H_2O$$

This reaction is normally described as dehydration of olated species. Oxolation is usually a slower process than olation.

It is important to briefly highlight the condensation behaviour of both the Al^{3+} and Si^{4+} cations. The aqueous chemistry of tetravalent silicon cations is dominated by the fact that they remains tetrahedrally coordinated over the whole pH range. The monomeric silica anions released into solution upon dissolution of the Si feedstock further copolymerize into higher oligomeric species which are negatively charged. The condensation rate of silica oligomers with aluminate anions increases with increasing silica ratio i.e. with an increasing oligomerization of the various silicates. The silicate and aluminosilicates polyanion chemistry is extremely complex and various techniques such as ^{27}Al NMR spectroscopic technique have contributed to the identification of the silicate and aluminosilicates polyanion structures (Barrer, 1982). The condensed phases are formed of corner sharing $[SiO_4]^{4-}$ tetrahedra in order to minimize electrostatic repulsion between cations. The trivalent aluminium cation gives aquo-cations $[Al(OH)_6]^{3+}$ at the low pH. It follows

an olation mechanism via nucleophilic addition of negatively charged OH groups onto positively charged metal cations (Jansen *et al.,* 1994). This later leads to the departure of the coordinated water molecules and the formation of 'ol' bridges.

Crystal growth which is the continued evolution of the nuclei to larger, macroscopic size, is generally agreed to involve the assimilation of dissolved solute into the ordered crystalline atomic form of the crystal surface and may involve a diffuse boundary near the surface in which the ordering process takes place. During the period preceding the formation of viable nuclei, different kinds of 'germ' nuclei form by chemical aggregation of the aluminosilicates precursor species and disappear again through polymerization. Due to these kinds of fluctuations, the 'germ' nuclei grow in time and form to become viable nuclei on which crystal growth occurs spontaneously (Barrer, 1982). The zeolite crystal growth is solution mediated and it occurs at the crystal-solution interface by condensation of dissolved species (secondary building units) on to the crystal surface (Barrer, 1982).Various efforts to identify the different species in liquid, gel or solid phases during the crystallisation process have also been conducted to understand the crystallisation kinetics that characterise zeolite synthesis (Dyer, 1988; Weitkamp and Puppe, 1999).

In general, the overall crystallization can be split into four stages: Formation of ring like structures of water molecules "icebergs" interconnected by hydrogen bonding, depolymerization of the condensed large molecules of the precursors, whereafter the depolymerized molecules start orienting around the water "icebergs" thus forming the nuclei, followed by the termination of nuclei formation leading to formation of a crystalline structure. The factors that influence the crystalline zeolite structure were highlighted by Szostak (1989) who classified them as:

i. Composition of the reaction matrix
   a. SiO_2/Al_2O_3 sources
   b. Concentration of OH^-
   c. Cations available in the solution, either organic or inorganic
   d. Amount of water
ii. Time of reaction

iii. Temperature; this is based on whether synthesis is done at the following temperature ranges; whether

a. ambient (25 °C – 60 °C),
b. low (90 °C – 120 °C),
c. moderate (120 °C – 180 °C), or
d. high (250 °C or higher)

iv. History dependent factors such as;

a. Stirring
b. Ageing
c. Nature of mixture (solution, sol or gel)
d. Order of mixing

Addition of seeds of a desired zeolite phase to the synthesis batch increases the rate of crystallization. This is can be explained to be due to; Added surface area and also promotion of secondary nucleation mechanisms which result in more rapid consumption of reagents and hence reducing supersaturation. Many other studies have also shown that mixed amorphous gel solutions aged at lower temperature prior to reacting at elevated temperatures provide time during which the solution can form nuclei, though at reduced rates, which can be activated at elevated temperature.

2.3.4.1 Influence of physical parameters on the synthesis of zeolites

i. Temperature and pressure

Initial investigations of synthesis of zeolites were performed under high temperature and pressure to try and mimic formation conditions of natural zeolites (Breck, 1974). In the 50's, synthesis at low temperatures was proposed by Union Carbide and led to the production of zeolites A, X and Y (Nagy *et al*, 1998 and Szostak, 1989).

Several factors in zeolites synthesis are thought to be attained by temperature variables for example:

a. The nature of zeolite phase formed; for example, high temperature favours production of more dense phases.

b. Variations of crystallization kinetics; for example, the ageing period is shorter at higher temperatures while metastable species are decomposed faster at higher temperature (Szostak, 1989).

ii. Pressure

Variation of pressure is not thought to be a major parameter in zeolite synthesis since crystallisation is normally performed under autogeneous pressure (Weitkamp and Puppe, 1999). There are certain specific cases in which pressure can play an important role for example, when synthesis is performed in the presence of volatile reagents such as ammonia and methane which might affect both the pH and/or concentration of dissolved species (Nagy *et al.*, 1998).

iii. Stirring or agitation

Mixing can be characterized as either tumbling or stirring using an impeller in autoclaves or even using a magnetic stirrer during the ageing or hydrothermal process. The effect of this physical parameter can lead to a change of the attributes of the synthesis gel and also affect the outcome of the zeolite process (Weitkamp and Puppe, 1999). Some of the reasons behind stirring the synthesis mixture can be attributed to enabling reagent dissolution, maintenance of the homogenous gel, assisting with structure break-up, maintaining uniform temperature across the reactor, transferring "nutrients" to growing crystals and modifying the local concentration of the reagents by producing synthesis mixtures with a more uniform concentration of reagents through the mixture (Nagy *et al.*, 1998).

iv. Time of reaction

Time is an important parameter since it plays a crucial role in the crystallization kinetics. For example, when preparing a pure phase zeolite, it is important to understand that a desired zeolite species can be a metastable product that can undergo further dissolution which can lead to more stable species (Nagy *et al.*, 1998). Here Ostwald's law of successive transformation is observed. Time, as a parameter of synthesis, can be optimised by applying the knowledge of the contribution of the many components in the synthesis mixture to minimize the crystallization time. Crystallization parameters must be adjusted to minimize the production of the other phases while also minimising the time needed to obtain the desired crystalline phase.

v. Temperature (type of heating and heating rate)

Heating can be done by placing the autoclave in an oven or surrounding the autoclaves with a heating mantle, or placing it in oil, sand-or a water bath or microwave. Inhomogeneous heating of the autoclave, due to poor heat transfer or local hotspots, may result in the formation of denser phases due to the higher temperatures in these zones. The rate at which heat is transferred through the autoclave is dependent upon the material that the autoclave is made of. Teflon-lined autoclaves, in general, take longer to reach a uniform reaction temperature. In literature, it has been noted that some zeolite types may be in synthesized in microwave system, where very rapid synthesis can take place (Kim *et al.*, 2004).

Temperature can alter several factors in zeolite synthesis such as the nature of the zeolite phase (high temperatures can produce more dense phases) and also vary the crystallization kinetics; particularly the induction time is normally shorter at higher temperatures (Nagy *et al.*, 1998).

2.3.4.2 Influence of chemical parameters in the synthesis of zeolites

Composition of the reaction mixture and also the kind of precursor materials used in the reaction media are very important parameters in zeolite synthesis. Variation of these parameters determine the properties of the resulting material, for example its structure, morphology, particle sizes, particle size distribution, homogeneity of elements within the crystallites and others (Nagy *et al.*, 1998).

i. Concentration of reactant species

This is one of the most important factors determining the outcome of crystallisation, because every zeolite has a specific chemical composition range, which can be very broad or extremely narrow. Some of the influences of the ratio of composition are: nucleation and crystallisation kinetics, the nature of the crystalline phases obtained, the framework composition, Si and Al distribution in the lattice and the crystal size and morphology (Breck, 1974). The chemical composition of a specific synthesis hydrogel is usually expressed in terms of molar ratios of oxides (Feijen *et al.*, 1994; Weitkamp and Puppe, 1999):

a SiO_2; Al_2O_3; b MxO; c NyO; d R; e H_2O

in which M and N stand for (alkali) metal ions, R for organic template and a-e are molar ratios.

The compositional ratios influence the nucleation and crystallization kinetics, nature of crystalline phase obtained the framework composition, Si and Al distribution in the lattice and the crystal size and morphology. This composition can also reflect other indirect parameters, such as the alkalinity, and the nature and amount of organic templates. Sodalite is the only material known to crystallize in the full compositional range Si/Al = 1 to infinity (Barrer, 1982).

ii. SiO_2/Al_2O_3 ratio of the synthesis mixture

The SiO_2/Al_2O_3 ratio in the synthesis gel places a constraint on the framework composition of the zeolite produced. All the aluminium present in the reaction mixture is normally incorporated into the framework structure, leaving varying amounts of silica or silicate solution, according to other factors such as hydroxide ion concentration and the presence or various inorganic and organic cations in the reaction mixture, with the exception of the aluminium-rich zeolite Na-A (Szostak, 1989).

The effects of changing SiO_2/Al_2O_3 ratio on the physical properties of a zeolite can be summarised (Szostak, 1989) as:

i. Increasing silica/alumina ratio
   a. Increases acid resistance
   b. Increases thermal stability
   c. Increases hydrophobicity
   d. Decreases affinity for polar adsorbates
   e. Decreases cation content

ii. Decreasing silica/alumina in a zeolite
   a. Increases hydrophilicity
   b. Increases cation exchange properties

The desired SiO_2/Al_2O_3 ratio of a zeolite chosen for a specific application can be obtained through adjusting this ratio in the synthesis mixture.

iii. Type of charge balancing cations

The inorganic cations such as Na, K, Li, and Mg are necessary during the zeolitisation process. They stabilise the framework structure of the zeolite during its formation, by creating charge neutrality since replacement of tetravalent silicon atoms by trivalent aluminium results in the formation of ionic sites in the vicinity of the aluminium atoms. The cations are situated in the pores and can be exchanged out of the crystalline solid upon completion of synthesis, as they are not framework species.

In aqueous solutions, cations are known to influence the ordering of water molecules. These cations can be divided into structure making and structure-breaking agents (Feijen *et al.*, 1994). Structure making cations are small cations such as Na^+ and Li^+ that interact strongly with water molecules because of their high charge density. Structure breaking agents such as NH_4^+, K^+ and Rb^+ interact with water molecules but break the original hydrogen bond. Excessive inorganic cation content may disrupt the formation of the required phase. Organised network of water molecules surrounding the cations can be (partially) replaced by silicate and aluminate tetrahedra and this contributes to the formation of cage like structures (Feijen *et al.*, 1994).

iv. Water concentration

In the conventional hydrothermal synthesis, zeolites have been synthesized in aqueous media. In this case, water is added in the stoichiometric amounts necessary for the dissolution of the silicon and aluminium sources. Apart from water's solvating and hydrolysing ability, it also enhances the formation of a zeolitic structure during growth by filling the micropore system as a guest molecule, thereby stabilising the porous oxide frame work. For most synthesis procedures ultra-pure water is used to avoid the complicating effects of ions such as calcium (Casci, 2005).

To quantify the amount of water in the synthesis, most researchers normally report it as a relative proportion to other chemicals involved in the synthesis process. A good example is work by Elliot (2006) where he reported ratio of water to aluminium (H_2O/Al) in the quantification of the water used during synthesis even though silicate to water (SiO_2/H_2O) or water to sodium hydroxide (H_2O/Na_2O) ratios can also be used.

Studies have also shown that it is possible to grow zeolites in other, nonaqeous media such as alcohols, pyridine and sulfolane. But water is the dominant solvent used for synthesis. The H_2O/SiO_2 and OH^-/SiO_2 ratios have a considerable impact on the ''molecular'' or ''polymeric'' species present in the reaction mix composition and the rate at which these species are incorporated into the three-dimensional structure of the zeolite (Weitkamp and Puppe, 1999; Criado, 2007).

v. Mineralising agent

OH^- is a strong mineralizing agent for bringing reactants into solution. It strongly influences the nature of the species (either monomeric or polymeric) present in the mixture, the concentration of dissolved silico-aluminate fragments, the charge of the species and also the rate of hydrolysis of solid and liquid phases (Nagy *et al.*, 1998).

The fluoride ion can also be used but it has a disadvantage since it prevents the polycondensation mechanism when it is in high concentration. This induces a compromise between the solubility of certain elements and inhibition of zeolites framework formation (Bekkum *et al.*, 1991). Conclusion of work done by Elliot (2006) indicate that OH^- influences the relative yields of zeolite phases produced and also plays a role in the changes in the rates of dissolution of different zeolite products to different extents changing the relative equilibrium yield ratios between different zeolite products.

2.3.5 Characteristics and modification of zeolite structures

Zeolites can be modified to obtain better properties especially for catalytic reactions. Some modification can be based on creation of secondary pores by either de-alumination or acid leaching (Nagy *et al.,* 1998) or by modifying external surface area or internal pore volume by blocking pores and also by varying the chemical compostion by isomorphous substitution of Al or Si by elements with ionic radii and coordination requirements which are compatible with the tetrahedral sites in the structures of the zeolite (Barrer, 1982).

2.3.6 Characterization of zeolites

In the study of zeolite formation, numerous characterisation techniques are used to identify the species present in the synthesis mixture, or characterize the product obtained (Nagy *et al.,* 1998) and some of these techniques are discussed below.

2.3.6.1 Mineralogy and crystallinity by X-ray diffraction spectroscopy

Identification of zeolite framework structure can be carried out on the basis of X-ray diffraction (XRD) which is the common method to determine identity and crystallinity of zeolites and gives a unique fingerprint of each phase. The crystal structure determination using X-ray powder diffraction (XRD) data played an important role in the development of the science and technology of zeolite molecular sieves and catalysts since the advent of synthetic zeolites. Through this technique, the researcher can follow crystallization mechanisms, modification processes, molecular sieve properties and catalytic behaviour.

The most significant information obtained from solid isolated from the synthesis mixture using the XRD technique include (Szostak, 1989):

i. Successful (or unsuccessful) formation of a crystalline material
ii. Presence of a single or mixture of phases
iii. Identification of the structure type or structure types comprising the mixture when there is presence of sufficient peaks
iv. Determination of new structures when complemented with other proper techniques

The analysis is performed on powdered samples which produce a diffraction pattern from the regular arrays of atoms or ions within the crystal. This pattern reflects the symmetry of the constituents of the zeolite framework and also the diffraction angles.
The calculations are based on the Bragg's formula:

$$n\lambda = 2\ d\sin\theta$$

Where;-

- n = An integer
- λ = Wavelength of incident rays
- d = Interplanar spacing

- θ = Diffraction angle

The Braggs formula provides finger print characteristic of the structure. The pattern is used for the identification of known structures by comparing with standard patterns of the JCPDS. An example of a typical diffraction pattern of zeolite Na-P1 is shown in Figure 2.5. During the zeolite synthesis, mixtures of different zeolite phases can be obtained. By changing the synthesis parameters, the zeolite phase purity can be optimised and the formation of secondary phases suppressed.

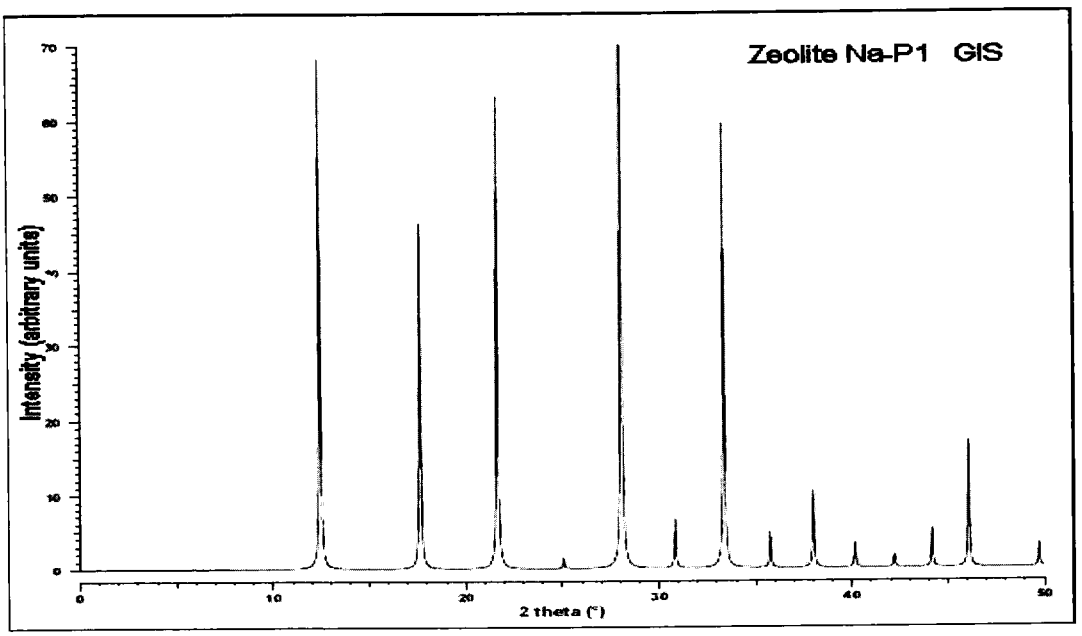

Figure 2-5: Simulated X-ray diffraction pattern of zeolite Na-P1 (Treacy and Higgins, 2007).

A quantitative measure of crystallinity of a zeolite (Szostak, 1989) is made using the summed heights of approximately eight peaks in the X-ray diffraction pattern. Percentage crystallinity is taken as the sum of the peak heights of the unknown material divided by the sum of the peak heights of a standard zeolitic material that has been designated to be 100% crystalline

% crystallinity = Sum of peak heights (unknown) ÷ Sum of peak heights (standard) * 100

Peak area (for example in the faujasite zeolites, the peak at 26.6 2 theta) can also be used to calculate the crystallinity as shown in the equation below.

$$\% \text{ crystallinity} = \text{Area (unknown)} \div \text{Area (standard)} * 100$$

2.3.6.2 Structural configuration by infra red spectroscopy

Vibrational spectroscopy obtainable by Infra Red spectroscopy (IR) provides information on a molecular level. This technique can be used to furnish direct information about the nature of surfaces and adsorbed surface species. Mid-infra red region of the spectrum is useful in the deduction of the structural information since it contains fundamental vibrations of the framework TO_4 tetrahedra. Each zeolite exhibits typical characteristic. Infra red - spectra and the spectra can be grouped into two classes named; (1) internal vibrations of the framework TO_4, which are insensitive to structural variations; and (2) vibrations related to the external linkage of the TO_4 units in the structure (Szostak,1989). Some common features such as asymmetric and symmetric stretch, double ring vibrations, T – O bending modes and pore opening modes can be observed.

The stretching modes involving mainly tetrahedral atoms are assigned to the spectral lines in the region of 650 – 820 cm^{-1}, these stretching modes are sensitive to Si – Al composition of the framework and may shift to a lower frequency with increasing number of tetrahedral aluminium atoms. The frequencies sensitive to the linkages between tetrahedral and the topology and the modes of arrangement of the secondary units of the structure in the zeolite occur in the region of 500 - 600 and 3000 – 420 cm^{-1}.

A band in the 500 – 650 cm^{-1} is assigned to the presence of double rings in the framework structure and is observed in all zeolites that contain the 4- and double 6- rings such as Zeolite X, Y, A and L. Frequencies between 300 – 420 cm^{-1} are associated with external linkages and also related to pore opening or motion of the tetrahedral rings which form the pore opening in zeolites (Breck, 1974).

The bands characteristic of the hydroxyl functions in the region of the infrared spectrum around 3000 cm^{-1} has been associated with the acidity and related acid activities of molecular sieves (Szostak, 1989).

2.3.6.3 Morphology by microscopy

Different techniques in the field of electron optical instrumentation are available to provide information concerning crystal shape and size and as well as other characteristics of zeolites. One of the most important techniques applied in zeolite research is Transmission Electron Microscopy (TEM) and Scanning Electron Microscopy (SEM) used in conjunction with scanning microprobe analysis which yields a great deal of information on zeolites (Szostak, 1989).

i. Scanning Electron Microscopy

For Scanning Electron Microscope (SEM), an electron probe is used to scan the surface of a specimen using deflection coils. The interaction between the primary beam and the specimen produces various signals from back scattered electrons, secondary electrons, X-rays, etc. which may be utilized to form an image of the surface. The appropriate signal is detected, amplified, and displayed on a cathode-ray tube screen scanned synchronously with the beam. One important advantage of SEM is that less stringent specimen preparation requirements are necessary and this permits samples to be examined in a largely unaltered state, since only a conducting surface layer is required. Zeolite samples are usually covered with a thin spluttered film of gold to ensure sufficient electrical conductivity of the sample so as to prevent the build-up of a surface charge which leads to distorted images. The gold film also serves to protect heat sensitive samples during analysis.

ii. Transmission electron microscopy

Transmission Electron Microscope (TEM) can achieve resolution of about 3Å at a magnification of approximately 106. The resolution can be improved by using special imageing techniques known as bright field, dark field, or lattice imageing. High resolution microscopy can provide information on structural defects within molecular sieve crystals and also generate information on the arrangement of channels and pores within the zeolite when enhanced with computer imageing (Szostak, 1989).

The surface scanning technique and the analysis of the characteristic X-ray radiation can also be applied in the transmission mode, which is, scanning transmission electron microscopy (STEM). This method has the advantage of better resolution compared with TEM, but has the disadvantage of difficult sample preparation.

2.3.6.4 Elemental composition by X-Ray fluorescence spectroscopy

The X-ray Fluorescent Spectroscopy (XRF) technique, which allows determination of elemental composition, involves the radiation of a sample with high energy x-rays by which electrons are expelled from the different atoms leaving "holes" in the low lying orbitals. An upper orbital electron then falls in this "hole" and the energy released may result in the generation of radiation which is called X-ray fluorescence or can lead to ejection of another electron, this secondary electron is called Auger effect. The x-ray fluorescence radiation is characteristic for the emitting atom and that makes the technique useful for qualitative and quantitative elemental analysis (Bekkum *et al.*, 1991). The XRF has its limitation since it is a bulk technique thus it is impossible to distinguish framework aluminium and non-framework aluminium in the zeolite product and this stresses the need of using other techniques.

2.3.6.5 Cation exchange capacity

Cation Exchange Capacity (CEC) can be defined as a measure of the charge compensating cations per unit of weight or volume of the zeolite. It represents the number of exchangeable extra framework cations available for exchange. It is a function of the Al substitution for Si in the zeolite framework structure; the greater the substitution, the greater the deficiency of positive charge, and thus the greater the number of alkali or alkaline earth cations required for electrical neutrality, which is signified by a higher cation exchange capacity.

Not all exchangeable cations are always available for ion exchange processes. This can be attributed to several reasons such as pore size of the zeolite, where some of the incoming ions may be too large to fit into the pores and channels of the aluminosilicate framework, and are thus excluded. Some of the exchangeable cations may be components of impurities, such as feldspar, quartz and salts, which were not completely crystallised during the "zeolitisation" process. Since

the structure of zeolites is made up of cages combined in a specific manner, some of the cations may become trapped in cages and thus inaccessible for exchange.

2.3.6.6 Selected area electron diffraction

Selected Area Electron Diffraction (SAED) is an important diffraction method that acts as a source of structural information that enables identification of individual microscopic sized crystallites. A computer program (process diffraction) helps to index a set of single crystal selected area electron diffraction pattern by determining which of the presumed structures can fit all the measured patterns simultaneously. By the use of the user supplied calibration data, the distances and angles can be measured in the digital patterns with a graphic tool when two shortest non-collinear vectors (spots) are clicked on.

2.3.6.7 Other techniques

i. Nuclear magnetic resonance analysis

Nuclear magnetic Resonance (NMR) is a technique is well suited to observe subtle changes in the zeolite catalyst as their composition is made of several NMR sensitive nuclei such as ^{27}Al, ^{29}Si and ^{17}O. NMR spectra can provide information on the bonding of atoms to the silicon and aluminium.

ii. Thermal analysis

The thermal stability of a zeolite can be determined since exothermic heat flows over 600°C is a general characteristic of the structural collapse of zeolites. It can also be used to give information on the water content and the amount of organic templating molecules which are occluded in the cavities and pores of zeolites during the synthesis process.

iii. Raman spectroscopy

The apparent relationship between zeolite structures and raman spectra has been noted for zeolites (Knight *et al.,* 1989). This technique is useful if zeolites being investigated possess similar structures and can also differentiate between bonding of Silicon.

iv. Ultraviolet –Visible Spectroscopy

Characterization of transition metals, complex ions or radicals present in the zeolite can be studied using this technique. By use of this technique, it can help to reveal the existence of cations at the external surface of the exchanged zeolites.

2.3.7 Applications of zeolites

The applications of zeolites have been widely studied. A review of the most significant applications from the literature can be grouped as follows:

2.3.7.1 Catalysis

Synthetic zeolites are known for their use as solid acid catalysts (Breck, 1974). The presence of Brönsted acid sites allows the use of zeolites to replace mineral acids in catalysis The first use of a zeolite as a catalyst was tested using zeolite Y by researchers of Union Carbide Corp. in 1959 (Dyer, 1988).

The versatility of zeolites makes them attractive as catalysts and this is due to their unique characteristics such as;

i. Ability to exhibit high thermal and hydrothermal stability which allows them to withstand use in high temperature and steam environments
ii. Their ability to be modified by isomorphous replacement of Al with elements such as Fe, B, Ga and Ti.
iii. Their macro porosity and near molecular pore dimensions allow the uptake of a relatively high concentration of molecules and also high diffusibility and size exclusion allows shape selective catalysis.
iv. The ion exchange properties of zeolites which can be used to introduce metals in a highly dispersed manner and also aid in the modification of intrinsic acid sites of zeolites (Bekkum *et al.,* 1991).

Environmental considerations to reformulate gasoline and reduce sulfur emissions have been responsible for the upsurge in the consumption of zeolites for catalytic applications. Their major

applications in catalysis is found in the refining and petrochemical industries where zeolites are utilised for catalytic cracking, hydrocracking, hydroisomerization and other processes such as dewaxing, aromatization and aromatic conversions.

2.3.7.2 Ion exchangers

Ion exchange capacity is among the most important properties of microporous materials. The ion-exchange capacity of zeolites depends on: (1) the nature of the cation species in the liquid phase, for example, the cation size and valence, (2) the pore size in the crystalline structure, and (3) the number of exchangeable cations bonded to the zeolite framework (Breck, 1974). This property enables zeolites to exchange their cations with those of the surrounding fluid during the process of cleaning waste water containing heavy metals.

2.3.7.3 Detergents builders and water softeners

Zeolites have been widely used to replace phosphates as water softening agents in detergent industries due to their high ion exchange capability. Pressure from environmentalists led to the phasing out of phosphate detergents (Nagy *et al.*, 1998). It has been noted that most of the zeolites such as Zeolite A, P and X used as detergent builder are characterized by high aluminium content.

2.3.7.4 Uses as adsorbents and desiccants

The dimensions of zeolite channels and their ability to adsorb gases and water have made zeolite molecular sieves suitable for a number of applications such as in processes for drying, purification, and separation of components, as well as in insulated glass windows and pressure swing absorption/vacuum swing absorption (PSA/VSA) processes for generation of high-purity gases.

2.3.7.5 Miscellaneous uses

Either natural or synthetic zeolites can be used in applications such as animal feed supplements, soil improvements, nuclear effluent treatment and some specific zeolites such as A, X or zeolites impregnated with Fe are used for $DeNO_x$ applications.

2.3.8 Zeolites from fly ash

As mentioned in section 2.2, fly ash is composed primarily of aluminosilicate glass, mullite (Al_6SiO_{13}) and quartz (SiO_2). Hence fly ash provides a ready source of Al and Si which can be used for the synthesis of zeolites. The compositional similarity of fly ash to some volcanic materials, precursor of natural zeolites, was the main reason that led Holler and Wirsching (1985) to pioneer the synthesis of zeolites from fly ash. A review of the synthesis of zeolites from fly ash done by Querol and co-workers confirms that the production of zeolites by treating fly ash with alkaline solution is a well known process (Querol *et al.*, 2002).

Class F fly ash (South African fly ash) has been found to be a good feedstock of Al and Si for zeolite synthesis because of its compositional dominance of aluminosilicate and silicate phases (Somerset *et al.*, 2004; Hendricks, 2005; Derkowski *et al.*, 2006). Zeolite synthesis from fly ash is one of the potential environmentally useful applications of fly ash to produce high value industrial products (Querol *et al.*, 1997). Major potential applications of zeolites synthesized from fly ash are based on their use as high capacity ion exchangers in industrial water waste treatment which is also coupled with their excellence to act as sorbents due to their large pore volumes (Holler and Wirsching, 1985; Flanigien, 1991; Querol *et al.*; 1997). These zeolites have also proven to be good candidates for use in soil decontamination (Singer and Berkgaut, 1995) and have shown great potential for use in the removal of post combustion gases such such as SO_x and NO_x (Querol *et al.*, 2002).

2.3.8.1 Methods of synthesis

All the methodologies developed by various authors are based on the dissolution of Al-Si-bearing fly ash phases with alkaline solutions (mainly NaOH and KOH solutions) followed by the hydrothermal crystallization of zeolite material as described in the following section.

i. Conventional methods of synthesis

The classic hydrothermal conversion of fly ash into zeolites has been reported by several authors (Querol *et al.*, 1995; Amrhein *et al.*, 1996; Berkgaut and Singer, 1996; Inada *et al.*, 2005). This is normally a single step involving direct hydrothermal conversion of a mixture of fly ash and alkaline solution (normally sodium hydroxide or potassium hydroxide) to zeolites. Even though

this is the simplest method to produce zeolites, this approach is not adequate because of the low (around 50 %) conversion of the fly ash to a zeolite phase as pointed out by Berkgaut and Singer in 1996. As highlighted in the introduction, more sophisticated procedures have been recently developed to improve this method. These developments include;

i. Introduction of an alkaline fusion step prior to hydrothermal treatment. In this method, the fly ash is mixed with either NaOH or Na_2CO_3 as fusion chemicals and then fused at temperatures above 500 °C to convert fly ash into soluble sodium aluminate and sodium silicate. The soluble materials are dissolved in alkaline solution then reacted under hydrothermal conditions. Even though it is possible to obtain a high rate of fly ash conversion to zeolites, the method is energy demanding since high temperatures are required during the fusion step.

ii. Adoption of a two-stage synthesis procedure that enables the synthesis of > 99% pure zeolite products from high-Si solutions obtained from a light alkaline attack of fly ash. This method was initially used by Hollman *et al.*, 1999. The method involved the extraction of silicon from fly ash, followed by hydrothermal reaction of the extracted silica with addition of aluminate solution in varying ratios to synthesize high purity zeolitic materials.

iii. Synthesis of zeolites under molten conditions without any addition of water (Park *et al.*, 2000).

iv. Introduction of a desilification step after the fusion step which showed an improvement of the solubility of aluminium and silica from fly ash into the alkali solution (Yaping *et al.*, 2008).

In the classic conversion of fly ash, a combination of different activation solution/fly ash ratios and applying specific regimes of temperature, pressure, and reaction time which may be varied, are used to obtain different zeolite types. Various studies have shown that zeolite content of the resulting material varied widely between 40.5 to 75 % (Querol *et al.*, 2002).

From the above discussion, the conventional synthesis of zeolites from fly ash can be summarized as either direct or indirect synthesis. In the case of the direct synthesis (Amrhein *et al.,* 1996), fly ash is hydrothermally treated with an alkaline solution while in the case of the indirect synthesis (Chang *et al.,* 1998; Hollman *et al.,* 1999) silica and alumina are firstly extracted from fly ash with hot alkaline solution and the resultant silicate and aluminate extracts are used for hydrothermal synthesis.

ii. Use of microwave in the synthesis of zeolites

Microwave heating has been shown to greatly accelerate the crystallization rate and to reduce synthesis time (Querol *et al.*, 1997; Kim *et al.*, 2004; Inada *et al.,* 2005). Microwave is absorbed directly into water as solvent and enables the rapid heating compared to a conventional heating process. The electromagnetic waves causes water dipole rotation, probably resulting in the activation of water molecules by breaking of hydrogen bonds.

2.3.8.2 Mechanism of formation from fly ash

The formation mechanism of zeolite from fly ash has been proposed to involve dissolution and depolymerization of the highly polymerized Si and Al containing mineral phases present in the fly ash and this is facilitated by the presence of an alkaline solution. The Al- and Si- bearing phases are dissolved during different stages of the zeolitisation in the following order; glass > quartz > mullite (Querol *et al* (2002).

The main reaction product of the alkaline activation of fly ash has been found to be an alkaline aluminosilicate - type gel regarded as a zeolite precursor (Criado *et al.,* 2007). Crystallisation follows after dissolution and in the process the precursor species condense by the formation of ring-like and other structural units which are important as building blocks to form zeolites (Scott *et al.,* 2001). The dissolution rate of Si^{4+} and Al^{3+} in fly ash is remarkably dependent on the OH^- concentration in the alkali solution, while Na^+ in the alkali makes a contribution to the crystallisation step of the zeolite (Murayama *et al.,* 2002). Nucleation, crystal growth and general mechanism of zeolites formation is discussed in section 2.3.4.

Factors influencing zeolitisation from fly ash include; fly ash properties, alkali concentration, temperature, time, cation type and content, water content, ageing period and seeding. Details of the effect of these factors are discussed in sections 2.3.4.1 and 2.3.4.2. It is important to mention that the properties of fly ash will have a significant influence on the composition and quantity of the zeolites formed. Of particular interest is the effect of the calcium content in fly ash material on the synthesis of zeolites. Fly ash with a calcium content exceeding 3 - 5 mass % of the fly ash has been found to have a suppressing effect on the crystallisation of zeolites (Catalfamo *et al.*, 1997).

2.3.8.3 Two step zeolite synthesis

The two step synthesis procedure was introduced in order to enhance the synthesis of zeolites. This was found to boost the dissolution of Al and Si from fly ash and also to enhance the crystallization of the zeolite leading to the production of purer phases of the zeolites (Hollman *et al.,* 1999).

For the first step, ageing has been found to lead to a shortening of the induction period of crystallization and this is attributed to enhancement of the dissolution leading to a concentration of precursor species. In order to fully understand the effects of this process, studies on chemical and structural changes in both the liquid phase and solid phase of the reaction mixture during the ageing and crystallization process need to be done. Different researchers have studied this mechanism of the ageing process and found that the influence of gel / slurry ageing on the kinetics of crystallization could be generally explained by the increase of nuclei formed in the liquid phase during ageing (Szostak, 1989).

The second step which involves thermal activation has been found to have positive influence on the zeolitisation process. Attempts to understand the crystallization process has lead to conclusions that zeolite crystallization takes place at the interface between the particle and the alkali solution. However this creates a challenge to the total conversion of fly ash to zeolites because as the reaction proceeds, aluminate ions and silicate ions may not be supplied from the fly ash because the growing particle surface is covered with the deposited material such as aluminosilicate gel and zeolite crystals (Murayama *et al.*, 2002).

2.3.9 Gismondine type zeolites

The Gismondine (GIS) framework topology is shared by the following natural zeolites; amicite, gobbinsite, and garronite and also by the synthetic zeolite P (Betti *et al.*, 2007). Natural Gismondine-type zeolites are normally formed under hydrothermal postmagmatic conditions. Their structures have two main connected channels (see Figure 2.6). Water in the channels is present in six different sites (Gottardi and Galli, 1985) and the temperature-dependent dehydration of these Gismondine-type zeolites in dried air is mainly consistent with the crystallographic sites of water molecules of the respective phase.

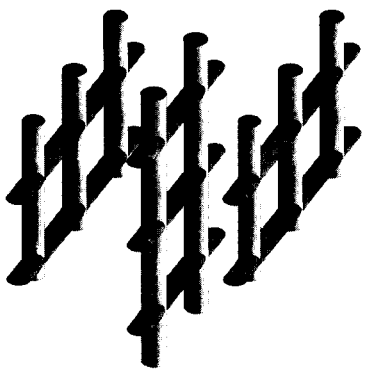

Figure 2-6: Tubular schematic of the two-dimensional channel system of Gismondine-type structures (Gottardi and Galli, 1985).

These Gismondine zeolites belong to the zeolite group comprised of four double-connected 4-ring building units consisting of $(Si,Al)O_4$-tetrahedra (Meier *et al.*, 1996). The four 2-ring units form "crankshaft" chains around a screw tetrad, to build up the three-dimensional framework (see Figure 2.7). According to Gottardi and Galli (1985), the highest topological symmetry of gismondinetype zeolite framework is tetragonal.

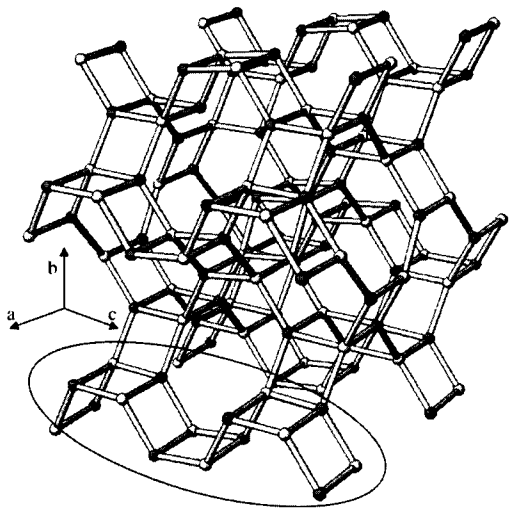

Figure 2-7: Stick-and-ball drawing of Gismondine framework "'double crankshaft'', where white balls = Si, gray balls = Al (Betti *et al.*, 2007).

2.3.10 Zeolite P

Zeolite P is classified as a synthetic member of the Gismondine (GIS) family (Bekkum *et al*, 1991) since it has the same framework topology as the Gismondine zeolites. Zeolite P class includes a series of synthetic zeolite phases which have the typical oxide formula;

$$M_2/nO.\ Al_2O_3.\ 1.80 - 5.00\ SiO_2.\ 5H_2O$$

Some of the known phases of zeolite P (Albert *et al.,* 1998) are:

i. High silica variety of NaP ($Na_{3.6}Al_{3.6}Si_{12.4}O_{32}.14H_2O$)
ii. Low silica NaP ($Na_8Al_8Si_8O_{32}.xH_2O$)
iii. NaP1 ($Na_6Al_6Si_{10}0_{32}.12H_2O$)
iv. NaP2 ($Na_4Al_4Si_{12}O_{32}.14H_2O$)

The unusual flexibility of the topology of zeolite P induces different real symmetries depending on the extra-framework ions, the Si/Al ratio and the degree of dehydration. The interesting properties of zeolite P are associated with the significant flexibility of its framework. For

example, dehydration of NaP zeolite results in a reversible 20 % decrease in unit cell volume (Zholobenko *et al.,* 1998).

Studies by Breck (1974) reported that Zeolite P undergoes two types of dehydration reactions; first order dehydration type involves sudden collapse of the zeolite structure in one or several direction when water is released. A displacement of the tetrahedra framework results in the reduction of the unit volume. However many of these collapse reactions are reversible. The second order dehydration type involves the continuous loss of water from the zeolite over a short temperature range to form a contracted structure. The second order type of dehydration is thought to affect the thermal stability of these zeolite phases and may create a challenge when considering commercial applications such as molecular sieves in adsorption and catalytic processes where water vapour at elevated temperatures may be encountered.

Even though Zeolite P may be limited in its applications as catalysts, it has been found to have significant potential in applications such as the removal of toxic elements during the waste water treatment (Hendricks, 2005; Petrik *et al.*, 2007), use as a geosynthetic liner and has also applications in ground water remediation (Czurdo *et al.,* 2002). Studies by Elliot (2006) have also shown that zeolite Na-P1 can be used in the fertilizer industries.

Studies by Breck (1974) have noted that synthetic zeolite P dominated the synthesis composition fields in the low temperature ranges of 100 °C to 150 °C. Other scientists who have been interested in zeolite Na-P1 have reported that it is a common product of fly ash hydrothermal transformation under alkaline conditions (Catalfamo *et al.*, 1993; Berkgaut and Singer, 1996; Woolard *et al.*, 2000; Hollman *et al.*, 1999; Scott *et al.*, 2001; Querol *et al.*, 1997, 2001). It is important to point out that most of these studies used class C fly ash which resulted in mixed phases whereas South African fly ash (class F) composition is more favourable because it has less calcium content.

Research work done by the Environmental and NanoSciences Group at the University of the Western Cape, had seen successful transformation of fly ash into impure zeolite P using the mild temperature method (100 °C) (Petrik *et al.*, 2007). The findings and also the low cost of

producing this zeolite has laid a good foundation for this study, which aims to improve the phase purity of the zeolite product. Since the quality of zeolites synthesized from fly ash also been found to be a major determinant in the efficiency of toxic element removal from waste water (Hendricks, 2005) the pure phase zeolite Na-P1 synthesized in this study is expected to show greater improvement of the toxic elements uptake.

2.3.11 Chapter Summary

The most relevant information concerning coal, fly ash, and zeolite synthesis from fly ash has been presented in this chapter. Information on zeolite Na-P1, though limited in the literature, has also been highlighted with emphasis on the potential of its synthesis from South African fly ash.

In the next chapter, experimental materials, set-up and sample preparation together with a description of the procedures used is presented in detail.

Chapter 3

3 EXPERIMENTAL

This chapter is divided in to three sections. Part A deals with optimizing the preparation conditions required to form pure phase zeolite Na-P1. Part B deals with application of statistical design of experiments in order to understand the interactions of synthesis variables and optimize the response variables. Part C deals with application experiments of the synthesized zeolite and also the use of brine solution as a substitute of ultra pure water during the synthesis process.

3.1 PART A: Synthesis of pure phase zeolite Na-P1

The major focus of this study was on establishing the synthesis condition that would enable the preparation of pure phase zeolite Na-P1. The experimental approach initially consisted of a one-step-at-a-time optimisation procedure using Arnot fly ash.

3.1.1 Materials and methods

Pulverized fly ashes that were collected from the ash collection systems at Arnot. Duvha and Hendrina Eskom coal fired power stations (see legend 1, 2 and 3 in figure 3.1) in South Africa were used as raw material for the zeolite synthesis.

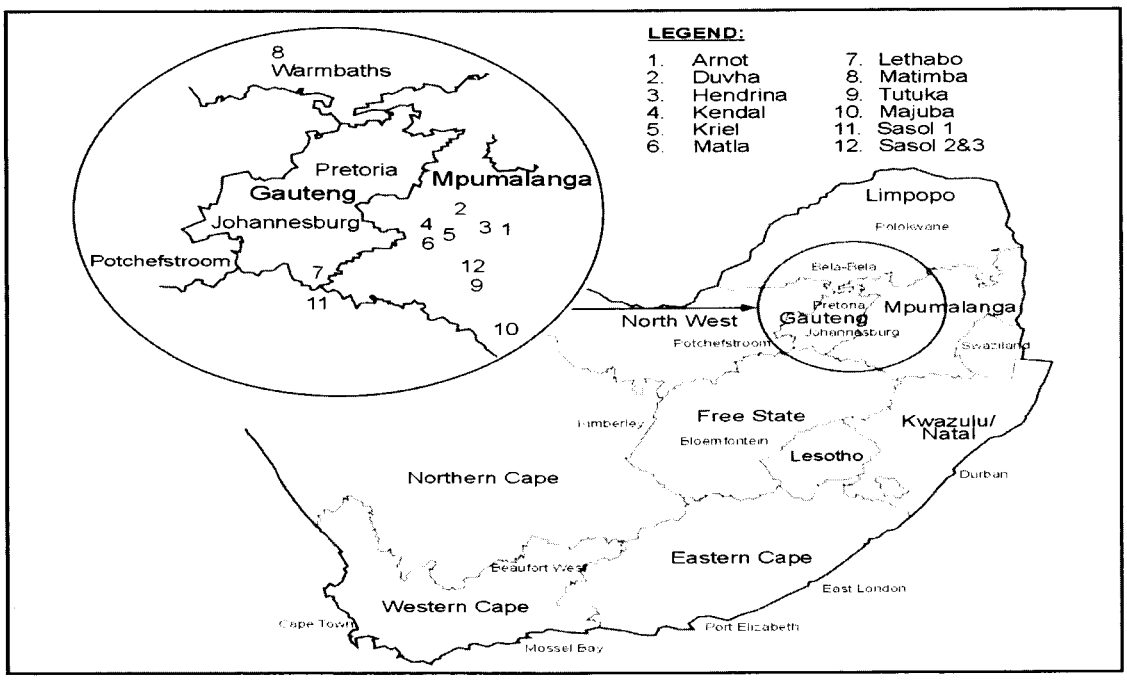

Figure 3-1: Location of important pulverised coal-fired thermal power stations in the Republic of South Africa (Krüger, 2003).

Table 3-1: Reagents used

Chemical	Source	Batch No.	Purity
Sodium hydroxide pellets	Kimix	39-07/10	99.00%
Ammonium hydroxide	Industrial Analytical	K07Q032	-
Ethanol	Kimix	203/8/63	99.50%
Sodium acetate trihydrate	Merck Chemicals	1032383	99.00%
Ammonium acetate	Kimix	MG7M571379	98.50%
Acetic acid	Kimix	2789/40/05	99.8%
Silicon powder	B & M Scientific cc.	F14S043	99.90%

3.1.1.1 Sample handling and storage

The fly ash samples were stored in sealed plastic container with an airtight lid. Containers were kept in dark cool rooms away from sources of moisture, out of direct sunlight and away from

fluctuating temperature. This was because upon exposure to the atmosphere many of the metastable assemblies of minerals phases in fly ash which are initially formed at high temperatures during coal combustion will alter to form thermodynamically stable minerals which might alter the overall initial composition of fly ash (Klink, 2003; Sonqishe, 2008).

3.1.1.2 Synthesis equipment

The set-up for the ageing process is as shown in Figure 3.2. Parr bombs with Teflon lining (Figure 3.3) were used in the hydrothermal treatment process. A typical slurry volume poured in the Teflon lining "cup" was 10 ml. The hydrothermal synthesis was conducted by placing the filled and sealed Parr vessels in to a Memmert hot air oven where temperature was controlled.

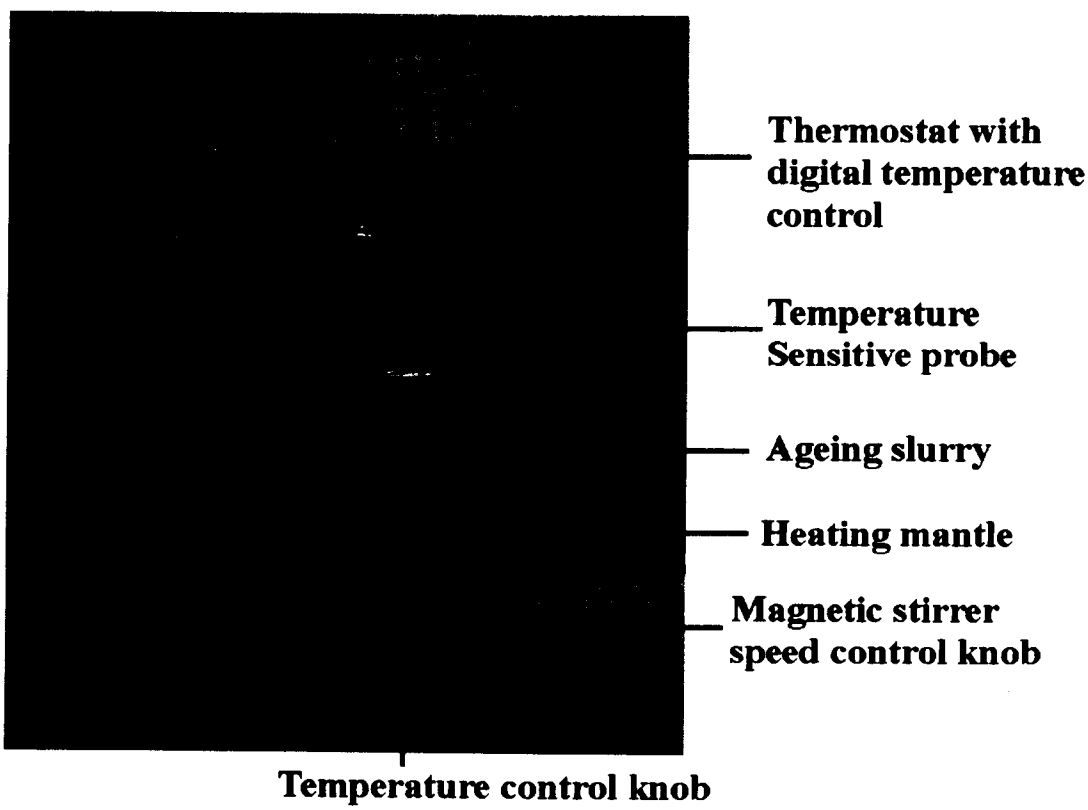

Figure 3-2: Experimental set-up during ageing process.

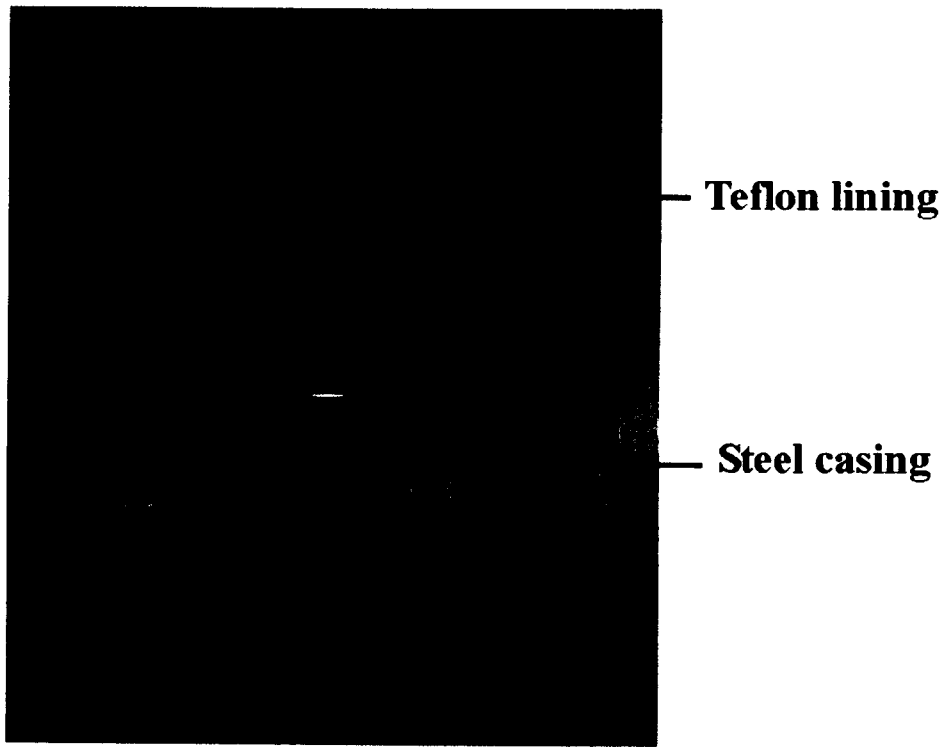

Figure 3-3: Parr bombs and Teflon lining used in the hydrothermal treatment process.

3.1.2 Synthesis procedure

A two step process for the synthesis of zeolites from fly ash adopted from Hollman *et al* (1999) was customised whereby a mixture of fly ash and alkaline solution was subjected to (1) the ageing step and (2) the hydrothermal treatment step. Experiments were undertaken in duplicate to ensure that erroneous results were quickly identified within a series of samples.

3.1.2.1 Ageing step

In this step, the mass ratio of fly ash to sodium hydroxide pellets was 1:1. The sodium hydroxide was dissolved in 100 ml of ultra pure water in a separate beaker and then added to the fly ash in a plastic 250 ml sealable bottle. A magnetic bar was added to the mixture; the bottle was sealed and then placed on a magnetic stirrer and the heating commenced on. The speed of rotation was set at 800 rpm with heater adjusted to a predetermined temperature of 48 °C which was controlled by a temperature probe inserted through the lid.

The ageing temperature and time were kept constant at 47 °C, and 48 hours respectively since previous studies had shown that these conditions were optimum for dissolution of silicon and aluminium from fly ash into the liquid phase (Thandi, 2008; Petrik *et al.*, 2007).

3.1.2.2 Hydrothermal treatment

After ageing, varying amounts of ultra pure water were added to the slurry while stirring and then the resulting homogenous solution was transferred in aliquots of 10 ml into a 23 ml Parr bomb. Crystallisation of the feedstock was achieved by placing the mixture in sealed Parr bombs in a thermostated Memmert hot air oven for a predetermined time and temperature (see experimental conditions in Table 3.2).

Table 3-2: Experimental conditions.

Parameter investigated	run	H_2O/SiO_2 after ageing process (molar ratio)	Ageing temperature (°C)	Ageing time (hours	Hydrothermal temperature (°C)	Hydrothermal time (hours)
1. Hydrothermal treatment temperature and time	1	0.39	47	48	100	12
	2	0.39	47	48	100	24
	3	0.39	47	48	100	36
	4	0.39	47	48	100	48
	5	0.39	47	48	120	12
	6	0.39	47	48	120	24
	7	0.39	47	48	120	36
	8	0.39	47	48	120	48
	9	0.39	47	48	140	12
	10	0.39	47	48	140	24
	11	0.39	47	48	140	36
	12	0.39	47	48	140	48
	13	0.39	47	48	160	12
	14	0.39	47	48	160	24
	15	0.39	47	48	160	36
	16	0.39	47	48	160	48
2. Water content during hydrothermal treatment step	17	0	47	48	140	48
	18	0.2	47	48	140	48
	19	0.26	47	48	140	48
	20	0.39	47	48	140	48
	21	0.49	47	48	140	48

In order not to miss conditions for synthesis of pure phase zeolite Na-P1, experiments were conducted by varying the hydrothermal treatment temperature and time concurrently.

3.1.2.3 Recovering of the zeolite

After hydrothermal treatment at the above (Table 3.2) predetermined time and temperature, the Parr bombs were removed from the oven and allowed to cool down to room temperature. The liquid phase was separated from the zeolite by filtration; pH was measured and the supernatant solution was kept for compositional analysis while the solid product was thoroughly washed with deionised water until a filtrate pH of 9 -10 was obtained.

When the pH of the rinse solution had reached 9, the phases were separated and the solid product was recovered quantitatively and dried overnight at 90 °C and then transferred into airtight plastic containers prior to characterization.

pH measurements

The measurement of pH was done using a HANNA HI 991301 portable pH/EC/TDS/temperature meter. Calibration of the pH meter before use was done using with buffer solutions at two 2 point automatic buffer recognition (at pH 4.01 and 7.01 or 10.01 as appropriate to the pH range being determined). It was also important to duplicate sample measurements at room temperature.

Electrical Conductivity measurements

Determination of the Electrical Conductivity (EC) was carried out using a portable HANNA HI 991301 pH/EC/TDS/temperature meter. It was important to calibrate the EC/TDS meter for accuracy before use and at times during determinations using a standard solution of 12.88 Ms/cm at room temperature. Duplication of the measurement was also done.

3.1.3 Characterization techniques

3.1.3.1 Elemental analysis

i. X-ray Fluorescence Spectroscopy analysis

In this case, the X-ray Flourescence spectroscopy (XRF) was used to carry out multielement analysis of the starting feedstock fly ash and the synthesized zeolitic materials. The samples were prepared by mixing 9g of fly ash or zeolitic material with 2 g of a binder (which was made up of 10 % C-wax binder and 90 % EMU powder). The mixture was then thoroughly shaken, poured

into the mould and pelletized at a pressure of 15 tons for about 1 minute using a Dickie and Stockler manual pelletizer. Loss on ignition (LOI) was measured by placing the samples in the furnace at 1000 degrees for at least 45 minutes.

Analyses were done on a Philips PW 1480 X-ray spectrometer. The spectrometer is fitted with a Chromium tube, five analyzing crystals namely LIF 200, LIF 220, GE, PE and PX and the detectors are a combination of gas-flow proportional counter and a scintillation detector. The gas -flow proportional counter uses P10 gas, which is a mixture of 90 % argon and 10 % methane. Major elements were analyzed on a fused glass bead at 40 kV and 50 mA tube operating conditions and trace elements were analyzed on a powder briquette at 50 kV and 40 mA tube operating conditions. Matrix effects in the samples were corrected for by applying theoretical alpha factors and measured line overlap factors to the raw intensities measured with the SuperQ Philips software.

ii. Inductively Coupled Plasma (Atomic Emission and Mass) Spectroscopy

Elemental analysis study of the zeolite filtrates collected after zeolite synthesis was done in order to gain a better understanding of the trace and major heavy metal species contained in the filtrates, and also to determine which element species stays trapped in the zeolite sample and which are released. The concentrations of ionic species in the post-synthesis aqueous supernatant solution were measured by the use of inductively coupled plasma atomic emission (ICP-AES) and mass spectrometry technique (ICP-MS). The instrument used for the majors is a Varian Radial ICP-AES, while traces were done on an Agilent 7500ce ICP-MS, using a High Matrix Introduction (HMI) accessory and He as collision gas. For both instruments, external calibration was performed daily, and results of a quality control standard verifying accuracy was included with every batch of samples analyzed. For ICP-MS analysis, internal standards were used to correct for matrix effects and instrument drift. Samples were diluted 20 times for majors and traces, with data corrected for dilution factors.

3.1.3.2 Mineralogical characterization by X-ray Diffraction Spectroscopy

i. Qualitative XRD analysis

The fly ash and synthesized zeolite samples (after being ground to a fine powder) were placed in sample holder and the crystalline phases were characterised using a Philips X-ray diffractometer with Cu-Kα radiation. The XRD instrument operating conditions were as given in Table 3.3.

Table 3-3: XRD operating parameters.

Radiation source	Cu-Kά
Radiation wavelength (λ)	1.542 Å
Range	104
Time constant	1 s
Preset	1000 counts/s
Voltage	40 kV
Current	25 mA
2 θ range	$4^{\theta} < 2\theta < 60^{o}$
2 θ /step	0.1^{o}
Anti-scatter slit	1^{o}

The phase identification was performed by searching and matching obtained spectra with the powder diffraction file data base with the help of JCPDS (Joint committee of powder diffraction standards) files for inorganic compounds.

ii. Quantification of mineral and amorphous phases in Arnot fly ash

After addition of 20 % Si (Aldrich 99 % pure) for determination of amorphous content and milling in a McCrone micronizing mill, the samples were prepared for XRD analysis using a back loading preparation method. It was analysed with a PANalytical X'Pert Pro powder diffractometer with X'Celerator detector and variable divergence- and receiving slits with Fe filtered Co-Kα radiation. The phases were identified using X'Pert Highscore plus software. The relative phase amounts (weight %) was estimated using the Rietveld method (Autoquan Program).

3.1.3.3 Physical characterization by morphological analysis

i. Scanning Electron Microscopy

An insight into the transformations which have taken place during hydrothermal treatment can be gained from the analysis of reactant and product morphologies. The morphology of the fly ash and zeolites prepared in this investigation was examined using a Hitachi X-650 scanning Electron Microanalyser equipped with a CDU- lead detector at 25kV. Samples were mounted on aluminum pegs and coated with a thin film of gold to make them conductive.

ii. Transmission Electron Microscopy

Samples were prepared by diluting the suspension of the synthesis products in ethanol, ultrasonicating and depositing a drop onto S147-4 Holey carbon film 400 mesh Cu grids. 200 kV Field Emission gunlens 1 was used with spotsize 3, at 200 kV using HRTEM Tecnai G2 F20 X-Twin MAT.

3.1.3.4 Fourier Transform Infrared Spectroscopy

Fourier Transform Infrared spectroscopy (FT-IR) was used to monitor evolution of crystallinity during synthesis and also provide information about molecular structure. FT-IR requires virtually no sample preparation so in this case, approximately 15 mg of the zeolite sample was placed on the Attenuated Total Reflectance (ATR) sample holder of a Perkin Elmer spectrum 100 FT-IR spectrometer. The sample was recorded in the range of 1800 – 250 cm^{-1}, baseline was corrected and the spectra smoothened. Vibrations common to zeolites were identified. The use of diamond cells with beam condenser or microscope allowed adjustment of the thickness of a sample by squeezing which enables analysis of microgram samples to be performed.

3.1.3.5 Cation Exchange Capacity

The Cation Exchange Capacity (CEC) was determined following a procedure adopted by Amrhein *et al* (1996). The reagents used were prepared as follows;

Sodium acetate 1 M: 136 g of sodium acetate trihydrate was added to a 1000 ml volumetric flask, dissolved in ultra pure water and diluted to 1000 ml. The pH of 8.2 was achieved by adding a few drops of acetic acid.

Ammonium acetate 1 M: 144 ml of glacial acetic acid was added to 2000 ml volumetric bottle and was diluted with ultra pure water to a volume of 1000 ml. 138 ml of concentrated ammonium hydroxide was added and the volumetric bottle was topped up with ultra pure water to a volume of about 2000 ml. The pH of the resulting solution was checked and if need be, a few drops of acetic acid were added achieve a pH of 8.2.

i. Procedure for determining CEC of fly ash

The untreated fly ash was first saturating using three repeated rinsing steps with 1.0 M sodium acetate (pH 8.2) and this was later followed by four washings with ultra pure water. The extracting of the cations was done with three aliquots of 1.0 M ammonium acetate (pH 8.2).

ii. Procedure for determining CEC for zeolite samples

0.5 g of zeolites was extracted with four 25 ml aliquots of 1.0 M ammonium acetate (pH 8.2). The zeolites were continuously shaken with the extracting solution for 15 min, centrifuged for 15 min, and then decanted. This was repeated a total of four times and the cumulative extract was brought to 100 ml.

The concentrations of exchangeable cations (Na^+, Mg^{2+}, Ca^{2+} and K^+) in the final solution were determined by the use of an Inductively Coupled Plasma – Atomic Emmission Spectrometer (ICP-AES). A slight modification was done on the procedure whereby the fourth washing with ammonium acetate was substituted with ethanol in separate experiments to see whether there was any difference in the values obtained.

3.1.3.6 Surface area and pore size determination

An important physical analysis of the synthesized zeolitic products was conducted by the application of gravimetric nitrogen Brunauer-Emmett-Teller (N_2-BET) surface analysis technique. The sample to be analysed (0.35 – 0.5g) was outgassed at 110 °C on the Flow Prep 060 using helium gas. Micromeritics Tristar instrument was used with nitrogen as the analysis gas based on a 5 point with 30 adsorption and 30 desorption points, together with a total pore size measurement.

3.1.3.7 Thermal stability analysis of the zeolitic product synthesized from fly ash

i. Temperature programmed XRD analysis

Temperature-induced phase transition or structural collapse of zeolite Na-P1 investigations were studied using automated temperature controlled X-ray analysis studies. PANalytical X'Pert Pro powder diffractometer with X'Celerator detector and variable divergence and fixed receiving slits with Fe filtered Co-Kα radiation was used. Mineralogical temperature-induced phase transition investigations were carried out by attachment of Anton Paar HTK 16 High-Temperature Chambers where the sample was directly heated with a heating strip. The mineral phases were identified using X'Pert Highscore plus software..

ii. Thermogravimetric analysis

Thermogravimetric analysis (TGA) of fly ash and zeolite Na-P1 synthesized from fly ash was performed using Mettler Toledo TGA (Model TGA/SDTA851e) with automated sample robot (Model TSO801RO). Temperature ramp was set as from 40 to 900 °C at 5 °C per minute with 30 ml per minute Synair as reactive gas and about 30 ml per minute N_2 as purge gas.

3.1.3.8 Section (Part A) Summary

In this section of chapter two; sample preparation, synthesis procedure, and characterisation techniques have been examined. The main focus of the next section (part B) will be on application of statistical design of experiments to gain more information in the attempts to optimize the quality of the zeolite Na-P1.

3.2 PART B: Statistical design for synthesis of zeolite Na-P1 from Arnot fly ash

The factorial design was used to evaluate two or more factors simultaneously. The treatments were combinations of levels of factors. The main advantage of the factorial designs over one-factor-at-a-time experiments are that they are more efficient and they allow interactions to be detected.

In an effort to make sure that the experimental error was taken care of, replication (which means running the same experiment in repeated trials) was adopted so that the effects of many uncertainties or random variations, such as the repeatability of measuring instruments or small fluctuations in conditions like atmospheric temperature was controlled.

3.2.1 Procedure for building statistically designed experiments

There are four interrelated steps that were followed in building a statically designed experiments, these steps were;

i. Definition of the objective of the study; for example in this case, the objective was to understand liner and non-linear interactions of parameters and find optimum synthesis conditions for obtaining better cation exchange capacity.

ii. Identification of variables that were be controlled during the experiment (design variables), and their levels or ranges of variation; in this case four variables were identified and they were to be varied in two levels.

iii. Definition of the variables that were to be measured to describe the outcome of the experimental runs (response variables), and examine their precision. For this study, the response was to be based on the improvement in the cation exchange capacity.

iv. The final step involved the choice of available standard designs, the one that was compatible with the objective, number of design variables and precision of measurements, and had a reasonable number of experimental runs.

3.2.2 Criteria for the choice of the computer program for designed experiments

Nowadays computers have become generally available for statistical use and numerous programs have been developed to perform calculations that have reduced the laborious nature of manual calculations.

The "Design of experiment" programme, is a structured, organized statistically valid method that is used to determine the relationship between the different factors affecting a process and the output of that process (Montgomery, 2001). Analysis of the results of these experiments helps in the identification of optimum conditions, the factors that most influence the results and those that do not, as well as details such as the existence of interactions and synergies between factors.

In the choice of the statistical computer program, it was important to consider a number of requirements as set forth by Mead (1991). The requirements for choosing the programme was based on the following criteria; namely that the program could;

1. Handle many variables for the same design structure, without repetition of information about that structure
2. Accept any structure of blocking and treatment factor
3. Perform all the calculations for each level of the design structure separately and present the results, with correct information about precision, for separate and combined analysis
4. Include terms representing sets of effects in the fitted model in any order as specified by the user, and the definition of the order of fitting terms must be simple, meaning that the program must be usable interactively
5. Allow inclusion of terms representing regression dependence on quantitative variables in the fitted model
6. Allow joint analysis of several variables, providing bivariate analysis, or more generally a multivariate analysis of variance.
7. Allow the analysis of subsets of the experimental units
8. Permit definition of non-normal error structures
9. Present and identify the results from any analysis in such a way that the user can define additional calculations and specify the form of presentation of information within the

operation of the program. These should include an extensive provision of graphical facilities, simple arithmetic operations and even matrix manipulations

10. Provide the user with all the information necessary to interpret the results, such as the initial subdivision of information in the analysis of variance, (ANOVA) including the tables of fitted mean values with standard errors for differences between means for all important effects
11. Written so that the facilities provided can be described and presented in such a manner that each user may obtain as much information as is necessary to interpret the results. This will involve the initial definition of the general statistical knowledge expected of the user.
12. Have facilities for consulting and summarizing the results of analysis from similar experiments and experimental materials. Implying that it should have data base of information that can be accessed easily when analyzing current data.
13. The program chosen should provoke the user to asses whether he or she fully understands the procedures and methods used. This is very crucial especially in this age where there are many computer statistical programs available, so that the user has an idea of detecting whether the program is statistically valid.

After considering the above criteria and consulting a number of statistics experts, "Design Expert" software (version 7.1) was chosen as the most appropriate program. The use of this software was also advantageous to the user since the same program was used by Douglas Montgomery (2001) to illustrate examples in his book "Design and Analysis of experiments".

A standard designs which provided a list of all experiments that were to be performed was generated using the software. The plans were in two-levels (see Table 3.4), i.e., they were based on measuring the examined property in only two boundary values of each variable synthesis parameter.

Table 3-4: Compositional factors and levels investigated for synthesis of zeolite Na-P1.

Factor	**Low level**	**High level**
A. $NaOH/SiO_2$ molar ratio	0.35	0.71
B. Ageing temperature	35 °C	55 °C
C. Hydrothermal treatment time	36 hours	66 hours
D. Hydrothermal treatment temperature	130 °C	150 °C

The experiments generated were randomized; meaning that the experimental units were allocated to treatments by a random process and not by any subjective or possibly biased approach. In a completely randomized design, there are two distinguishable components of variation; variation between the units receiving the same treatment and of units receiving different treatment

The importance of randomization is that it enables production of groups for studies that are comparable in unknown as well as known factors which are likely to influence the outcome, apart from the actual treatment under study. When carrying out the analysis of variance F tests it is usually assumed that the treatments have been applied randomly.

The full 2^4 factorial design (as shown in Table 3.5) had 32 experimental runs instead of 16 due to duplication.

Table 3-5: 32 Experiments used for a 2^4 factorial plan.

Table 3.5: Run	$NaOH/SiO_2$ (molar ratio)	Ageing temperature (°C)	Hydrothermal treatment time (hours)	Hydrothermal treatment temperature (°C)
1	0.71	55	36	130
2	0.35	55	60	150
3	0.71	55	60	150
4	0.35	55	60	130
5	0.71	55	36	130
6	0.35	35	36	150
7	0.71	55	60	150
8	0.35	35	60	150
9	0.35	55	60	130
10	0.35	55	36	130
11	0.35	35	36	130
12	0.35	55	36	130
13	0.71	55	60	130
14	0.35	35	60	150
15	0.35	35	36	150
16	0.71	35	60	130
17	0.71	35	36	150
18	0.71	55	36	150
19	0.71	35	36	150
20	0.71	55	36	150
21	0.35	55	36	150
22	0.35	35	36	130
23	0.71	35	36	130
24	0.71	35	60	150
25	0.71	55	60	130
26	0.35	55	60	150
27	0.71	35	60	130
28	0.35	35	60	130
29	0.71	35	36	130
30	0.35	35	60	130
31	0.35	55	36	150
32	0.71	35	60	150

3.3 PART C: Application experiments and use of brine during the synthesis procedure

This section details the methodology used during application of synthesized zeolitic samples to treat brine solution from Emalahleni water reclamation plant and also the use of this brine solution as a substitute for ultra pure water during the synthesis process.

Brine samples

The brine samples were collected from stage three treatment section of the Emalahleni water reclamation plant (situated in the Witbank coalfields of South Africa's Mpumalanga province). The samples were transported on ice via a courier to the University of Western Cape, Chemistry Department and refrigerated at 4 °C as soon as they reached the destination. This was done to preserve their integrity (Klink, 2003). The samples kept in the fridge were unfiltered and not acidified in order to determine for pH and EC analysis before use. But before the use of the samples, they were filtered through a 0.45 μm membrane and pH and EC was determined after which they were acidified with 1 ml concentrated HNO_3 for trace element analysis.

3.3.1 Brine treatment experiments

The sorption of toxic elements from the brine by the use of the zeolite Na-P1 synthesized from the Arnot fly ash was studied on a batch wise mode. Experiments were conducted in 50 ml glass flasks using 0.5 g of the adsorbent in contact with 10 ml of brine solution at 26 ± 1 °C. The flasks were shaken in a mechanical shaker for one hour and the solutions were transferred to 50 ml centrifuge tubes where they were centrifuged for 15 minutes and later the solutions was filtered. The major and trace elements were analysed as highlighted in section 3.1.4.1.

3.3.2 Use of brine solution as a substitute of ultra pure water

The effect of using brine solution instead of ultra pure water during the hydrothermal synthesis process was investigated to establish whether it would be possible to replace ultra pure water with brine. The same procedure that was used to synthesize zeolites using ultra pure water (refer to section 3.1.3) was followed to synthesize zeolites from Arnot, Duhva and Hendrina fly ashes.

Chapter 4

4 RESULTS AND DISCUSSION

4.1 PART A: Synthesis of pure phase zeolite Na-P1

In this section, the results obtained during experiments (Section 3.1) which conducted to find the optimum conditions to prepare pure phase zeolite Na-P1 are discussed based on chemical and mineralogical analysis of products and replicability of the experimental results, thermal stability of the synthesized zeolites, morphological transformation of fly ash during the various stages of synthesis, cation exchange capacity and the surface area and pore volume of the zeolites.

4.1.1 Elemental composition of the Arnot fly ash

The XRF results of the elemental composition of Arnot fly ash is reported in the table 4.1 below. The information obtained was fundamental since it provided data for major and trace elemental composition of the matrix of the fly ash. The analysis was done in triplicate i.e. sample AF – 1, 2 and 3.

Table 4-1: XRF of Arnot fly ash.

Major Oxides (mass %)	AF - 1	AF - 2	AF - 3	Mean mass (%)	Std deviation
SiO_2	50.93	51.08	50.73	50.91	0.1782
Al_2O_3	31.03	30.75	30.94	30.91	0.1438
Fe_2O_3	3.47	3.48	3.43	3.46	0.0314
MnO	0.02	0.02	0.01	0.02	0.0029
MgO	1.46	1.49	1.49	1.48	0.0198
CaO	6.23	6.19	6.18	6.2	0.0242
Na_2O	0.10	0.10	0.11	0.10	0.0061
K_2O	0.620	0.60	0.60	0.60	0.0094
P_2O_5	0.58	0.55	0.57	0.56	0.0156
TiO_2	1.66	1.65	1.65	1.65	0.0095
SO_3	0.24	0.25	0.25	0.24	0.0037
Loss On Ignition	3.67	3.85	4.04	3.85	0.185
Sum (%)	100	99.99	99.99	99.99	0.0008
SiO_2/Al_2O_3	1.64	1.66	1.64	1.65	0.012

Trace elements (ppm)	AF - 1	AF - 2	AF - 3	Mean mass (ppm)	Std deviation
As	18	18	20	18.48	1.009
Ce	158	156	161	158.43	2.8466
Co	17	14	14	14.92	1.5922
Cu	48	52	53	51.15	2.3773
Nb	44	46	45	44.96	0.8418
Ni	64	65	68	65.81	2.2044
Pb	63	65	68	65.38	2.2651
Rb	30	27	29	28.45	1.5823
Sr	1100	1026	1058	1061.36	37.1695
Y	46	42	21	36.28	13.1364
V	82	84	89	85.11	3.7107
Zn	42	44	49	45.01	3.4915
Zr	407	404	401	403.98	3.2189

The average SiO_2/Al_2O_3 ratio of Arnot fly ash was found to be 1.65. This ratio is of paramount importance since it will directly govern both the Si/Al ratio of the zeolite product and also the incorporation of Al in the framework structure. Attempts to change the Si/Al ratio of the synthesis mixture often leads to the formation of undesired crystalline impurities or amorphous phases or even formation of completely different zeolites phase (Nagy *et al.,* 1998). Cr_2O_3 and B were not analysed due to experimental constraints.

The major elemental chemistry of the Arnot fly ash is consistent with $SiO_2+Al_2O_3+Fe_2O_3 \geq 70\%$ meaning that it is "class F" fly ash (ATSM method C 618). This is a typical composition of fly ash from combustion of bituminous coal from South Africa (Gitari *et al.,* 2005). The Loss-On-Ignition (LOI), was 3.85 mass % and this measures the unburned carbon remaining in the fly ash and it is an important chemical parameter since it can be used as a screening tool for fly ash for use in concrete and also help to predict the quality of zeolites synthesized from fly ash.

It is important to point out that the presence of CaO and MgO play a significant role when considering fly ash as the feedstock for zeolite synthesis. The reason is that Ca^{2+} and Mg^{2+} act as competing cations during synthesis. It has also been confirmed that Ca^{2+} has structure breaking

properties hence interference with the zeolite crystallization process (Catalfamo *et al.*, 1997). Therefore, low content of CaO signalled that there was a higher likelihood of zeolite crystallization without much interference.

4.1.2 Mineral composition of Arnot fly ash

The qualitative and quantitative X-ray Diffraction spectra of the Arnot fly ash based on the analysis highlighted in section 3.1.4.2 is presented in Figure 4.1.

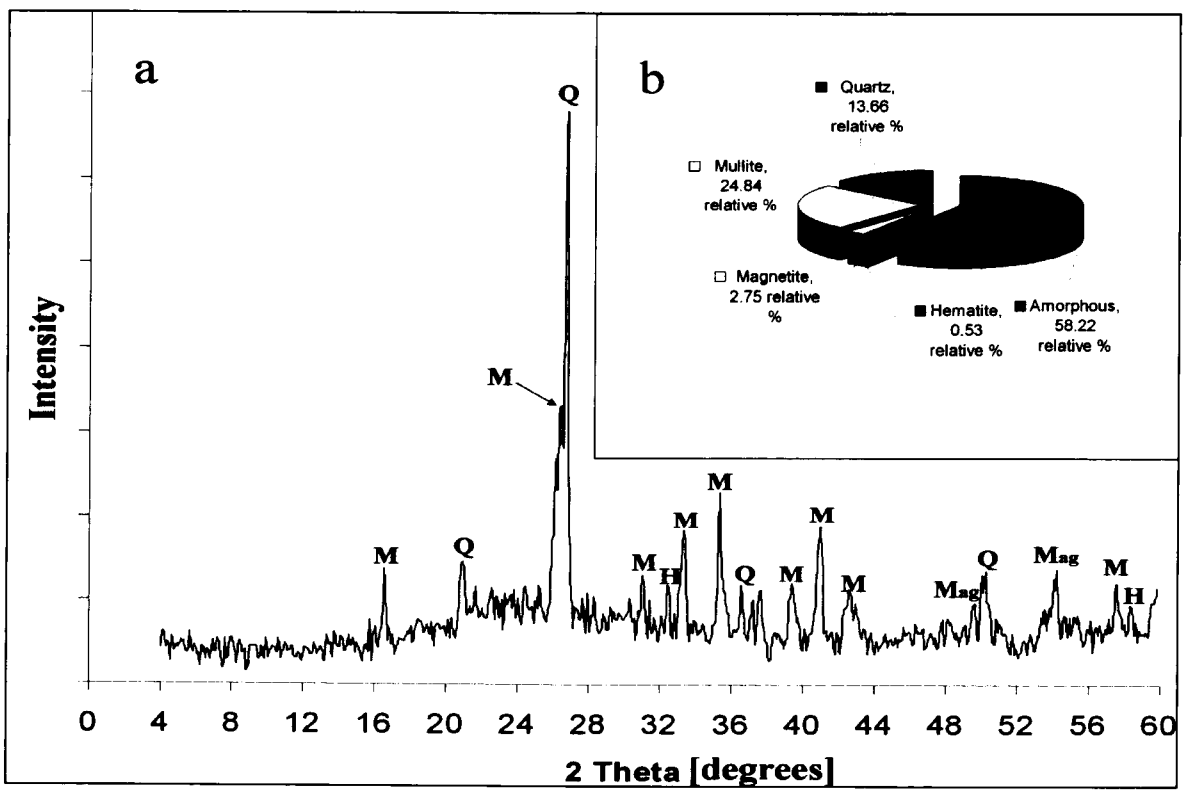

Figure 4-1: XRD of Arnot; a) Qualitative analysis b) Quantitative analysis (Q = Quartz, M = Mullite, H = Hematite, Mag = Magnetite).

From the XRD pattern of Arnot fly ash presented in Figure 4.1, it was found that the predominant phases were quartz (SiO_2) with major peak at 26.9 degrees 2θ and less intense peaks also identified, mullite ($3Al_2O_3.SiO_2$), major peaks at 26.4 degrees 2θ (i.e as a shoulder on the quartz peak), magnetite, and hematite. The presence of amorphous phases are identified as a broad diffraction 'hump' in the region between 18 to 32 degrees 2θ (Inada *et al.*, 2005;

Murayama *et al.*, 2002; Hui and Chao, 2006). The quantification results presented in Figure 4.1 (b) shows that the quantity of the phases identified were in the following order; Amorphous (58.22 %) > Mullite (24.84 %) > Quartz (13.66 %) > Magnetite (2.75 %) > Hematite (0.53 %).

4.1.3 Elemental composition of zeolitic material synthesized from Arnot fly ash

The X-ray Fluorescence Spectroscopy (XRF) data on the elemental composition of zeolites prepared from Arnot fly ash using ultra pure water according to Section 3.1.4.1 is presented in Table 4.2.

Table 4-2: Major oxides and trace elemental analysis of the zeolitic materials synthesized from the Arnot fly ash using ultra pure water.

Major oxides	Percentage of major
SiO_2	36.69
Al_2O_3	25.17
Na_2O	6.53
CaO	6.07
Fe_2O_3	2.28
MgO	2.21
TiO_2	1.58
MnO	0.06
K_2O	0.13
P_2O_5	0.04
SO_3	0.06
Cr_2O_3	0.04
NiO	0.01
H_2O^-	7.04
LOI	11.92
Total	99.81

The SiO_2/Al_2O_3 was found to be 1.45. This was less that the value identified in the raw fly ash showing that there was wastage of the feedstock. Na_2O was higher than in the starting fly ash and this was because of the incorporation of Na as a charge balancing cation since NaOH was used

as the alkaline solution. CaO in the zeolitic sample was almost similar to the content identified in the fly ash since Ca can also act as a charge balancing cation. Due to experimental constrains relating to the sample size of the synthesized zeolitic product, trace elements were not analysed but looking at their concentration in the supernatant solution (Section 4.1.5.3) it seems that most of them were removed as waste in the supernatant after filtering the zeolitic solid product.

4.1.4 Mineralogy of synthesized zeolitic product

The mineral phases identified by X-ray Diffaction (XRD) in products obtained after variation of synthesis conditions using Arnot fly ash is presented in the sections that follow.

4.1.4.1 Variation of hydrothermal treatment time and temperature

According to Feijen *et al* (1994), increasing the synthesis temperature is expected to increase the nucleation and growth of zeolite crystals. Increased mullite digestion is also expected to occur as the synthesis temperature is increased (Querol *et al.*, 1997). Catalfamo *et al.*, 1993 also noted that there is a greater increase in Si dissolution from fly ash compared to Al, this results in an increase in Si/Al ratio in solution which influences the gel composition and consequently the zeolite type.

i. Synthesis at 100 °C with variation of hydrothermal treatment time

Figure 4.2 shows XRD spectra of the transformations of different phases in the fly ash as a function of time when hydrothermal synthesis was done at 100 °C.

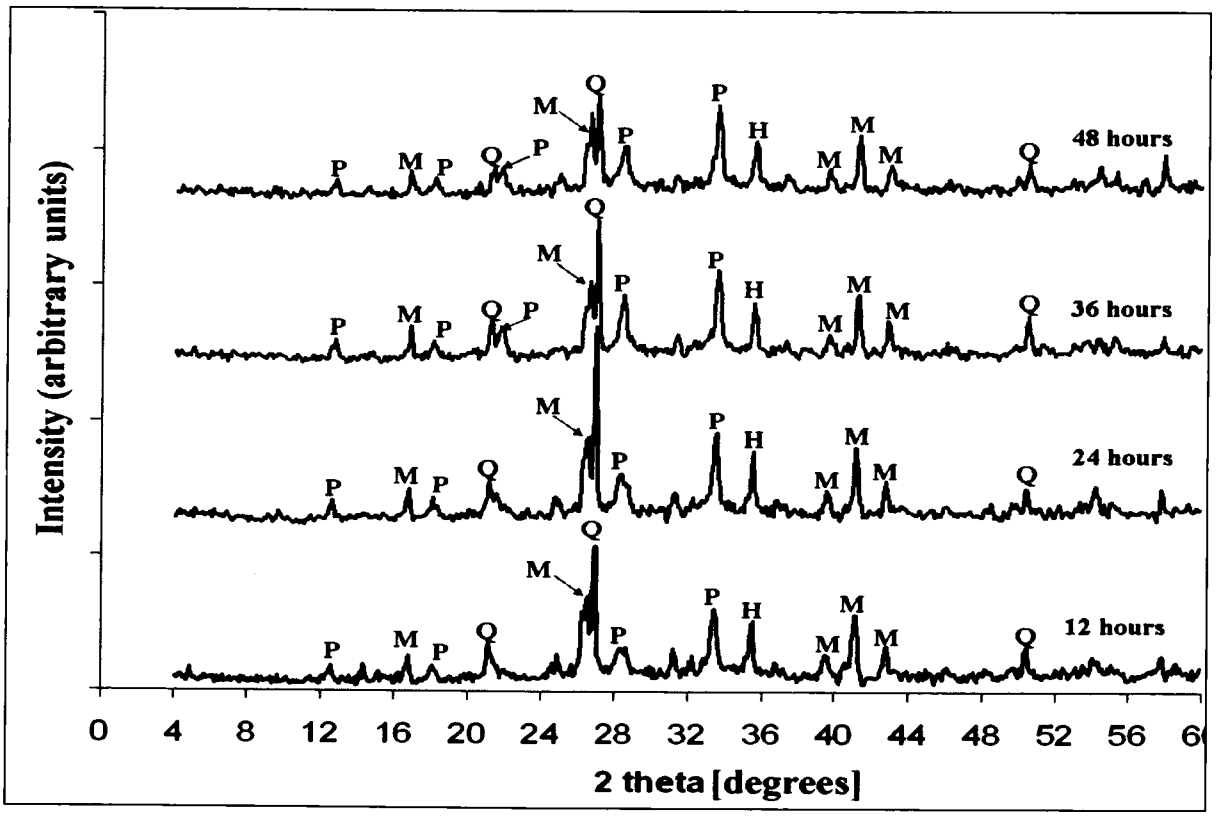

Figure 4-2: XRD patterns of products synthesized at 100 °C with variation of time (P = Zeolite Na-P1, Q = Quartz, M = Mullite, H = Hematite).

It can be seen in Figure 4.2 that the broad hump between 18 to 32 degrees 2θ (Figure 4.1), signifying the presence of amorphous phase, disappeared meaning that this glassy phase was consumed in the zeolitization process. The major zeolitic phase produced was identified as zeolite Na-P1 ($Na_6Al_6Si_{10}O_{32}.12H_2O$). Some undissolved quartz, mullite and hematite phases from the fly ash were also present in the product even after 48 hours synthesis time at 100 °C. Similar observations were pointed out by Catalfamo *et al* (1993) who also noted that the amorphous glassy phase was more soluble than crystals such as quartz and mullite in alkali solutions.

ii. Synthesis at 120 °C with variation of hydrothermal time

Failure to achieve pure phase of zeolite Na-P1 at 100 °C, resulted in experiments being performed at 120 °C to achieve alkaline conversion of fly ash. The product obtained at the next level of elevated hydrothermal temperature (at 120 °C) is shown in Figure 4.3.

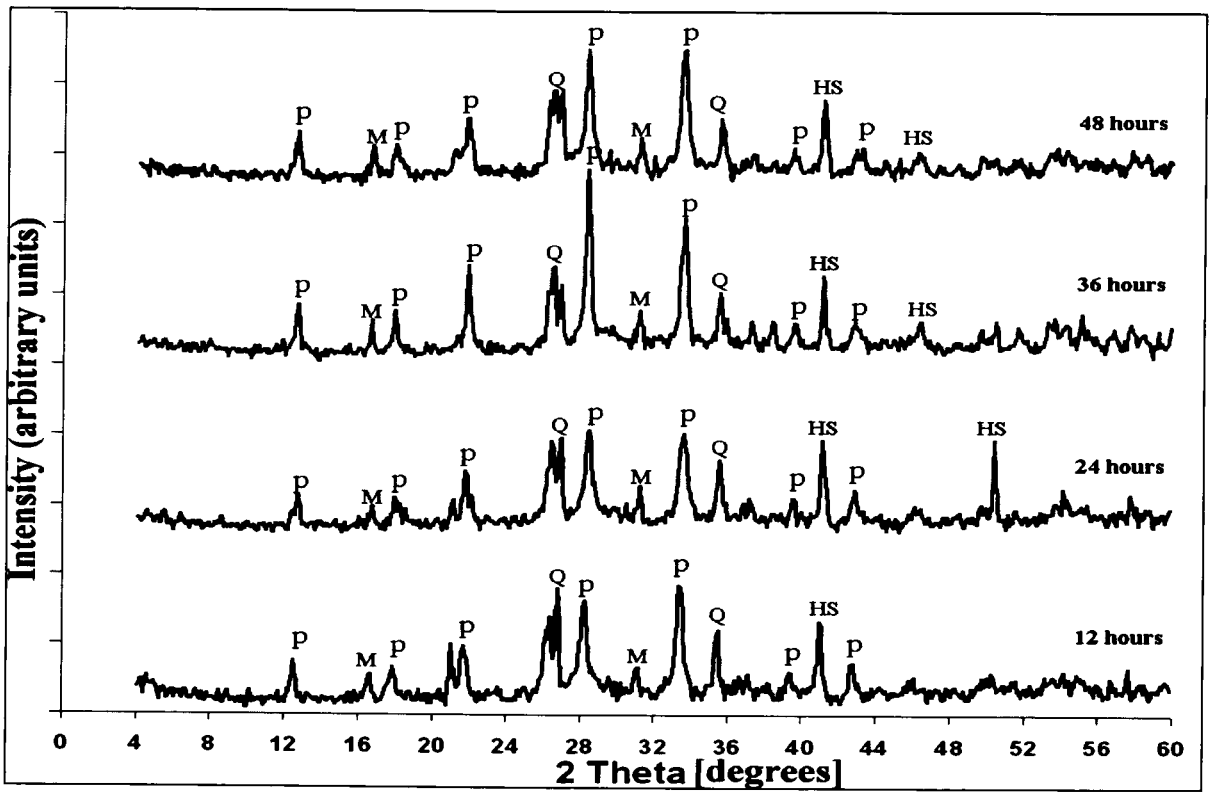

Figure 4-3: XRD patterns of products synthesized at 120 °C with variation of time (P = Zeolite Na-P1, Q = Quartz, M = Mullite, HS = Hydroxy-sodalite).

Similar observations as had been observed in section 4.2.3.1.1 were also made when the hydrothermal synthesis temperature was set at 120 °C. Time variation did not seem to influence the quality of the zeolites produced. A new zeolite phase (Hydroxy-sodalite) was formed but since this was not the targeted zeolite, it prompted trials at the next level of hydrothermal treatment temperature (140 °C).

iii. Synthesis at 140 °C with variation of hydrothermal time

The results of XRD spectra of product obtained at the elevated hydrothermal synthesis temperature of 140 °C are presented in Figure 4.4 (see Section 3.1.2.2 for experimental details).

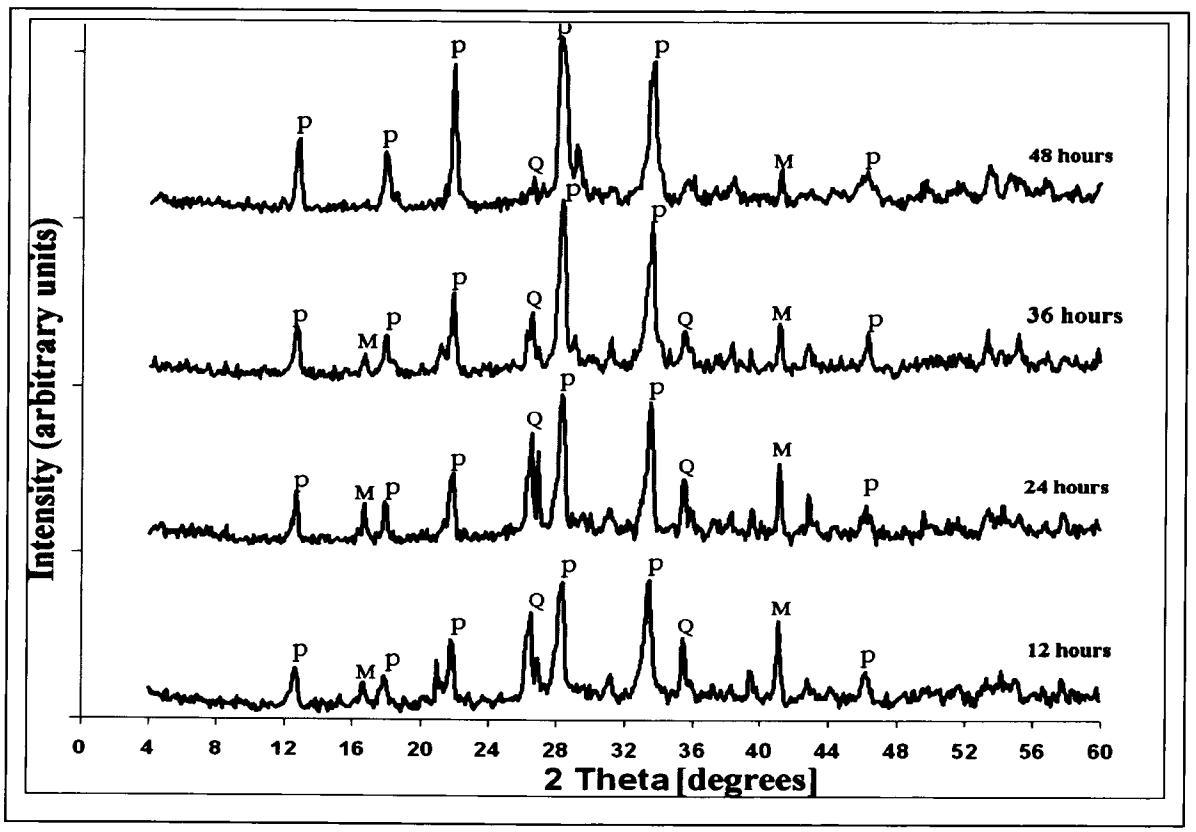

Figure 4-4: XRD patterns of products synthesized at 140 °C with variation of time (P = Zeolite Na-P1, Q = Quartz, M = Mullite).

As shown in Figure 4.4, there was almost a total consumption of quartz and mullite phases at this higher applied temperature meaning that they were progressively available as feedstock for the zeolitisation process. Hematite peaks were not identified meaning that it had been completely digested during the dissolution process. Zeolite Na-P1 in nearly pure phase was formed when hydrothermal treatment was prolonged from 12 hours to 48 hours. This can be observed from the progressive increase in the intensity of zeolite Na-P1 peaks, whilst peaks of other crystalline phases were minimized over the time of the experiment.

Calculation of relative percentage crystallinity was done by summing and normalising the peak heights of five major peaks (around degrees 2 θ = 12, 23, 28, 33 and 46). The normalised peaks of zeolite Na-P1 synthesized at 140 °C for 48 hours was assumed to be 100 % crystalline for the purpose of comparing with spectra of the zeolites synthesized at 12, 24 and 36 hours. The reason for basing the comparison on the major peaks was because they are least affected by the degree of hydration hence minimal interference is expected.

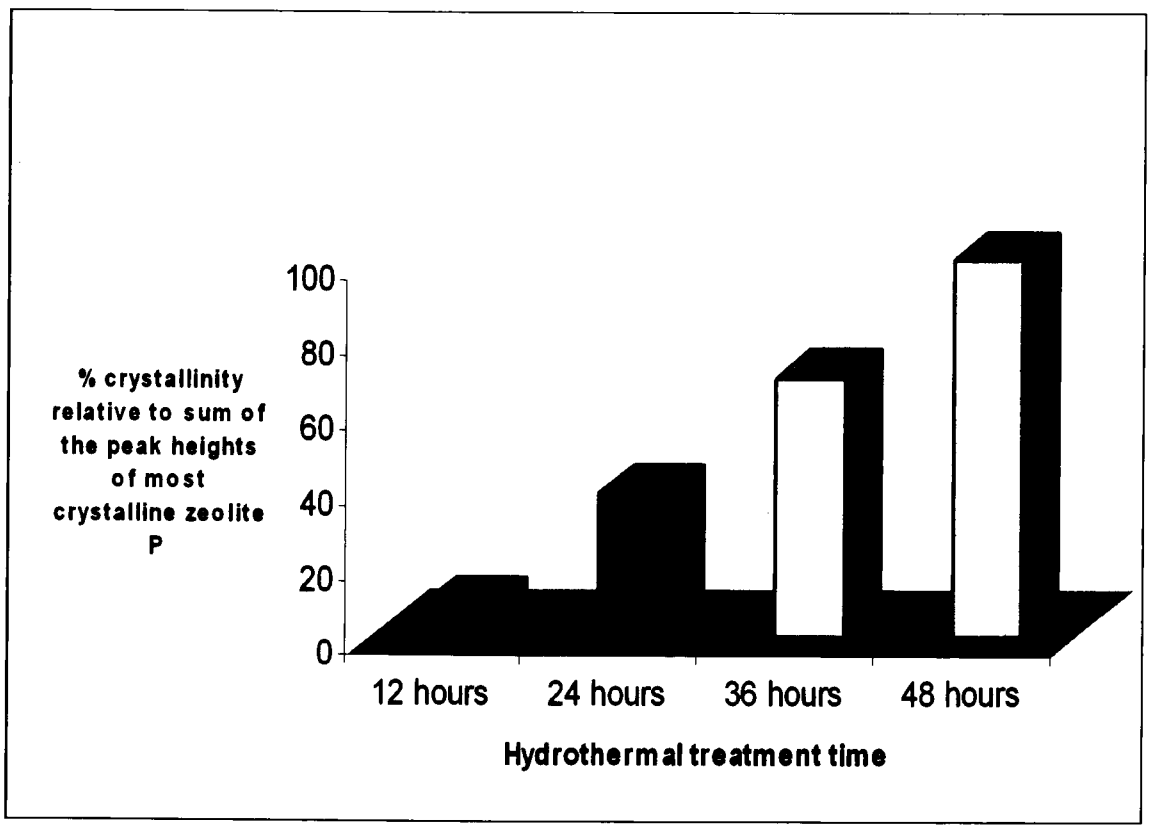

Figure 4-5: Relative % crystallinity for zeolite Na-P1 synthesized at 140 °C by varying hydrothermal synthesis time.

As shown in Figure 4.5, percentage crystallinity was directly proportional to the increase in the hydrothermal treatment time.

iv. Synthesis at 160 °C with variation of hydrothermal time

The almost pure phase zeolite Na-P1 obtained in previous section (4.1.4.1 part iii) prompted investigations at a hydrothermal treatment temperature of 160 °C which is shown in Figure 4.6 (see Section 3.1.2.2 for experimental details).

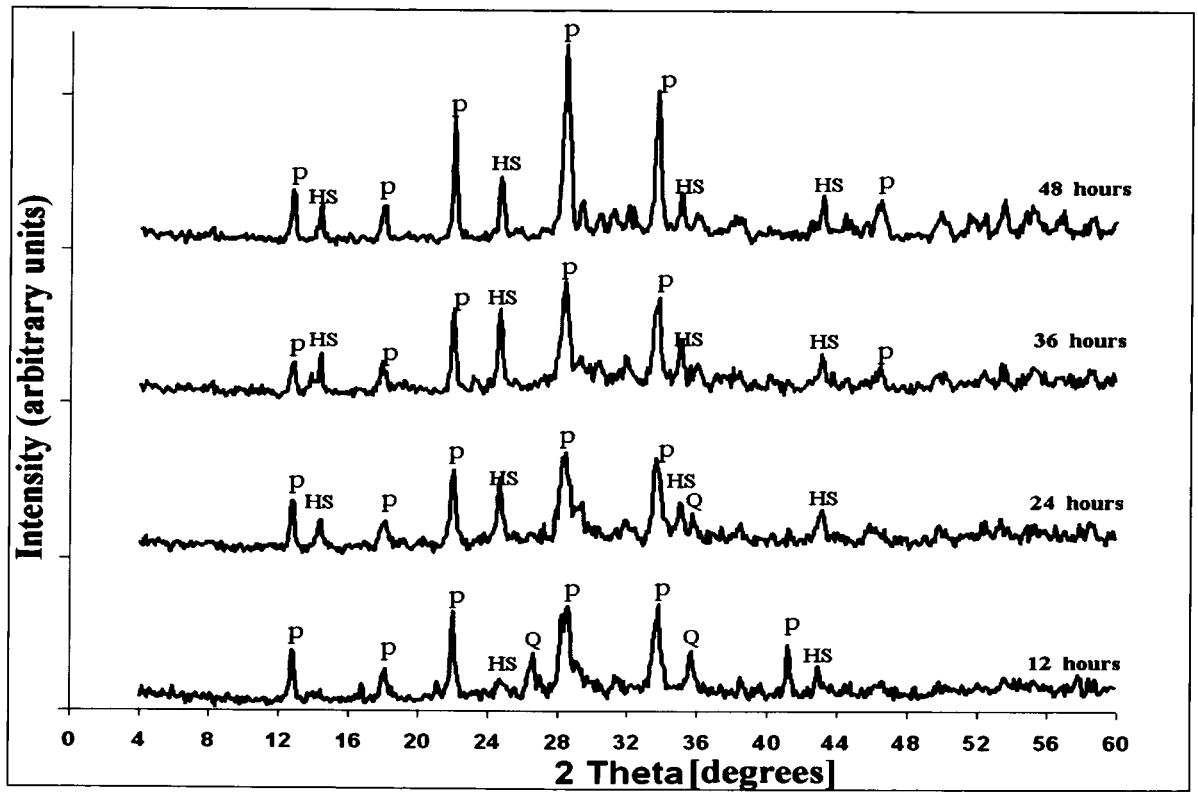

Figure 4-6: XRD patterns of products synthesized at 160 °C with variation of time (P = Zeolite Na-P1, Q = Quartz, HS = Hydroxy-sodalite).

When synthesis was performed at 160 °C, it was noticed that quartz and mullite were completely digested as time progressed but it was also evident from XRD spectra (Figure 4.4) that an impure phase namely Hydroxy-sodalite was formed simultaneously as the synthesis time was extended. Studies by Singer and Berkgaut (1995) also pointed out that zeolite Na-P1 would be the first zeolite to form but found that it can be gradually be replaced by Hydroxy-sodalite with increasing reaction time and temperature. In this case, the formation of the Hydroxy-sodalite phase was not desired since the target was pure phase zeolite Na-P1.

To conclude the study of variation of hydrothermal treatment time and temperature, the synthesis products obtained in the experiments conducted at 160 °C were found to follow Ostwald's rule of successive phase transformation which suggests that the first phase to crystallise from solution will be the hydrothermally least stable phase but with time this phase will be followed by more stable and denser phases (Barrer, 1982), due to dehydroxylation.

In the preliminary experiments at the temperatures of 100, 140 and 160 °C, the best synthesis temperature and time was found to be at 140 °C for 48 hours even though there were still some traces of quartz and mullite in the almost pure phase. In order to achieve the most pure phase zeolites, variation of water content during the hydrothermal synthesis was studied.

4.1.4.2 Variation of water during the hydrothermal synthesis

The findings obtained whilst varying the amount of water (as described in table 3.2) used during hydrothermal synthesis (at 140 °C and 48 hours) are presented in Figure 4.7. This additional water was added after ageing since a constant amount (100 ml) had been used during the ageing process as discussed in section 3.1.2.1.

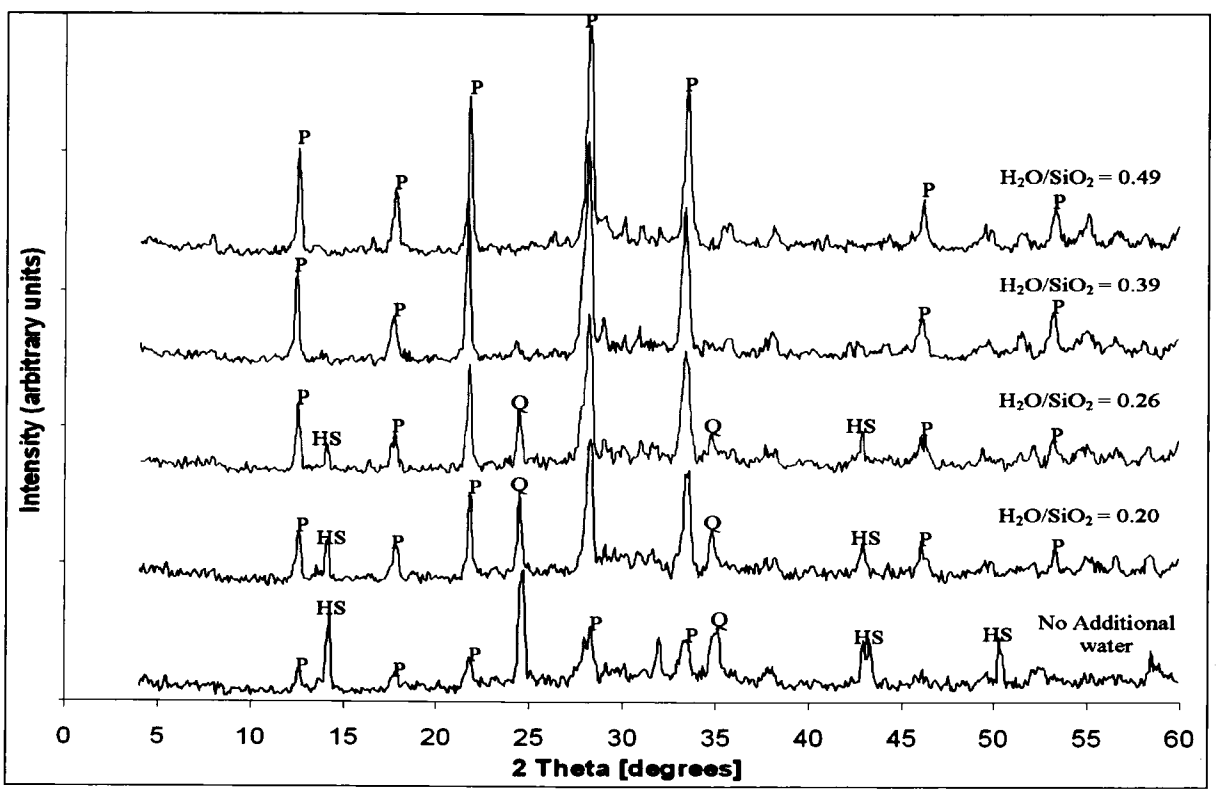

Figure 4-7: XRD patterns of products synthesized at 140 °C for 48 hours with variation of water content during the hydrothermal synthesis (P = Zeolite Na-P1, HS = Hydroxy-sodalite, Q = Quartz).

It was interesting to observe that addition of more water after ageing enabled the formation of a relatively pure phase zeolite Na-P1. This can be explained by the fact that when undergoing the

ageing process, the dissolution takes place and this leads to saturation of ionic species in the mixture which hinder further dissolution but on addition of more water it creates the conditions for further dissolution of the fly ash matrix.

Even though the highest quantity of water during the hydrothermal treatment step showed an improvement of the quality of zeolites, it is important to highlight that very high quantities of water can restrict production rate. This is because the maximum amount of liquid placed in any given hydrothermal reactor should be less than 2/3 to avoid an excess pressure build up due to phase changes of liquid into gas (Fansuri, 2008). Too much water can also change the degree of supersaturation which will slow the crystallization kinetics. In addition, the use of excessive amount of water can also increase the cost of zeolite synthesis since there is a large amount of supernatant that will require treatment before disposal.

Figure 4.8 shows that the relationship of percentage crystallinity (refer to section 4.1.4.1 part iii) of zeolite Na-P1 and quartz for products obtained from experiments in which the water content of the molar regime was adjusted in the hydrothermal stage.

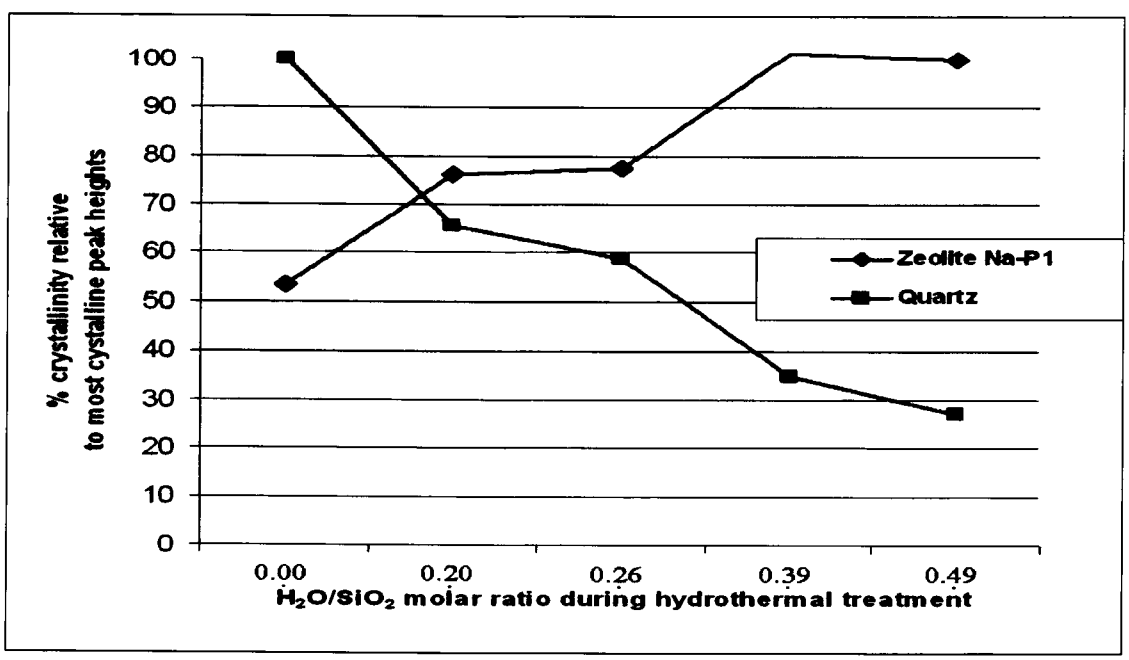

Figure 4-8: Comparison of relative % crystallinity of quartz and zeolite Na-P1 synthesized at 140 °C (48 hours) by varying H_2O/SiO_2 molar ratio during hydrothermal treatment.

The peaks of zeolite Na-P1 were found to be inversely proportional to the quartz peaks suggesting that the dissolution of quartz phase and the concomitant monomerization of Si, made it available as a feedstock in the synthesis process. Similar observations were also noted by Singer and Berkgaut (1995) who also suggested that the decrease in the intensity of quartz peaks in the XRD spectra pattern was as a result of zeolitisation.

4.1.5 Use of other fly ashes to synthesize zeolite Na-P1

Upon identification of the synthesis condition for conversion of Arnot fly ash to pure phase zeolite Na-P1, the same conditions were applied (see Section 4.1.4.2) to the fly ashes sourced from Hendrina and Duhva power stations. Initially, the fly ashes were characterised using XRF and XRD as shown in Table 4.3 and Figures 4.9 (a) and (b). The XRD quantitative comparison is presented in Figure 4.10. The XRF analysis was done in triplicate i.e. sample HF 1 – 3 and DF – 1- 3 for Hendrina and Duvha fly ash respectively.

Table 4-3: XRF analysis of Hendrina and Duhva fly ashes.

	Hendrina fly ash						**Duhva fly ash**				
Major oxides (%)	**HF-1**	**HF-2**	**HF-3**	**Mean (%)**	**Std deviation**		**DF-1**	**DF-2**	**DF-3**	**Mean (%)**	**Std deviation**
SiO_2	49.8	49.72	49.86	49.79	0.0679		55.4	54.79	54.58	54.92	0.428
Al_2O_3	31.59	31.75	31.91	31.75	0.1631		27.08	27.36	27.37	27.27	0.1646
Fe_2O_3	3.20	3.17	3.15	3.17	0.0275		4.79	4.78	4.77	4.78	0.0111
MnO	0.00	0.00	0.00	0.00	0.0011		0.05	0.05	0.05	0.05	0.0014
MgO	1.01	0.98	0.95	0.98	0.0292		1.14	0.99	1.08	1.07	0.0739
CaO	4.62	4.65	4.59	4.62	0.0332		3.72	3.67	3.67	3.69	0.0311
Na_2O	0.09	0.09	0.09	0.09	0.0004		0.05	0.09	0.07	0.07	0.02
K_2O	0.63	0.63	0.63	0.63	0.002		0.65	0.67	0.66	0.66	0.0085
P_2O_5	0.67	0.66	0.67	0.67	0.0041		0.61	0.61	0.62	0.61	0.0075
TiO_2	1.45	1.46	1.45	1.46	0.0029		0.3	0.3	0.3	0.3	0.0049
SO_3	0.24	0.23	0.23	0.23	0.0045		1.7	1.71	1.72	1.71	0.0097
Loss On Ignition	6.68	6.63	6.45	6.59	0.121		4.43	4.45	4.45	4.44	0.0115
Sum of Concentration	99.98	99.98	99.98	99.98	0.0014		99.92	99.48	99.33	99.58	0.3094
SiO_2/Al_2O_3	**1.58**	**1.57**	**1.56**	1.57	0.0073		**2.05**	**2**	**1.99**	2.01	0.0278

Trace elements (ppm)										
	HF-1	HF-2	HF-3	Mean (ppm)	Std deviation	DF-1	DF-2	DF-3	Mean (ppm)	Std deviation
Co	13	12	13	12.55	0.717	33.4	32.86	33.7	33.32	0.4281
Cu	53	51	50	51.03	1.5036	51.95	50.62	50.06	50.88	0.974
Nb	37	40	42	39.67	2.5883	38.39	38.44	38.79	38.54	0.2179
Ni	58	60	56	58.12	2.1554	70.38	74.39	72.11	72.29	2.0108
Pb	68	69	59	65.37	5.2994	83.64	80.48	83.72	82.61	1.848
Rb	31	30	33	31.18	1.6045	41.81	42.12	42.5	42.14	0.3456
Sr	1198	1186	1201	1194.85	8.0243	966.07	950.51	955.66	957.41	7.9268
Y	16	17	13	15.31	2.0818	77.34	76.58	76.22	76.71	0.5718
V	85	84	86	85.12	0.9857	128.66	124.82	123.18	125.55	2.813
Zn	95	92	94	93.69	1.2976	115.89	120.28	118.68	118.28	2.2197
Zr	418	425	430	424.09	6.0389	530.81	527.29	525.41	527.84	2.7412

The average SiO_2/Al_2O_3 ratio for Hendrina and Duvha were found to be 1.57 and 2.01 respectively. As mentioned earlier, in section 4.1, this ratio is very important in the achievement of the zeolite type that can be synthesized. Cr_2O_3 and B were not analysed due to experimental constraints. The lower CaO content of Duvha could result in the lower alkalinity of the solution during ageing and hydrothermal synthesis which could affect the rate or depolymerization and monomerization process (Catalfamo *et al.*, 1997).

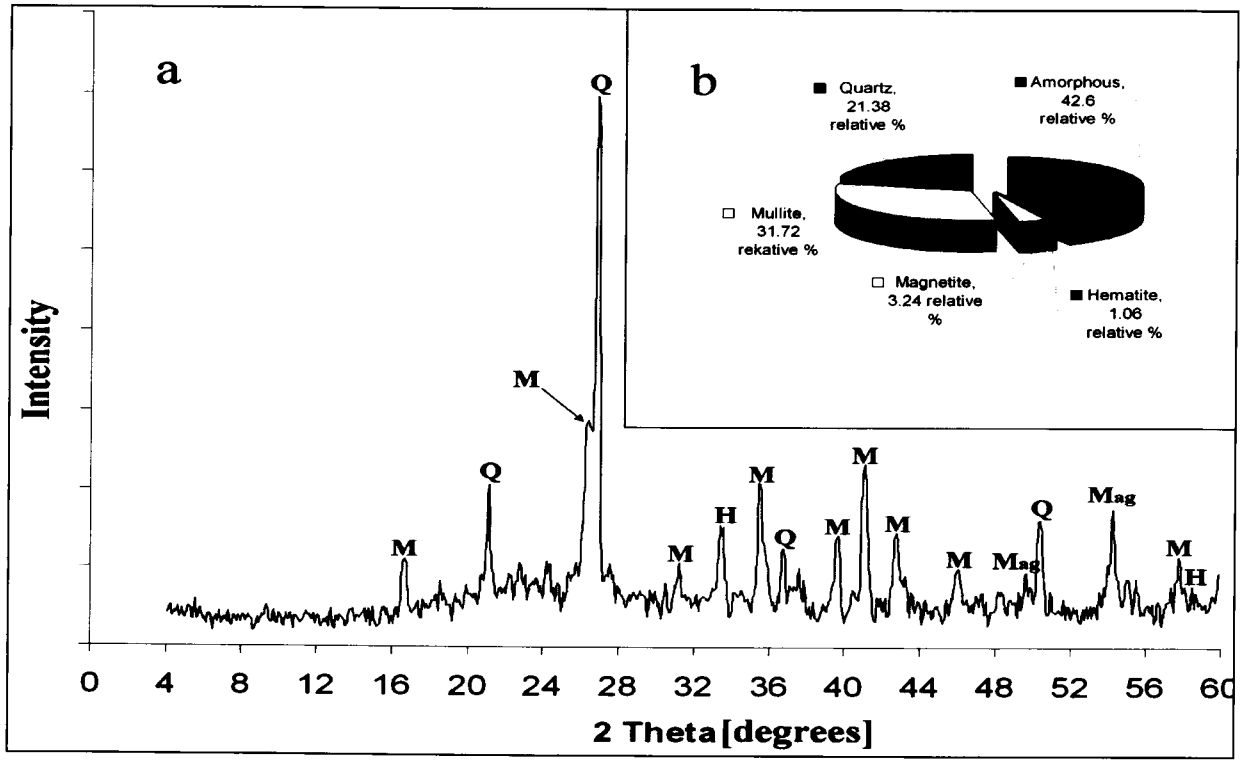

Figure 4-9: (a) XRD pattern of Hendrina fly ash (Q = Quartz, M = Mullite, H = Hematite, Mag = Magnetite).

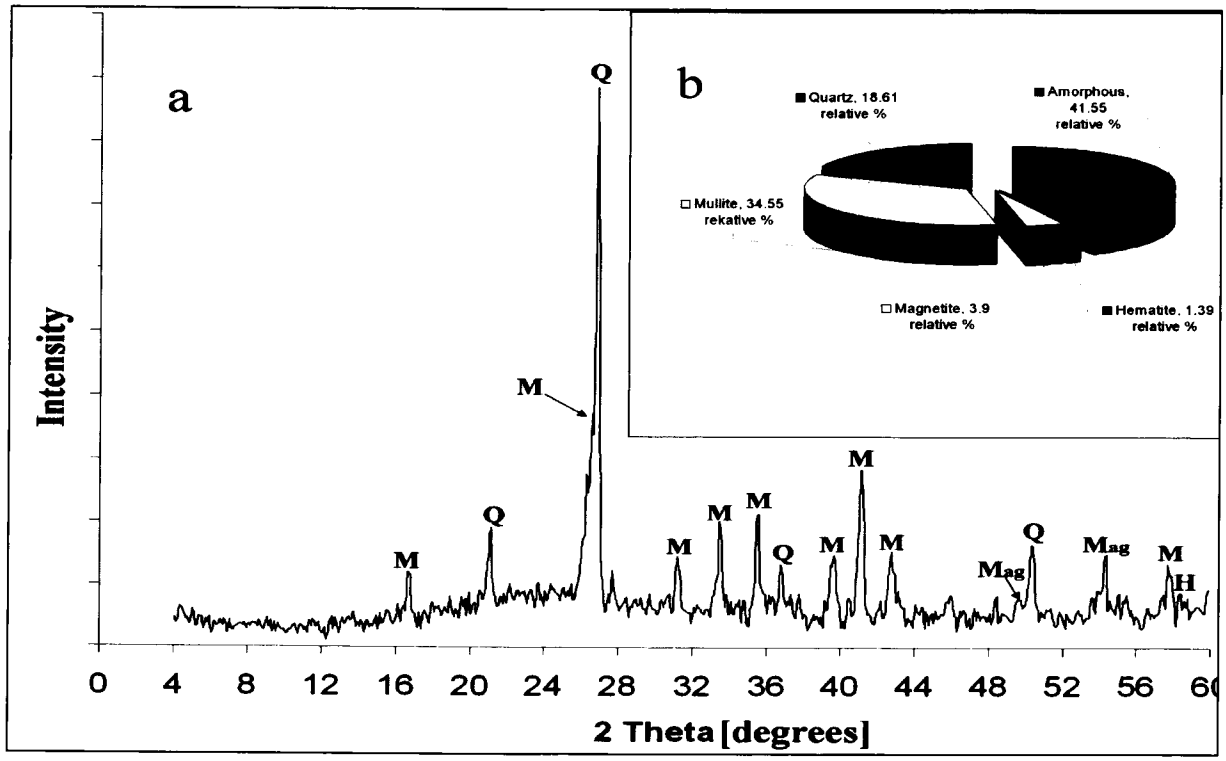

Figure 4.9 (b): XRD pattern of Duhva fly ash (Q = Quartz, M = Mullite, H = Hematite, Mag = Magnetite)

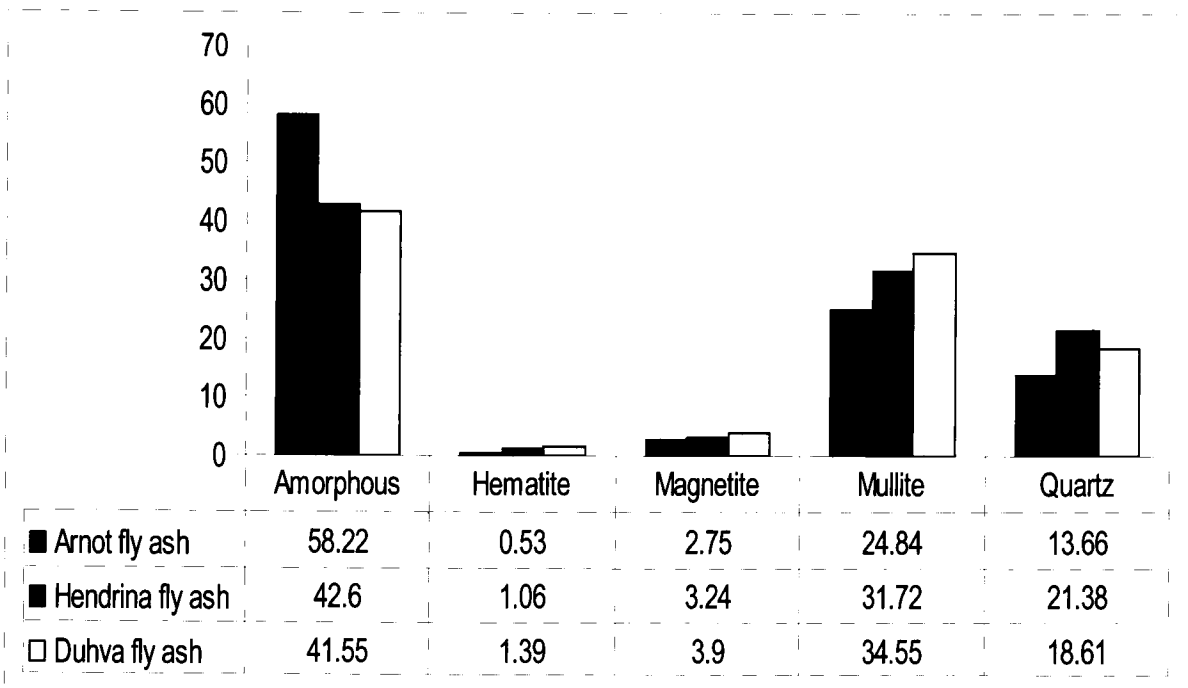

	Amorphous	Hematite	Magnetite	Mullite	Quartz
■ Arnot fly ash	58.22	0.53	2.75	24.84	13.66
■ Hendrina fly ash	42.6	1.06	3.24	31.72	21.38
□ Duhva fly ash	41.55	1.39	3.9	34.55	18.61

Figure 4-10: Quantitative XRD comparison of Arnot, Hendrina and Duhva fly ashes.

From the quantitative XRD spectra of Arnot (see Figure 4.10), Duvha and Hendrina, it is noticeable that Arnot fly ash has a higher content of the amorphous phase and has the lowest quantity of quartz, mullite hematite, and magnetite phases. Low levels of the mullite phase have been found to encourage zeolite synthesis (Rayalu *et al.*, 2001) and this is attributed to the fact that mullite is resistant to dissolution during direct hydrothermal treatment. The quantities of hematite and magnetite were not significantly different from the three fly ashes though it can still be noted that Arnot fly ash had the lowest content. The presence of the above phases makes all these fly ash sources potential candidates for synthesis of zeolite Na-P1.

4.1.5.1 Mineralogy of product synthesized from Duvha and Hendrina fly ashes

Figure 4.11 presents the comparison of the XRD spectra of zeolite Na-P1 synthesized from Arnot, Hendrina and Duhva fly ashes. The conditions for synthesis were held constant to those identified during optimisation of synthesis conditions from Arnot fly ash.

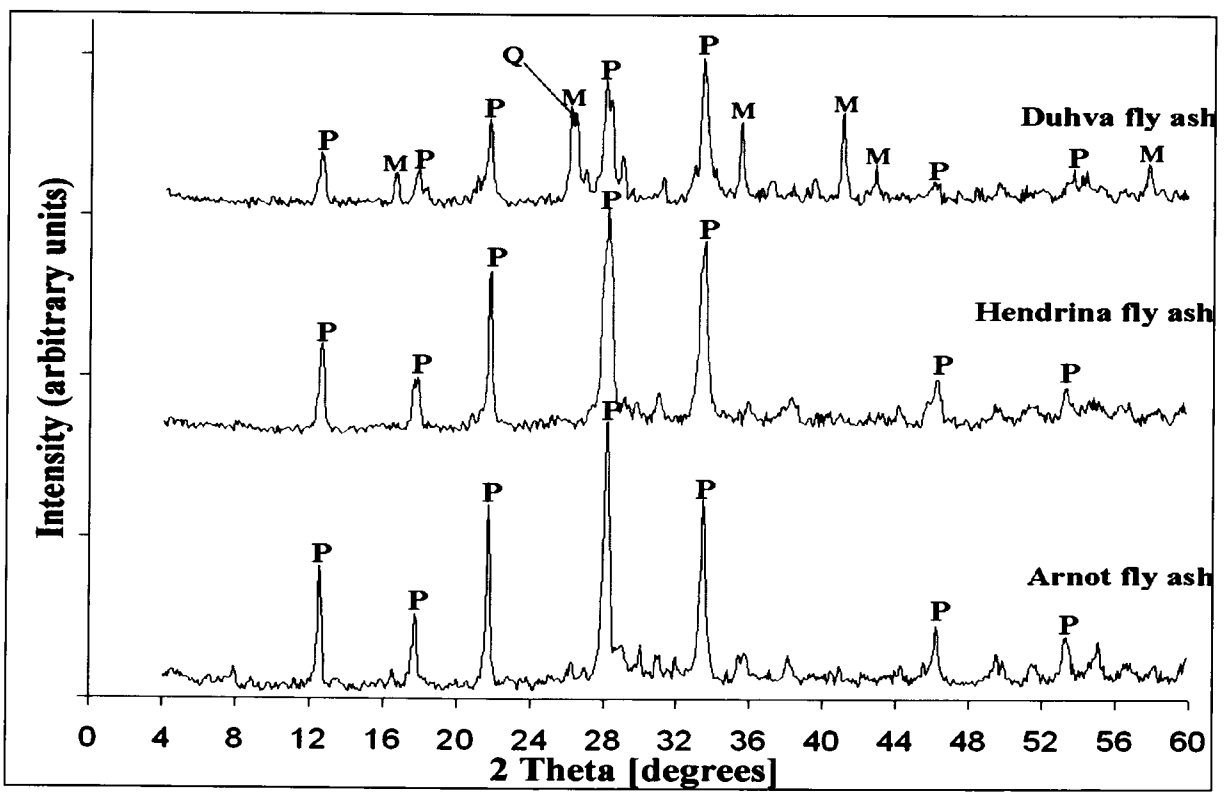

Figure 4-11: XRD patterns of products synthesized at 140 °C for 48 hours using Arnot, Hendrina and Duvha fly ashes (P = Zeolite Na-P1, M = Mullite, Q = Quartz).

The spectra in Figure 4.11 above clearly shows that there was not much difference in the zeolite Na-P1 obtained when Hendrina fly ash was used under the same synthesis conditions as were applied for the Arnot fly ash. The Duvha fly ash however, showed incomplete dissolution of feedstock quartz and mullite phases which was expected due to the difference in the chemical and mineralogical composition as noticed from the XRF and XRD results.

The failure to obtain pure phase zeolite Na-P1 using Duhva fly ash was a good indication that the conditions applied were not sufficient to guarantee full dissolution of quartz and mullite. In this case, it is important to note that a separate investigation is needed to identify the best synthesis conditions for this fly ash source, which fell outside the scope of this study. The pure phase zeolite was not formed in this case and may be due to the lower alkalinity of the solution as a result of the lower CaO content of Duvha fly ash or the ageing time and temperature may not be adjusted yet to allow high solubilisation of silica and aluminium components from fly ash. Moreover, the hydrothermal treatment time and temperature may not have been high enough to initiate and sustain the crystallization of the zeolite Na-P1.

4.1.5.2 Elemental analysis of product from Hendrina and Duhva fly ashes

In the attempt to understand the chemical composition of the synthesized zeolites prepared as a set out in section 4.1.5, Table 4.4 presents the results of the elemental content (as major oxide) for zeolites synthesized from Duhva and Hendrina fly ashes.

Table 4-4: Elemental composition of zeolite Na-P1 from Duhva and Hendrina fly ashes (XRF).

Major oxide %	Duhva fly ash	Hendrina fly ash
SiO_2	33.946	35.161
Al_2O_3	31.814	22.565
Na_2O	5.491	9.173
CaO	3.651	4.358
Fe_2O_3	2.284	1.777
TiO_2	1.949	1.244
MgO	1.121	1.481
MnO	0.04	0.04
K_2O	0.141	0.125
P_2O_5	0.043	0.059
SO_3	0.026	0.062
Cr_2O_3	0.035	0.034
NiO	0.02	0.029
H_2O^-	7.652	8.188
LOI	10.994	13.909
Total	99.207	98.203

The SiO_2/Al_2O_3 ratio for zeolitic products synthesized from Duvha and Hendrina were found to be 1.07 and 1.56 respectively. Comparing the SiO_2/Al_2O_3 ratio of the starting Duhva fly ash with the corresponding zeolitic product, the ratio was too low indicating that there was much wastage as it can be reflected in the analysis of the supernatant (see table 4.5). The corresponding SiO_2/Al_2O_3 ratio of the Hendrina fly ash was almost similar to the zeolitic product meaning that there was proper utilisation of the feedstock during the synthesis process. The Si/Al ratio difference in zeolite samples affects the brönsted acid sites (exchangeable cation sites) hence influencing the cation exchange capacity of the final synthesis product.

The synthesis of zeolite Na-P1 from Hendrina fly ash showed a far much higher uptake of the Na^+, Ca^{2+}, and Mg^{2+} than Duvha fly ash. These cations act as a charge balancing cation and can also reflect the degree of crystallisation of the zeolitic product which in this case can correlate well with the XRD spectra in Figure 4.11. It is noted that the zeolitic material still contained

some elements that were originally in the fly ash even though the Cr_2O_3, B, and other trace elements were not analysed due to experimental constraints. The presence of Ti, Fe, Cr and Ni in the synthesis product may imply that they were isomorphously substituted for Al in the zeolitic framework or probably adsorbed or precipitated as hydroxides.

4.1.5.3 Elemental analysis of post synthesis supernatant

Results of the post synthesis supernatant of the products prepared using the three fly ashes as detailed in Sections 3.1.2 and 4.1.5 is presented in Table 4.5

Table 4-5: Elemental composition of post synthesis supernatant for zeolites synthesized with different fly ash feedstock sources.

Concentration in ppm			
Element	**Arnot**	**Duhva**	**Hendrina**
Si	341.10	612.13	219.50
Al	100.78	98.46	94.74
P	98.25	174.05	131.70
K	21.57	23.88	23.33
V	8.34	6.53	8.95
B	4.92	2.41	3.38
Fe	2.09	5.55	1.55
Concentration in ppb			
Element	**Arnot**	**Duhva**	**Hendrina**
Pb	898.45	1564.50	957.25
As	767.00	1254.50	910.25
Zn	369.55	461.55	843.95
Mo	359.25	547.25	422.60
Se	143.65	107.90	108.05
Ca	131.21	123.86	148.60
Cr	113.52	90.33	239.65
Sr	108.20	133.25	129.45
Ba	85.19	190.80	318.45
Mn	65.15	99.62	53.15
Cu	50.85	63.98	69.65
Be	11.31	8.81	36.66
Cd	1.23	1.05	3.25
Co	0.99	1.71	2.36
Ni	0.97	0.03	1.87

Analysis of fly ash and zeolite products had earlier shown that during the zeolitization process, charge balancing cations contained in the fly ash, such as Mg, Ca, Na and K, were incorporated in the zeolite, as was expected. However, the fate of the heavy metals in fly ash is of major importance. It was deemed necessary to establish whether the zeolite product adsorbed these elements or whether they were released as waste during the zeolitization process. The results in Table 4.5 show that not all Ca and K present in the feedstock solution was taken up into the zeolite product since their presence was detected in the waste post synthesis supernatant. It seemed that the Na supplied had mostly been taken up in the zeolite product implying that it is the main exchangeable and charge balancing cation hosted on the zeolite framework, as is expected for these materials.

Some residual Si and Al from the fly ash feedstock that had not participated in the formation of the zeolite product was also detected in the filtrate, showing some wastage of the Si and Al feedstock materials; meaning that the process was not fully optimized yet to give a good yield on the Si and Al feedstock utilization. Somewhat different levels of trace elements were released depending upon the ash source used. It was found that trace metals such as V, Fe, B, Pb, As, Zn, Mo, Se, Cr, Sr and Ba were to a large extent extracted from the fly ash during the zeolitization process and reported to the waste effluent and were not taken up in the zeolite product during formation. This would imply that the waste effluent after synthesis could be a source for some of these elements to be extracted and recovered, or that its disposal could be problematic unless these elements were removed, prior to disposal of the supernatant.

4.1.5.4 Replicability of synthesis of zeolite Na-P1

For the purposes of demonstrating the replicability of the experimental methodology, replication of the synthesis procedure for the most pure phase zeolite Na-P1 was performed and the XRD spectra of the replicate products of zeolite Na-P1 from Arnot, Duvha and Hendrina fly ashes are compared as presented in Figure 4.12.

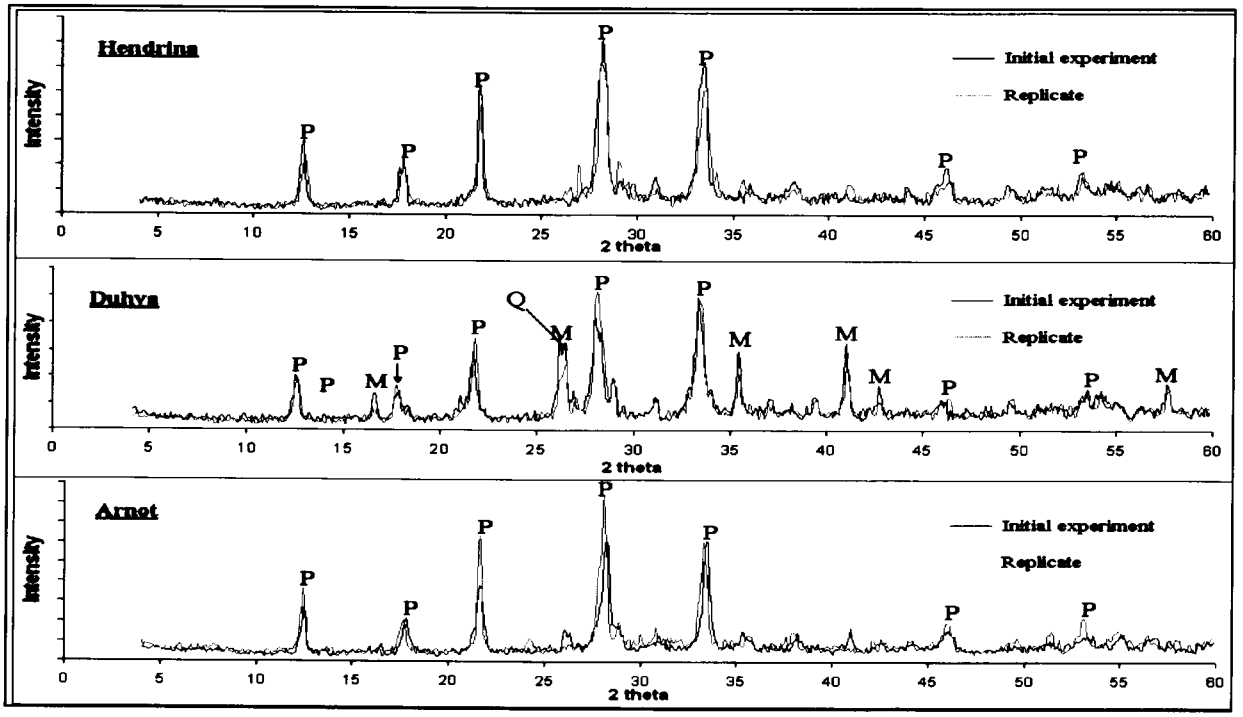

Figure 4-12: XRD patterns to show replicability of synthesis of zeolite Na-P1 (P = Zeolite Na-P1, M = Mullite, Q = Quartz).

A slight increase of crystallinity was observed in the case of zeolite Na-P1 from Arnot fly ash but the other replicates were nearly identical indicating good replicability of the procedure.

4.1.6 Structural analysis of synthesized zeolite

The Fourier Transform Infra – Red Spectroscopy (FT-IR) vibration bands from the analysis of products, that were prepared according to the procedure highlighted in section 3.1.4.4, were assigned in accordance to the generally accepted practice for silicates and the zeolite family of compounds as shown in Table 4.6.

Table 4-6: Overview of mid-Infra red vibrations of zeolites (Breck, 1974; Weitkamp and Puppe, 1999).

Internal tetrahedra	Asym. stretch	1250 – 950
	Sym. stretch	720 – 650
	T-O bend	500 – 420
External tetrahedra	Double rings	650 – 500
	Pore opening	420 – 300
	Sym. stretch	750 – 820
	Asym. stretch	1150 – 1050

The spectrum for Arnot fly ash (Figure 4.13) shows the three wide bands characteristic of aluminosilicates: the band at 460 cm^{-1} was associated with T–O bending vibrations (Fernandez-Jimenez and Palomo, 2005); the bands appearing at around 704, 780 and 800 cm^{-1} were associated with T–O (T = Al, Si) symmetric stretching vibrations that correspond to quartz present in the original fly ash; the band appearing at 1053 cm^{-1} was associated with T–O (T = Al, Si) asymmetric stretching vibrations.

Colthup *et al.*, 1964, suggested that the shoulder at around 950 cm^{-1} is probably due to the presence of a glassy phase while the bands at 1135 and 700 cm^{-1} are likely to be from the asymmetrical stretching vibration and symmetrical vibration of the Al–O–Si groups, respectively. The bands found at 700 cm^{-1} are likely to be from mullite (Farmer, 1988). Fernandez-Jimenez and Palomo (2005) also reported that those bands at around 550 and 560 cm^{-1} which are identifiable in Figure 4.13 are associated with octahedral aluminium present in the mullite phase. Silicate bands are found to be broad and diffuse because of

the overlapping of different types of silicate molecular vibration resulting from various silicate minerals (Mollah *et al.*, 1999).

The vibrations common to all zeolites are the asymmetric stretching modes, which appear in the region 950–1250 cm^{-1}. The FT-IR spectra of the alkaline activated fly ash products (zeolites) show interesting differences when compared with the spectrum of fly ash. Coincident with the progressive transformation of fly ash, characteristic zeolite bands appeared on the spectra. The bands in the region of 400–420 cm^{-1} are related to the pore opening or motion of the tetrahedral rings, which form the pore opening of zeolites. The bands in the region of 420–500 cm^{-1} are attributed to internal tetrahedron vibrations of Si–O and Al–O of the zeolitic materials (Ríos *et al.*, 2008).

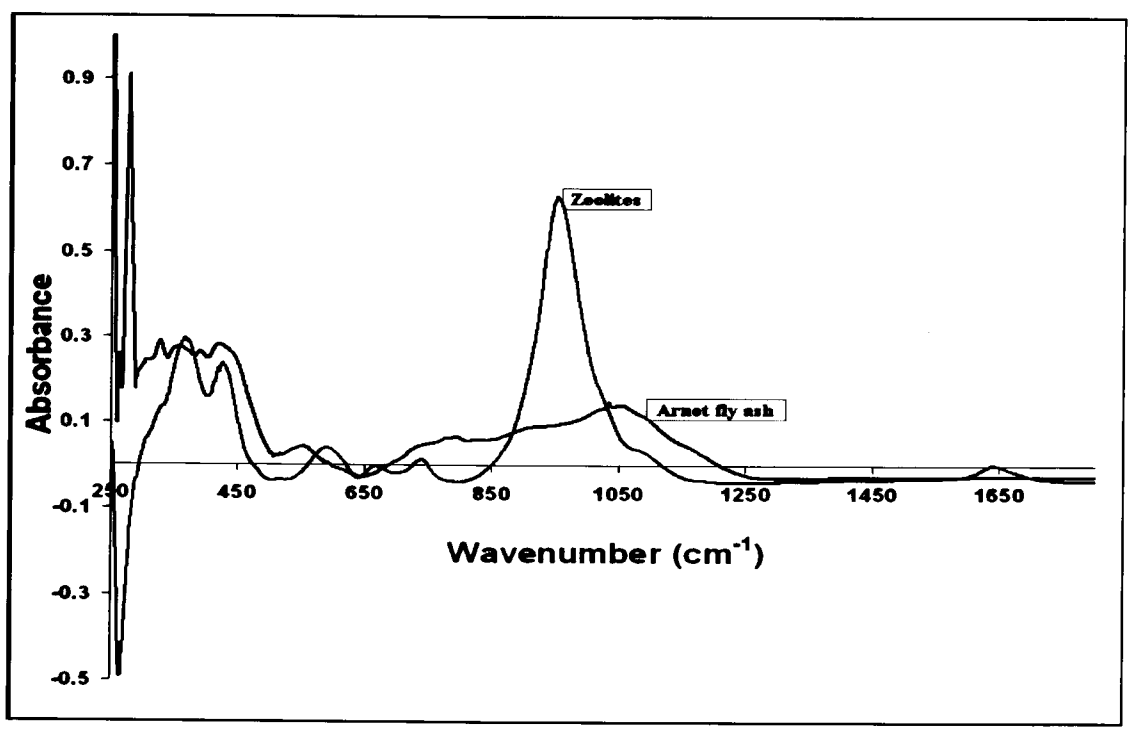

Figure 4-13: Comparison of Arnot fly ash and the corresponding zeolite (prepared in section 4.1.4.2) by FT-IR.

When zeolites were synthesized at 140 °C by varying hydrothermal time, the T-O band associated with stretching vibrations shifts (in zeolites) are in ranges that can be

perceived and these shifts are shown to depend on the reaction time (Figure 4.14). For example, the band at around 1053 cm^{-1} of the original fly ash becomes sharper and shifts towards lower frequencies in the zeolite sample. It was also found that there was more displacement and the peak at 1053 cm^{-1} is the sharpest when treated for 48 hours indicating that the vitreous component of the fly ash is reacting with the alkaline activator (NaOH) to form zeolites. This observation is in agreement with the XRD results. The water molecules attached to the zeolite framework causes characteristic structure-sensitive bands due to water bending vibrations at 1630 cm^{-1}.

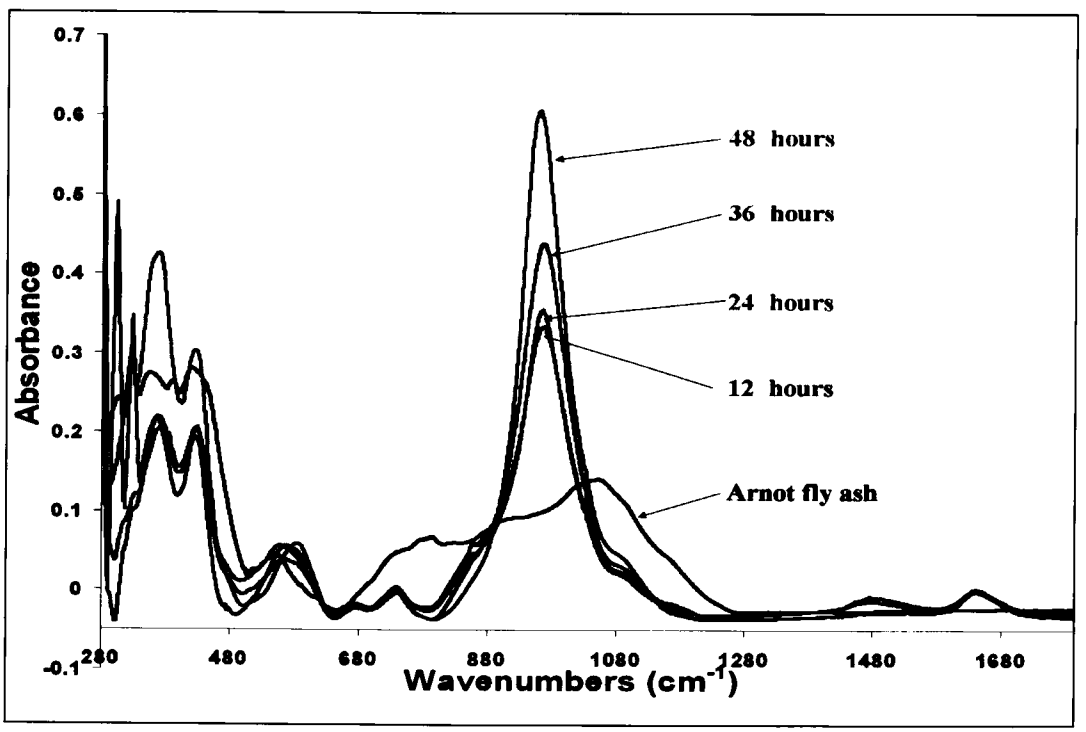

Figure 4-14: FT-IR spectra of zeolites synthesized at 140 °C by varying time of hydrothermal treatment.

It is important to point out that the joint presence of T-O vibrations (T = Al , Si) of both the fly ash and the crystalline zeolites synthesized yields overlapping spectral bands that make interpretation difficult. This can be attributed to the fact that the unreacted fly ash (having both crystalline and vitreous phases) and the reaction products (zeolites) are all constituted of SiO_4 and AlO_4 (Fernandez-Jimenez and Palomo, 2005) and the only

difference is their degree of structural order. The vibrations associated with the amorphous material in the raw fly ash samples have wide and imprecise bands which makes it hard to derive their full structural information. However the structural bands of zeolites in this region can clearly be distinguished in region 300 – 420 cm^{-1}.

4.1.7 Morphological transformation during the synthesis process

4.1.7.1 Scanning electron microscopy analysis

Figure 4.15 shows the scanning electron miscroscope (SEM) images of the Arnot fly ash matrix, the fly ash after ageing process and the synthesized zeolite that was made according to procedure set out in Section 3.1.2. The SEM image of the surface of the Arnot fly ash particle was observed to be smooth and spherical because the glass phase covers the particle (Inada *et al.*, 2005). The morphology of fly ash grains is determined by the heating and cooling regimes in the pulverised coal boiler. Micro spheres, typically between 30 and 100 μm in diameter, can be described as hollow cenosphere or non crystalline glass beads (Shao *et al.*, 1997).

The physical characteristics of combustion residues of coal including particle size, particle shape or morphology, hardness and density are a function of the particle size of feed coal, type of combustion and the particulate control device (Vories and Throgmorton, 2002). The image of the fly ash particle after ageing process shows that there was partial dissolution of the particles indicating that the ageing period was not sufficient to bring the fly ash matrix in to solution. After the hydrothermal treatment, the granular crystalline products could be observed and from the XRD analysis, it was identified to be Zeolite Na-P1.

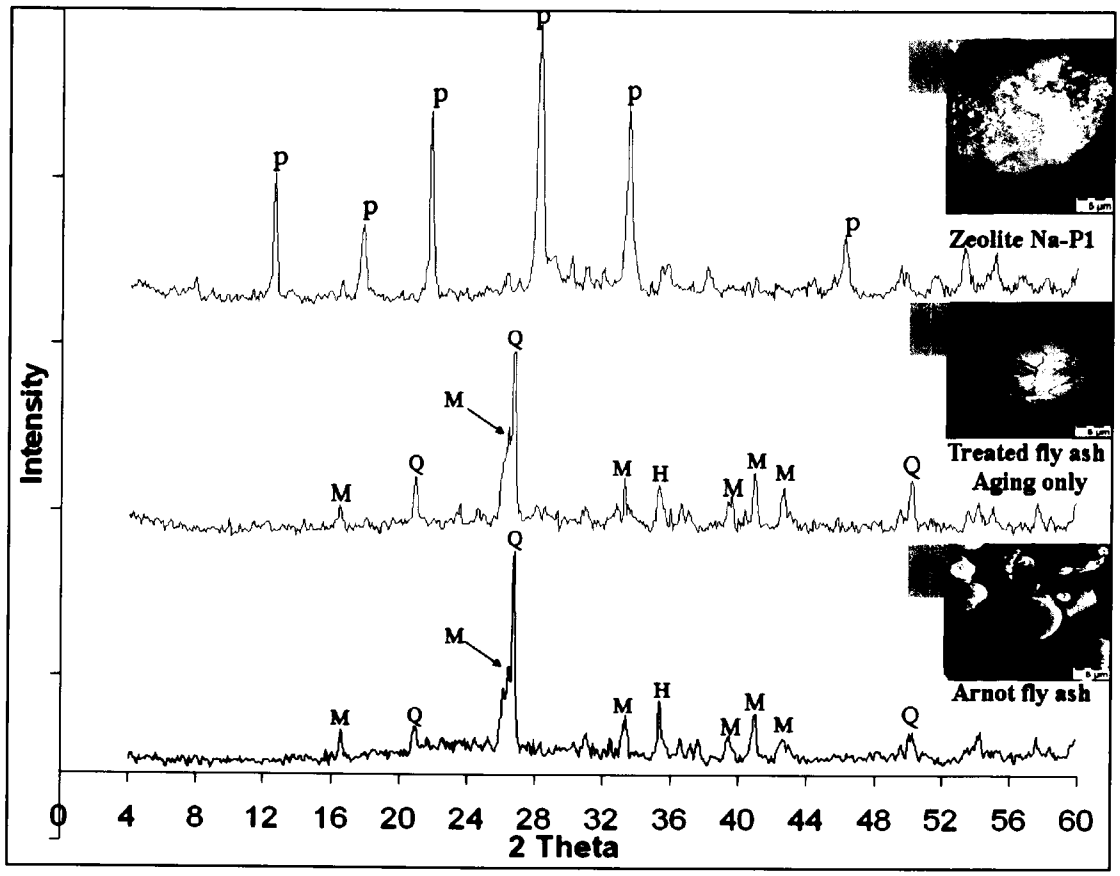

Figure 4-15: XRD patterns and SEM images correlation of raw Arnot fly ash, treated fly ash (after ageing) and synthesized zeolite (as at 140°C for 48 hours with H_2O/SiO_2 ratios as 0.49).

The formation mechanism of zeolites from fly ash has been proposed to be as follows: Dissolution of the SiO_2 and Al_2O_3, especially from the glassy phase, in alkaline solution, formation of aluminosilicate gel as zeolite precursor and crystallization of zeolite during supersaturated conditions (Murayama *et al.,* 2002). Many studies (Walek *et al.*, 2008) have reported that the hydrothermal crystallization process mainly begins on the surface of the undissolved or partially dissolved fly ash particle and this has been found to restrict access of hydroxyl ions that would have enhanced the dissolution of Si and Al from the fly ash phases. Studies by Chun-Feng *et al* (2008) have also reported that the dissolution of the Si from fly ash is higher than that of Al since the content of armophous SiO_2 in the fly ash is higher than that of amorphous Al_2O_3, this implies that zeolitisation of zeolites

on the surface of fly ash hinders the amount of Al that may be dissolved from fly ash. A schematic illustration of formation of zeolite from fly ash is presented in Figure 4.16 by the use of SEM images.

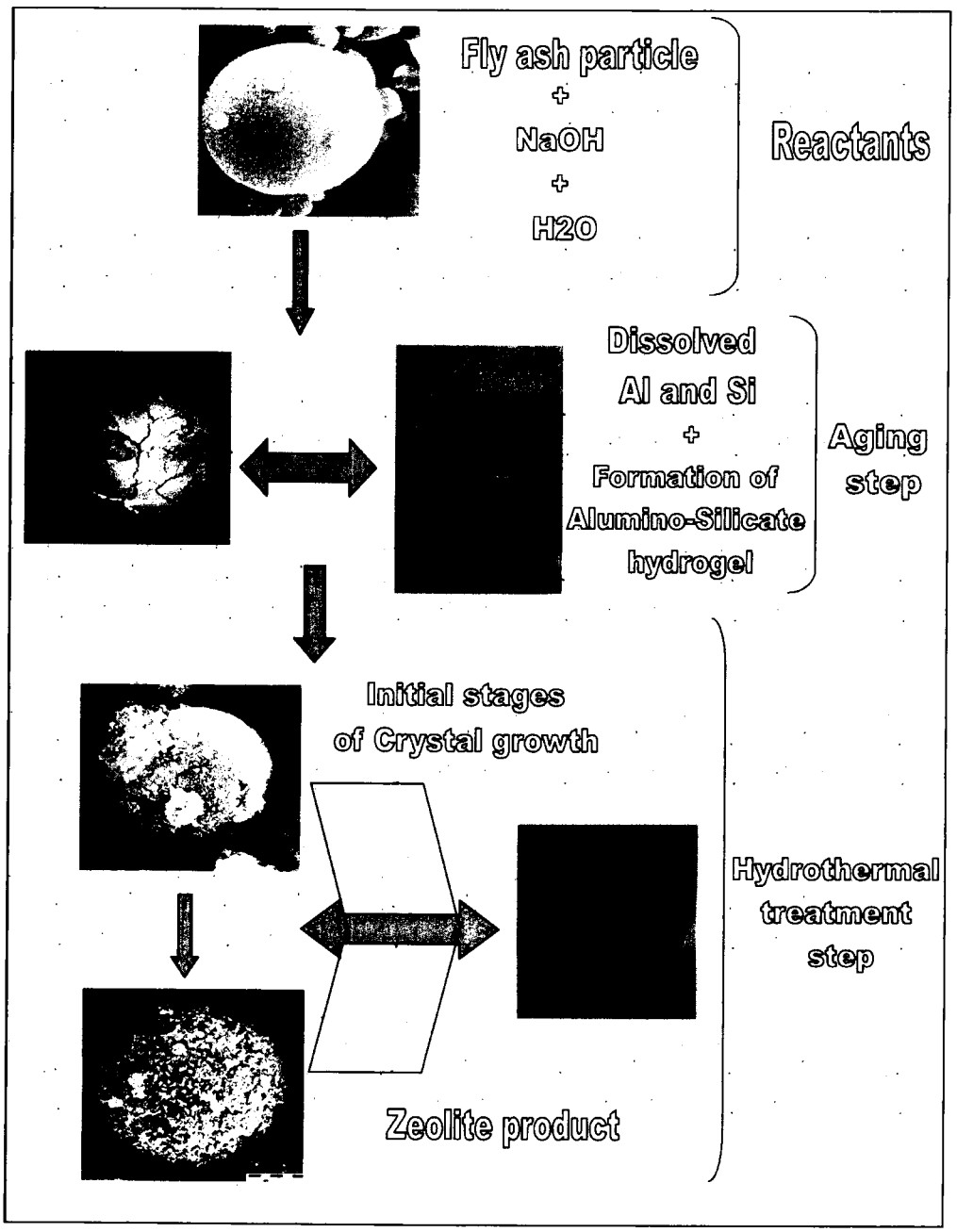

Figure 4-16: An illustration of reaction mechanism for formation of zeolite by use of SEM images.

Figure 4.17 shows the crystallinity of zeolite Na-P1 product when the water content during the hydrothermal synthesis step was varied. This correlates well with the results of XRD analysis discussed in section 4.1.4.2.

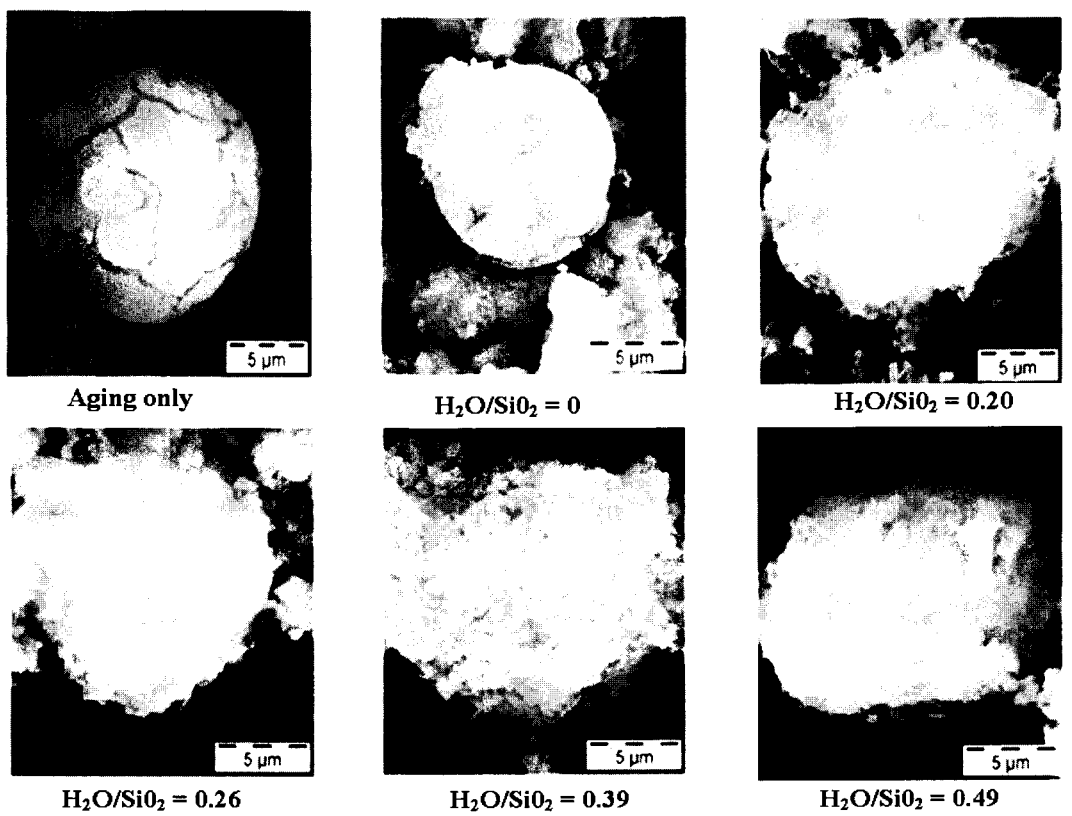

Figure 4-17: SEM images showing the products obtained with variation of water content during the hydrothermal treatment process.

The progressively increasing crystallinity over addition of water during the hydrothermal treatment can be reflected in agglomeration of crystals (Figure 4.17) which were individually lathe shaped as shown by the HRTEM in the next section.

4.1.7.2 High resolution transmission emission microscopy analysis

The formation of the porous well structured crystalline zeolitic material (zeolite Na-P1) formed during the hydrothermal synthesis when ageing temperature and time was 47 °C and 48 hours respectively while hydrothermal treatment temperature and time at 140 °C

and 48 hours respectively with H_2O/SiO_2 ratios of 0.49) was also confirmed by the use of High Resolution Transmission Microscopy (HRTEM) analysis as shown in Figure 4.18.

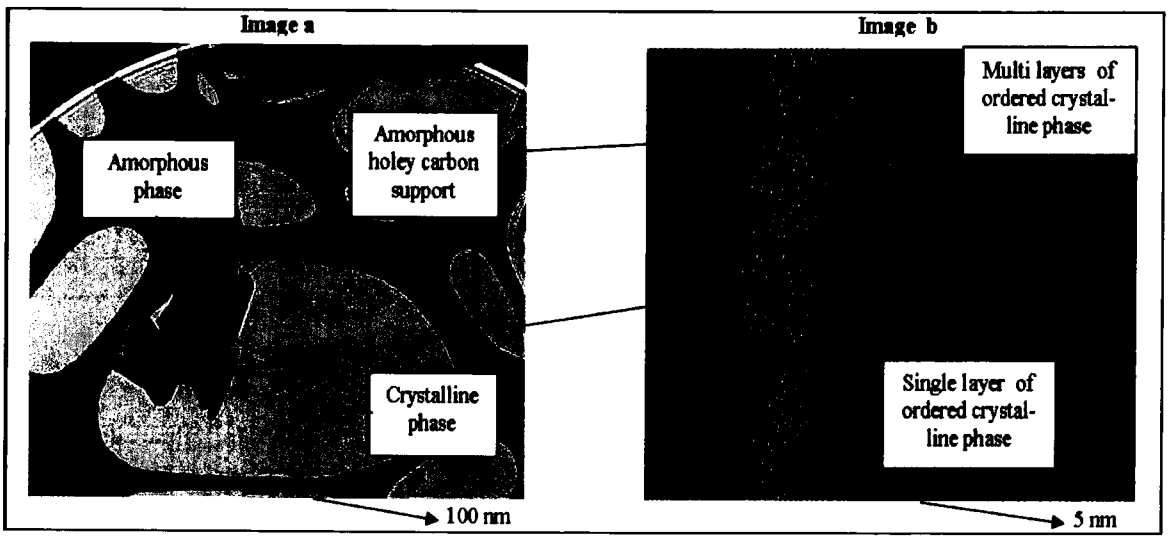

Figure 4-18: HRTEM images of the zeolitic material synthesized from Arnot fly ash.

Upon magnifying to 100 nm, the individual zeolite particles appeared lathe like (thin and long). By tilting the sample holder by 8.3 degrees, one could distinguish between the crystalline phase and areas of the product that were not crystalline because the particles that were crystalline showed some changes in diffraction contrast (the black particle in Figure 4.18 (a)). Upon further magnification (5 nm) of the particles that had showed diffraction contrast, the HRTEM study confirmed the presence of well ordered porous crystalline matrix as is shown in Figure 4.18 (b).

4.1.8 Thermal stability analysis of zeolite Na-P1 synthesized from fly ash

Thermal stability of the higher purity zeolite Na-P1 synthesized at hydrothermal treatment temperature and time of 140 °C and 48 hours respectively with H_2O/SiO_2 molar ratio of 0.49 was determined according to procedure outlined in Section 3.1.3.7. The results are presented in the sections that follow.

4.1.8.1 Temperature programmed X-ray diffraction spectroscopy

Studies conducted by Breck (1974) reported that zeolite P undergoes dehydration reactions which leads to collapse of the zeolite structure. Hence, it was important to understand the temperature ranges of the structural collapse especially of the zeolite Na-P1 synthesized from fly ash. The information gained from this study was of importance when deciding the right temperatures to do the degassing during the BET analysis. Figure 4.19 presents results obtained from temperature programmed XRD analysis from 25 °C to 600 °C.

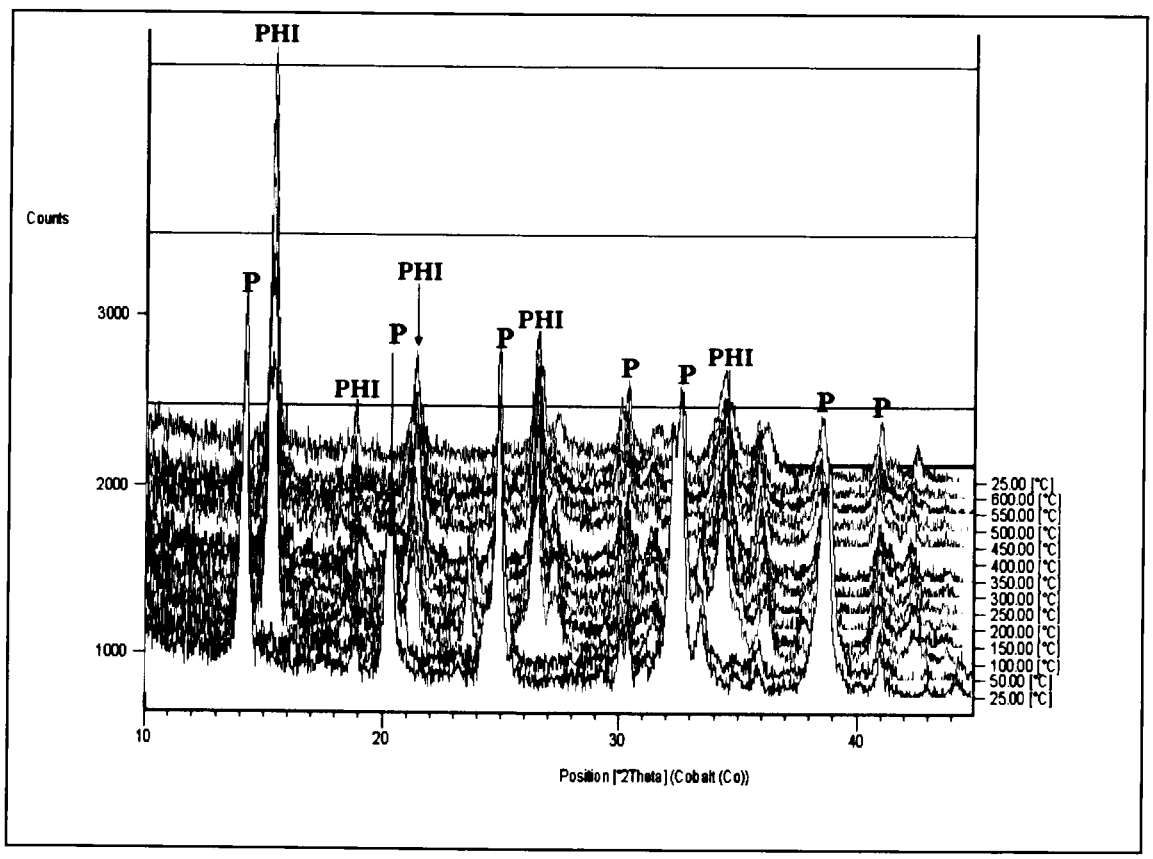

Figure 4-19: Temperature step change XRD spectra of zeolite Na-P1 (P = Zeolite Na-P1, PHI = Zeolite Na-PHI).

As shown in Figure 4.19, it was interesting to observe that phase transformation of zeolite Na-P1 (JCPDS file number 39 219) to a new phase, which was identified as zeolite Na-PHI (JCPDS file number 24-1046), occurred at around 100 °C. Contraction of the pore

sizes of the zeolite Na-P1 upon phase transformation is expected since the new phase peaks at low 2θ are shifted to the right meaning that the zeolite Na-PHI is a small pore zeolite.

These results can also be correlated with studies reported by Breck (1974) which showed that 16 % of pure zeolite P showed structural collapse at 165 °C while the remaining part persisted but then complete recrystallization of a new phase occurred at 530 °C. The results also differ with findings reported by Nagy *et al* (1998) which gave an indication that the temperature stability range for Gismondine zeolites was between 250 °C and 400 °C.

As a verification of the phase transformation observed at 250 °C, degassing of the zeolite Na-P1 was done at 250 °C (refer to Section 3.1.3.7 for degassing conditions) and the XRD results presented in Figure 4.20 show that heating zeolite Na-P1 led to formation of another phase (zeolite Na-PHI). Almost similar observations were noted by Derkowski *et al.,* 2006 where heating of the zeolite Na-P1 lead to a phase transformation to zeolite Na-PHI. Studies by Dyer in 1988 reported that the metastable nature of zeolites implied that they can be converted from one mineral structure to another, (through Ostwald ripening) it was also suggested that in some cases, it even occurred at room temperature (Dyer, 1988). The loss of intracrystalline water, as discussed in Section 2.3.9, seems to be contributing to this structural transformation.

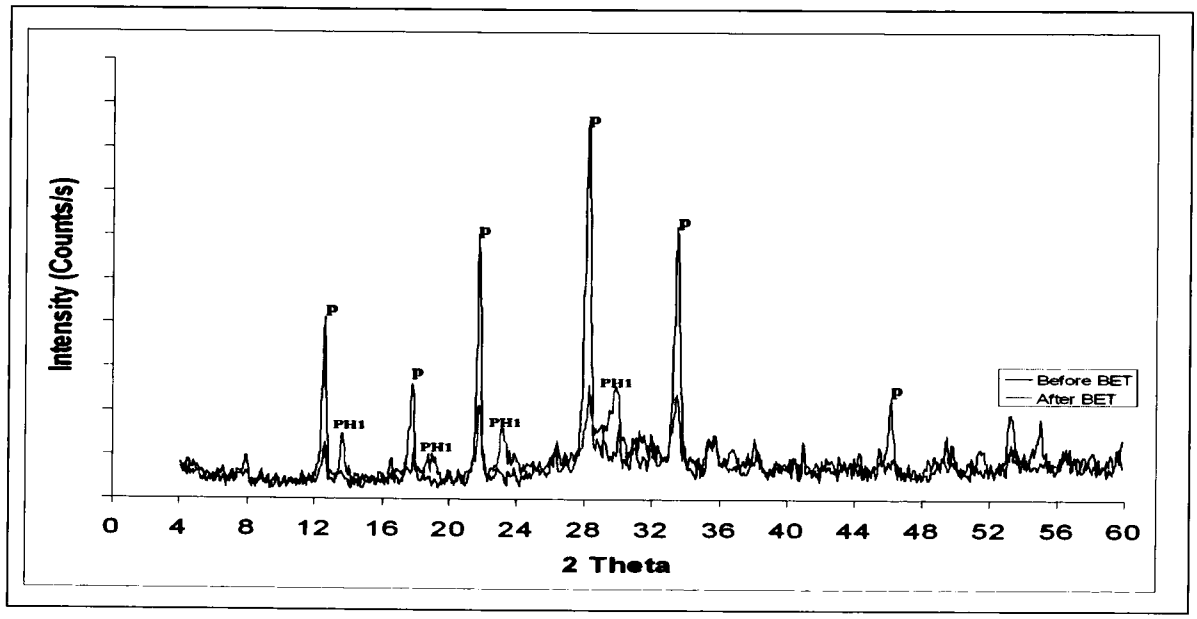

Figure 4-20: XRD patterns for zeolite samples before and after N_2-BET analysis (P = Zeolite Na-P1, PHI = Zeolite Na-PHI).

4.1.8.2 Thermogravimetric analysis

Figure 4.21 shows the temperature dependent weight loss of the zeolite Na-P1 synthesized from Arnot fly ash according to the procedure given in Section 3.1.2 in this case the conditions for synthesis of pure phase zeolite Na-P1 (ageing and hydrothermal temperature and time of 47 °C, 48 hours, 140 °C and 48 hours respectively with the water content after ageing being at SiO_2/H_2O molar ratio of 0.49) were applied.

The heating allowed the correlation of the elimination of adsorded and enclatherated water content with the weight loss. It can be noted that there are two distinct weight loss regions. The first, between 80 °C and 112 °C, is because of evaporation of adsorbed water which is probably removed from mesopores rather than from the intracrystalline channels as was suggested by Zholobenko *et al.,* 1998. The temperature for desorption of water from the internal pore voids occurred over the temperature region of 100 – 300 °C and the region is higher than the boiling point of water because of the slow release of the water molecules.

The other sharp weight loss occurred between 450 °C and 680 °C, this is ascribed to dehydroxylation (this is the loss of water due to condensation of silanol groups forming siloxane bonds). Comparing the thermal behaviour of zeolite Na-P1 with that of Arnot fly ash in Figure 4.22, it can be noted that the distinct weight loss exhibited by zeolite Na-P1 was due to its microporous voids which allowed a high surface area for much adsorption of water which is unlike the starting material (Arnot fly ash). The TGA of the zeolite Na-P1 sythesized from Hendrina and Duhva fly ashes also showed the same weight loss behaviour (see Figure AI and A2 in the appendix).

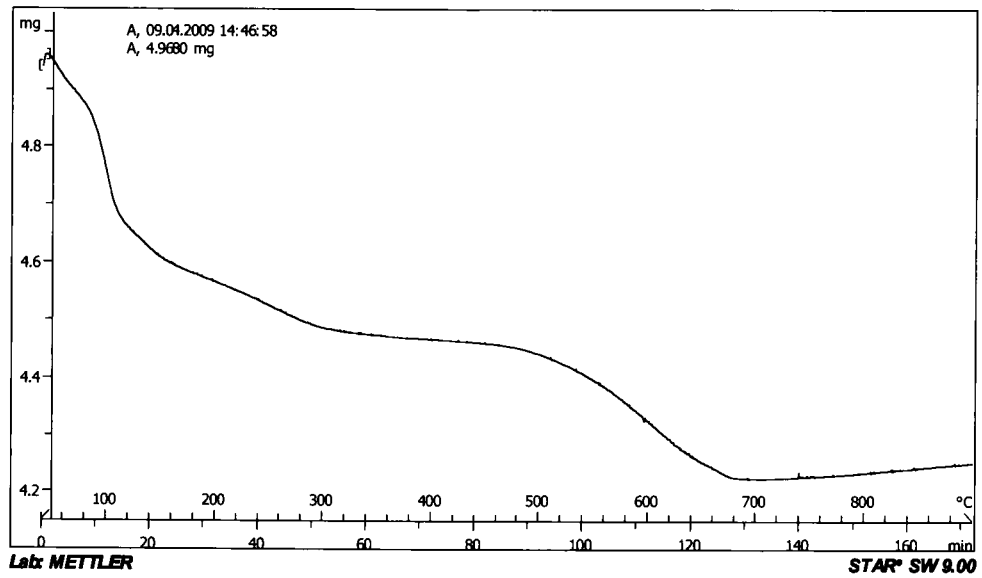

Figure 4-21: Weight-temperature behaviour of zeolite Na-P1 by TGA.

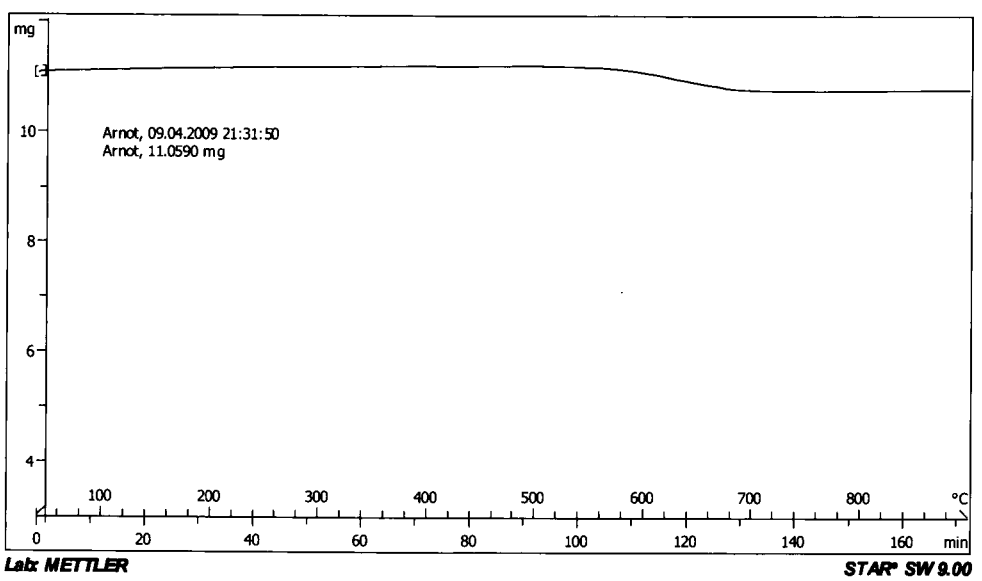

Figure 4-22: Weight-temperature behaviour of Arnot fly ash by TGA.

The implication of the TGA results are that zeolite Na-P1 synthesized from fly ash is not stable at temperatures above 500 °C and hence this creates a limitation for its application in conditions that may call for elevated temperatures. It is important to point out that it was not clear from TGA studies that structural reorganisation or collapse occurred.

4.1.9 Determination of cation exchange capacity

The weight of the zeolite sample used to determine the cation exchange capacity was 0.5g as specified in Section 3.1.3.5. The concentrations of cations obtained from ICP-AES analysis were converted to meq (milliequivalents) per g of sample as follows (Radojević & Bashkin 1999):

Mass (mg) of cation per gram of zeolite = Volume (L) x Cca / (weight of zeolite sample used)

Where Cca is the concentration of cationic species in the sample extract in mg l^{-1},

Therefore, meq of cation g^{-1} of sample = [Volume (L) x Cca/ (weight of zeolite sample used)] / (equivalent weight of the cation)

Equivalent weight of the cation is the mass needed to provide 1 mole of charge or atomic weight divided by the valence
Therefore:
meq Ca g^{-1} sample = [0.1 x Cca / 0.5] / 20.0
meq Mg g^{-1} sample = [0.1 x Cca / 0.5] / 12.2
meq Na g^{-1} sample = [0.1 x Cca / 0.5] / 23.0
meq K g^{-1} sample = [0.1 x Cca / 0.5] / 39.1

The calculated milliequivalents per g of each cation (Ca^{2+}, Mg^{2+}, Na^{+}, and K^{+}) was summed up to get the total cation exchange capacity (CEC) of the zeolitic material. Table 4.2 gives a comparison of CEC values obtained for fly ash and zeolites Na-P1 synthesized at different conditions.

Table 4-7: Comparison of CEC values for fly ash and different zeolite samples.

Sample	CEC (meq/g)
Fly ash	0.48
Zeolites product (100 °C/48hrs)	2.98
Zeolites product (140 °C/48hrs)	3.91
Zeolite at 140 °C/48hrs (modification by use of ethanol during the fourth washing)*	4.11

The cation exchange results presented in Table 4.7 show a correlation with the zeolite phase purity and crystallinity. This trend confirmed the XRD results shown in Section 4.2.3.1. The CEC value obtained for zeolites synthesized at 140 °C had a higher value compared to zeolites synthesized at 100 °C. Comparing the CEC values obtained in this study with other values obtained from literature (Table 4.8), it is evident that the values obtained in this study (4.11meq/g) are the highest reported. The value obtained was also close to that theoretical value of commercial zeolite Na-P1 (5 meq/g).

Table 4-8: Comparison of cation exchange capacity values of zeolite Na-P1 obtained in other studies.

Si/Al ratio	Synthetic conditions	Zeolite product (JCPDS 39-0219)	CEC	Reference
1.27	2M NaOH at 100 °C for 24 hours	Zeolite Na-P1	3.0	Inada *et al.*, 2005
2.40	3M NaOH at 125 °C for 24 hours	Zeolite Na-P1	3.1	Querol *et al.*, 2007
2.20	1M NaOH at 110 °C for 24 hours	Zeolite Na-P1	0.7	Mouhtaris *et al.*, 2003
1.65	5M NaOH at 140 °C for 48 hours	Zeolite Na-P1	4.11	Current study

4.1.9.1 Cation exchange capacity based variation of hydrothermal treatment time

Figure 4.23 show the CEC for materials prepared when the hydrothermal treatment time for zeolites synthesized from Arnot fly ash was conducted at 140 °C (Section .3.1.2, Table 3.2).

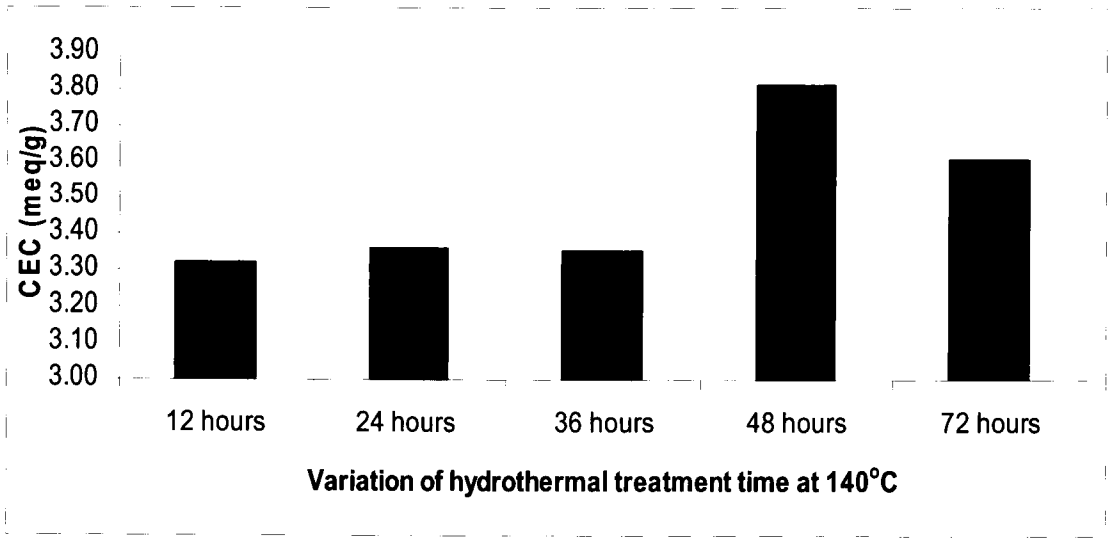

Figure 4-23: Effect of variation of hydrothermal treatment time on cation exchange capacity.

The trend established using the XRD technique (Section 4.1.4.2) was confirmed by the determination of the cation exchange capacity. The synthesis of zeolites at 140 °C for 48 hours gave the highest CEC value (3.81). It is important to point out that the water content during the hydrothermal treatment process had not been optimized for these materials. The reason for the decline in the CEC value when synthesis was conducted at 72 hours was due to the formation of hydroxysodalite, according to Ostwald's ripening principle, which is a small pore zeolite hence, having a lower pore volume and hence a lower capacity for ion exchange.

4.1.9.2 Cation exchange capacity based on variation of water content

Figure 4.24 shows the effect of variation of water content during the hydrothermal treatment process. The materials were prepared as described in Section 3.1.2 (Table 3.2). The amount of water added after ageing and prior to hydrothermal synthesis is presented as H_2O/SiO_2 molar ratio.

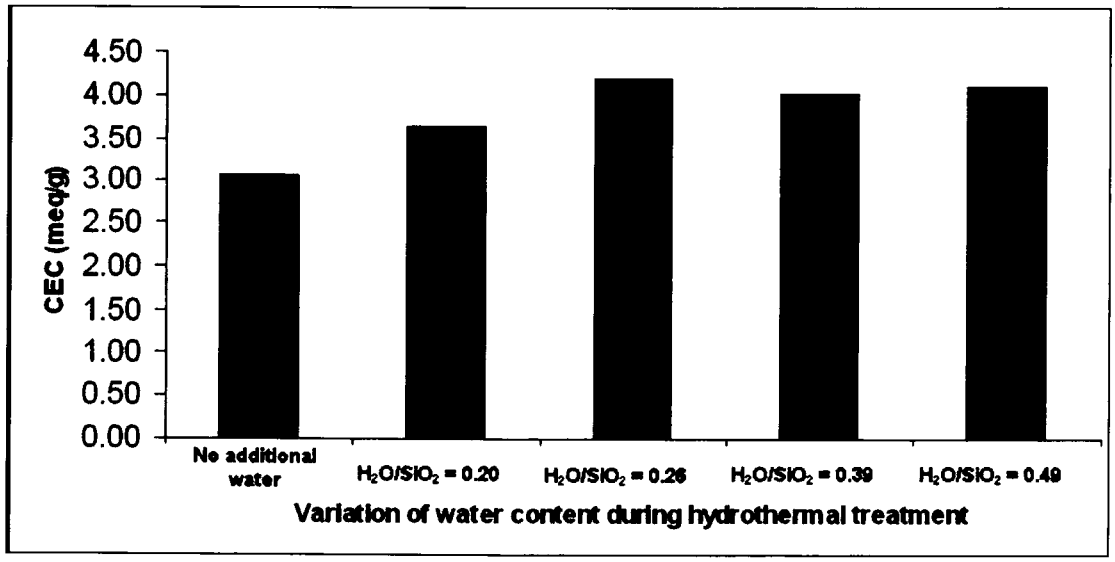

Figure 4-24: Effect of variation of water content during the hydrothermal treatment stage on cation exchange capacity.

The trend observed in Figure 4.24 shows that an increase in water content improved the CEC values. The trend had earlier been established by use of the XRD technique as was shown in Section 4.1.4.2. The value obtained when synthesis was conducted at 140 °C for 48 hours when H_2O/SiO_2 molar ratio was between 0.26 and 0.49 was found to be 4.10 meq/g and this sample proved from the XRD data to be the most crystalline sample as shown in Figure 4.7. These results show that the procedure is replicable and that similar products were obtained even when the H_2O/SiO_2 molar ratios were varied between 0.26 – 0.49.

4.1.10 BET analysis

Table 4.9 presents the results obtained for N_2-BET surface area, pore diameter and volume of the zeolite Na- P1 synthesized from Arnot fly ash at the specified conditions. The Nitrogen adsorption/desorption isotherm (Figure A1) did not clearly show the expected clear cut type I isotherm which is ascribed to microposity (lowell *et al.*, 2006) although a hysteresis loop was present at relative pressures between 0.4 and 0.9 which revealed some intragranular mesoporosity of the zeolite.

This isotherm was used to calculate the specific surface area by the BET method. The pore distribution was determined by BJH method.

Table 4-9: Surface area, pore diameter and volume of the zeolite Na- P1 synthesized from Arnot fly ash.

Synthesis conditions (Variation of Hydrothermal treatment time)	BET surface area (m^2/g)	Micro-pore area (m^2/g)	Micro-pore Volume (cm^3/g)
No Hydrothermal treatment	30.5693	3.9294	0.0018
Hydrothermal treatment: 140 °C for 24 hours	58.6358	7.1088	0.0032
Hydrothermal treatment: 140 °C and 48 hours	67.6320	7.5536	0.0034

N/B: For the above synthesis conditions, the ageing temperature and time was held constant at 47 °C for 48 hours respectively while H_2O/SiO_2 molar ratio during the hydrothermal treatment was at 0.49.

Table 4.9 shows that the surface area of the material obtained after ageing step without hydrothermal treatment was low (30.5693 m^2/g). There was a significant increase in the product's surface area after hydrothermal treatment for 24 hours at 140 °C (58.6358 m^2/g) and 48 hours (67.6320 m^2/g) which is ascribed to the formation of zeolite Na-P1 and which is confirmed by the XRD analysis (Section 4.1.4.1, Figure 4.4). The growth of many zeolitic crystals as was seen in the SEM images (Section 4.1.7) could also point towards the increase of the surface area due to their smaller particle size compared to the fly ash. Woolard *et al*, 2000 prepared zeolite P with a surface area of 62.66 m^2/g. The increase in surface area also confirms the improvement of the quality of the zeolite Na-P1 that had earlier been established by XRD and CEC results.

The absence of clear cut type I isotherm in Figure A1 and the low micro-pore area obtained could be due to the narrow channels dimensions of zeolite Na-P1 ($0.31 \times 0.44\ nm^2$ and $0.28 \times 0.49\ nm^2$) which could block the adsorption of Nitrogen inside the pores (Baelocker et al., 2007). Therefore, it is important to point out that, had

the above analysis been done using Argon as the adsorbent instead of Nitrogen, the surface area would have been expected to be higher than the reported values (Table 4.9) because the use of argon adsorption has an advantage since it enables a thorough analysis of the micro-pore level by filling of pores of dimensions 0.5 – 1 nm at a much higher relative pressure compared to nitrogen adsorption (Lowell *et al.*, 2006).

The micro-pore surface area might have also been lower than expected probably because of the effect of the pore blocking effects of the cations that are dispersed in the channels of the zeolite. A further reason could also be due to degassing temperatures applied, which may have caused structural reorganisation to zeolite Na-PHI as was confirmed by XRD analysis (Section 4.1.8.1). Thus BET data should be interpreted with caution and assessed in conjunction with XRD and CEC results, since under the conditions applied it is apparently mainly the external surface area of the agglomerated crystals that is probed.

4.2 Part B: Results for statistically designed experiments

In this section, the results for the statistical approach based on the experimental design explored in section 3.2 are discussed. The results and discussions are discussed based on mineralogical analysis and cation exchange capacity of the synthesized zeolites. Analysis of variance, confidence interval, response surface methodology is also highlighted.

The general sequence used during the statistical analysis of 2^k design is as summarized below (Montgomery, 2001);

1. Estimation of factor effect. In this case, their signs and magnitude are established. This enables the experimenter to gain preliminary information regarding which factors and interactions may be important and also determines the direction of adjustment to improve the response.
2. Formation of initial model. It is usually recommended that the full model be chosen (i.e. having the main effects and interactions).
3. Performing statistical testing. Normally, the use of Analysis of variance (ANOVA) is employed to carry out the formal test for significance of main effects and interactions.
4. Refining the model. In this case, the nonsignificant variables are removed from the full model.
5. Analysing residuals. This is normally done to check model adequacy and also assumptions.
6. Interpretation of results. This involves graphical representation of either main effects or interaction plots or response or contour plots.

As mentioned in section 3.2, a computer software package (Design Expert) was employed in the analysis of the results. Although most of the calculations were generated using the software, the formulae and some manual calculation are also highlighted in the results.

4.2.1 Qualitative XRD spectra analysis

Figure 4.25 shows qualitative XRD scans of the products obtained from the experiments that were statistically designed.

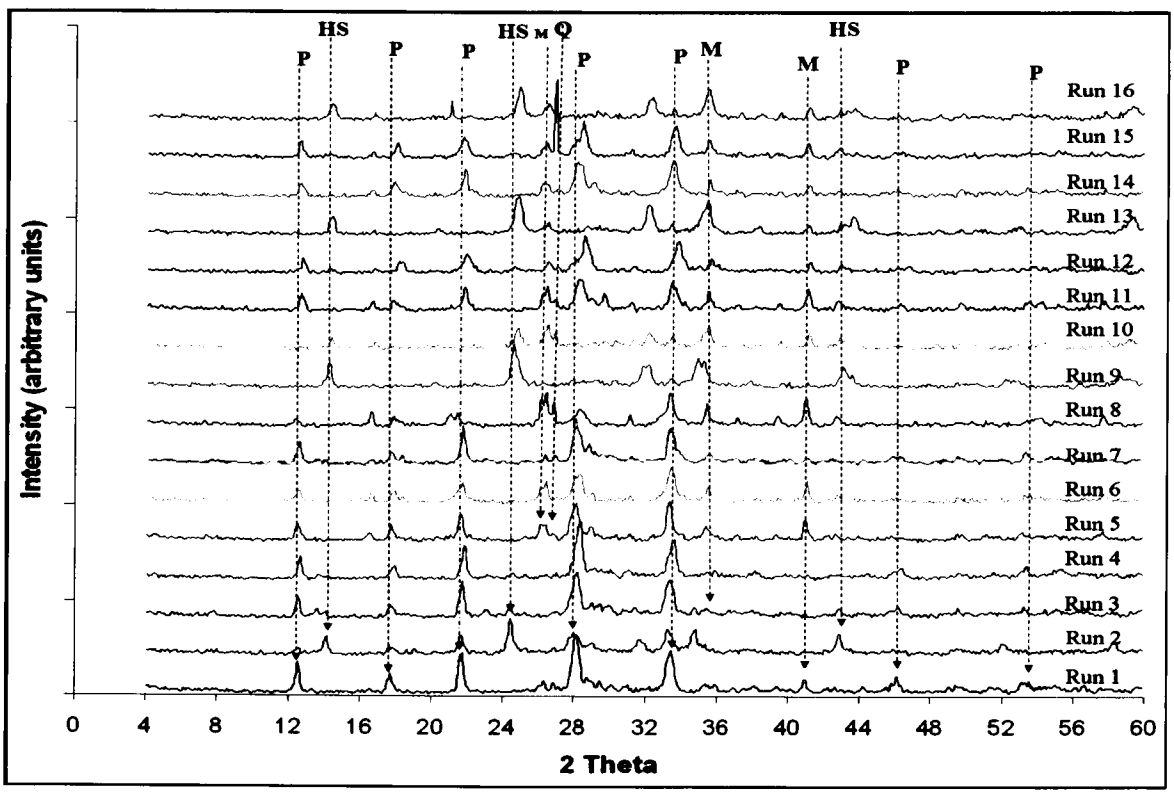

Figure 4-25: Comparison of XRD patterns for statistically designed experiments (P = Zeolite Na-P1, HS = Hydroxy-sodalite, Q = Quartz, M = Mullite).

As discussed in Section 2.3, the variation in the resulting mineralogical, phase and compositional purity is expected since synthesis conditions govern the end product. It can be noted from Figure 4.25 that zeolite Na-P1 (p), mullite (m), quartz (q) and hydroxyl-sodalite (HS) phases were identified.

4.2.2 Effect of synthesis variables on cation exchange capacity of zeolite Na-P1

Having confirmed the reliability and replicability of the CEC values obtained from experiments conducted using by the one-step-at-a-time approach, the results of the statistically designed experiments can be analyzed with confidence. Table 4.10 presents the results of the response factor, cation exchange capacity, determined from product obtained according to the experimentally applied conditions as described in section 3.2.

Figure 4.26 show the replicability of the randomized experiments. Normally, failure to replicate designed experiments often results to misleading conclusions since there is no internal estimate of error (Montgomery, 2001). Therefore, risk of fitting the model to noise was avoided by replication of each test combination as highlighted in Table 3.5 in Section 3.2.

Table 4-10: Cation exchange values for the statistically designed experiments (refer Table 3.5).

Randomized experiments	Run 1	Run 2	Run 3	Run 4	Run 6	Run 8	Run 10	Run	Run 13	Run 16	Run 17	Run 18	Run 21	Run 23	Run 24	Run 28
CEC	3.04	2.9	2.02	1.92	4.25	4.01	2.42	3.33	1.79	3.48	4.72	3.3	3.47	2.3	4.85	2.7
Duplicate Experiments	Run 5	Run 26	Run 7	Run 9	Run 15	Run 14	Run 12	Run 22	Run 25	Run 27	Run 19	Run 20	Run 31	Run 29	Run 32	Run 30
CEC	2.34	2.42	2.09	2.34	3.47	3.7	2.11	3.47	2.09	3.38	5.65	2.79	3.23	2.67	4.11	1.68
Average CEC	2.69	2.66	2.06	2.13	3.86	3.86	2.27	3.40	1.94	3.43	5.19	3.05	3.35	2.49	4.48	2.19
Stdev	0.4950	0.3394	0.0495	0.2970	0.5515	0.2192	0.2192	0.0990	0.2121	0.0707	0.6576	0.3606	0.1697	0.2616	0.5233	0.7212
Std error	0.35	0.24	0.035	0.21	0.39	0.155	0.155	0.07	0.15	0.05	0.465	0.255	0.12	0.185	0.37	0.51

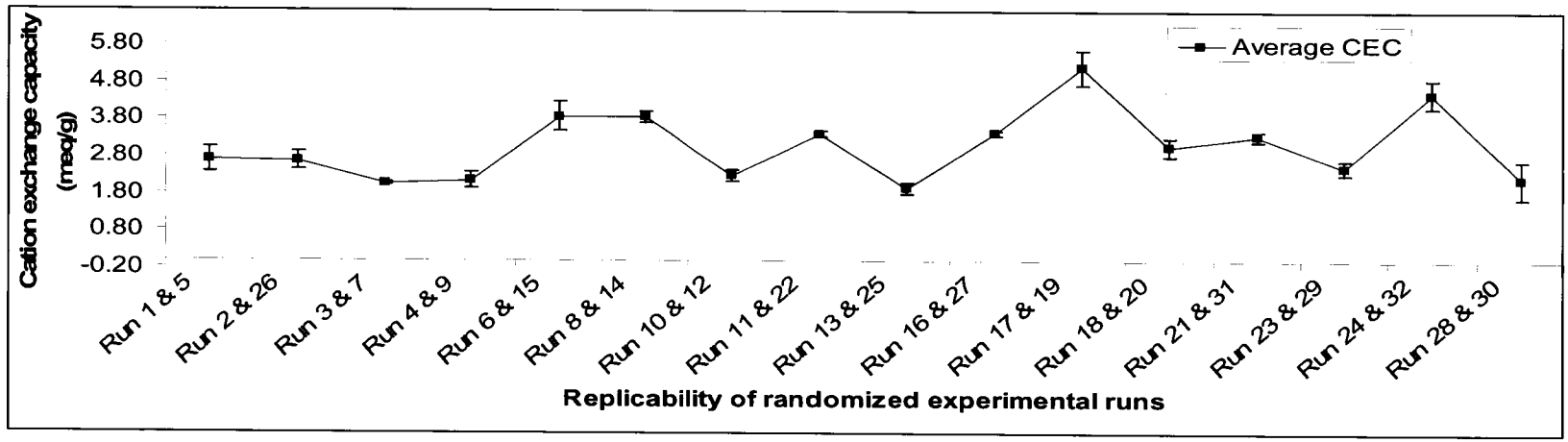

Figure 4-26: Replicability of designed experiments (Error bars represents standard error of average cation exchange capacity).

Summary of information during statistical analysis can enable the experimenter and the reader to connect the experimental units with the actual analysis (Design-Expert 7.1 user's guide, 2001). The summary of the factorial design is as shown in Table 4.11.

Table 4-11: Design summary for statistically designed experiments.

Study Type: Factorial		Runs	32
Initial Design: 2 Level Factorial		Blocks	No Blocks
Center Points : 0			
Design Model : 4FI			

Factor: Name	Units	Type	Low Actual	High Actual	Low Coded	High Coded	Mean	Std. Dev.
A : $NaOH/SiO_2$	Molar ratio	Numeric	0.35	0.71	-1	1	0.53	0.18
B : Ageing temperature	°C	Numeric	35	55	-1	1	45	10
C : Hydrothermal treatment time	hours	Numeric	36	60	-1	1	48	12
D : Hydrothermal treatment temperature	°C	Numeric	130	150	-1	1	140	10

Response Name	Units	Observations	Analysis	Minimum	Maximum	Mean	Std. Dev.	Ratio	Trans	Model
CEC	meq/g	32	Factorial	1.68	5.65	3.061875	0.951855	3.363095	None	R3FI

It is often convenient to write down the treatment combinations in the order (1), a, b, ab, c, ac, bc, abc, d, ad, bd, abd, cd, acd, bcd, abcd. This is referred to as standard order (or Yates' order for Dr. Frank Yates). Using this standard order, the contrast coefficients used in estimating the effects are as shown in Table 4.12. Contrast coefficients are a numerical way of embodying the hypothesis to be tested (Crawley, 2005). Contrast coefficients guarantee a valid comparison and also orthogonality.

It is important to note that the contrast coefficients for estimating the interaction effect are just the product of the corresponding coefficients of the main effects. There are actually three different notations that are widely used for the runs in 2^k design; the first contrast coefficient is either +1 or -1, often called the geometric notation. The second is the use of lowercase letter labels to identify the treatment combinations. The final notation uses 1 and 0 to denote high and low factor levels, respectively, instead of + and -. The table of plus and minus signs for the contrast constants for the 2^4 design are shown in Table 4.11. From these contrasts, we may estimate the 16 factorial effects.

Table 4-12: Contrast constants for the 2^4 design.

Run number	Run label	A	B	AB	C	AC	BC	ABC	D	AD	BD	ABD	CD	ACD	BCD	ABCD
1	(I)	-	-	+	-	+	+	-	-	+	+	-	+	-	-	+
2	a	+	-	-	-	-	+	+	-	-	+	+	+	+	-	-
3	b	-	+	-	-	+	-	+	-	+	-	+	+	-	+	-
4	ab	+	+	+	-	-	-	-	-	-	-	-	+	+	+	+
5	c	-	-	+	+	-	-	+	-	+	+	-	-	+	+	-
6	ac	+	-	-	+	+	-	-	-	-	+	+	-	-	+	+
7	bc	-	+	-	+	-	+	-	-	+	-	+	-	+	-	+
8	abc	+	+	+	+	+	+	+	-	-	-	-	-	-	-	-
9	d	-	-	+	-	+	+	-	+	-	-	+	-	+	+	-
10	ad	+	-	-	-	-	+	+	+	+	-	-	-	-	+	+
11	bd	-	+	-	-	+	-	+	+	-	+	-	-	+	-	+
12	abd	+	+	+	-	-	-	-	+	+	+	+	-	-	-	-
13	cd	-	-	+	+	-	-	+	+	-	-	+	+	-	-	+
14	acd	+	-	-	+	+	-	-	+	+	-	-	+	+	-	-
15	bcd	-	+	-	+	-	+	-	+	-	+	-	+	-	+	-
16	abcd	+	+	+	+	+	+	+	+	+	+	+	+	+	+	+

4.2.2.1 Estimation of factor effect

In the process of judging the significance of effects, the analysis of variance is the formal way to determine which factors are nonzero. Use of normal probability plots can also be used to assess the importance of the effects. To enable the experimenter narrow down to the contribution of the various effects, a tentative percentage contribution of each model term to the total sum of squares is generated by the software (Table 4.13). The percentage contribution is often a rough but effective guide to the relative importance of each model. The model terms that are of least significance are marked as "error" and this is useful during the refinement of the analysis process (Design-Expert 7.1 user's guide, 2001).

Table 4-13: Tentative Model for estimation of Factor Effects.

	Term	Effect	Sum of Squares	Percentage contribution
Require	Intercept			
Model	A-$NaOH/SiO_2$	0.19625	0.308113	1.06
Model	B-Ageing temperature	-1.0975	9.63605	33.24
Model	C-Hydrothermal treatment time	-0.44	1.5488	5.34
Model	D-Hydrothermal treatment temperature	0.9925	7.88045	27.18
Model	AB	-0.3725	1.11005	3.83
Error	AC	0.07	0.0392	0.14
Error	AD	0.0575	0.02645	0.09
Error	BC	-0.19625	0.308113	1.06
Model	BD	-0.47625	1.814513	6.26
Error	CD	-0.15125	0.183013	0.63
Error	ABC	-0.29375	0.690313	2.38
Error	ABD	-0.34875	0.973013	3.36
Error	ACD	-0.31375	0.787513	2.72
Error	BCD	-0.04	0.0128	0.04
Error	ABCD	0.4	1.28	4.414876
Error	Lack Of Fit		0	0
Error	Pure Error		2.3945	8.258922
	Lenth's ME	0.538247		

4.2.2.2 Analysis by the use of normal probability plots

Some factors can be included to make the model hierarchical. The hierarchy principle indicates that if a model contains high-order terms, it should also contain all of the lower-

order terms that compose it (Montgomery, 2001). Hierarchy promotes a type of internal consistency in a model, and many statistical model builders rigorously follow this principal. In this analysis, hierarchical term A is added after manual regression to obey the hierarchy principle which is reflected in the analysis of variance. The normal probability plots for these effects are shown in Figure 4.27.

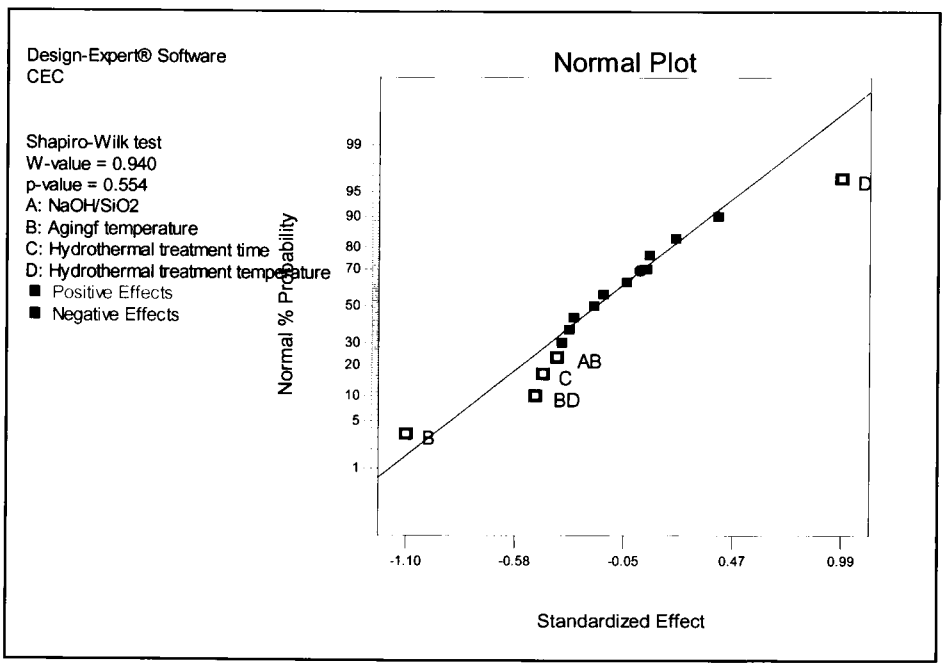

Figure 4-27: Normal probability plot.

All the effects that lie along the line are negligible, whereas the significant effects are far from the line. The important effects that emerge from this analysis are the main effects of Factor B (Ageing temperature), C (hydrothermal treatment time), D (hydrothermal treatment temperature) and the interactions AB (between $NaOH/Si_2O$ molar ratio and hydrothermal treatment temperature) and BD (between ageing and hydrothermal treatment temperature).

4.2.2.3 Statistical testing by analysis of variance

Analysis of variance (ANOVA) serves two main purposes; the first is to provide a subdivision of the total variation between the experimental units into separate components, each component representing a different source of variation, so that the relative importance

of the different sources can be assessed. Secondly, it gives an estimate of the underlying variation between units which provide a basis for inferences about the effects of the applied treatments (Mead, 1991).

The analysis of variance, which is a collection of models, can be generated computationally using the design expert software. However, manual computing can also be used although it becomes complicated with higher order designs.

The analysis of variance for the reduced model containing only the main effects A, B, C and D, and AB and BD interactions is as shown in Table 4.14. This computer generated summary contains the usual sum of squares, degrees of freedom, mean squares, test statistic F and p-value (upper bound value because the probabilities less than 0.0001 are defaulted to 0.0001).

Table 4-14: Analysis of variance for selected Factorial Model (part 1).

Source	Sum of Squares (SS)	Degrees of freedom (df)	Mean Square (MS)	F Value	p-value Prob > F
Model	22.30	6.00	3.72	13.88	< 0.0001
A-$NaOH/SiO_2$	0.31	1.00	0.31	1.15	0.29
B-Ageing temperature	9.64	1.00	9.64	35.98	< 0.0001
C-Hydrothermal treatment time	1.55	1.00	1.55	5.78	0.02
D-Hydrothermal treatment temperature	7.88	1.00	7.88	29.43	< 0.0001
AB	1.11	1.00	1.11	4.15	0.05
BD	1.81	1.00	1.81	6.78	0.02
Residual	6.69	25.00	0.27		
Lack of Fit	4.30	9.00	0.48	3.19	0.02
Pure Error	2.39	16.00	0.15		
Cor Total	28.99	31.00			

Where; F value: is a test for comparing model variance with residual (error) variance.

Prob > F : the probability of seeing the observed F value if the null hypothesis is true

In the first line of the analysis of variance, the overall summary for the reduced factorial model is presented and the model sum of squares (SS) is calculated as;

$$SS_{\text{reduced model}} = SS_A + SS_B + SS_C + SS_D + SS_{AB} + SS_{BD} = 22.30$$

The number of degrees of freedom (df) for any main effect is the number of levels of the factor minus one, and the number of degrees of freedom for an interaction is the product of the number of degrees of freedom associated with the individual component of the interaction.

The assessment of the overall strength of the treatment effect can be formally be justified by the use of F distribution which is given by;

$$F = \text{MS reduced model} \div \text{MSE} = 3.72 \div 0.48 = 13.88$$

Where MS is the treatment mean squares for the reduced model and MS_E is the error mean square. The Model F-value of 13.88 (Table 4.14) implies the model is significant. There is only a 0.01% chance that a "Model F-Value" this large could occur due to noise. For a completely randomized design model, the power of the F-test to detect treatment differences depends on the average of the squares of treatment deviations

The error or residual sum of squares is composed of a pure error component arising from the replication and a lack of fit component consisting of the sum of squares for the interactions that were dropped from the model (AC, AD, BC, CD, ABC, ABD, ABCD, BCD and ACD). Once again, the regression model representation of the experimental results is given in terms of both coded and natural variables.

Values of "Prob > F" less than 0.0500 in Table 4.14 indicate which model terms are significant. In this case B, C, D AB and BD are significant model terms. Values greater than 0.1000 indicate the model terms are not significant.

Table 4-15: Analysis of variance for selected Factorial Model (part 2).

Standard deviation of mean measure	0.51749	R- Squared (R^2)	0.76908
Mean of the main measure	3.06188	Adjusted R^2	0.71367
Coefficient of Variation (C.V) %	16.9011	Predicted R^2	0.62167
PRESS	10.9689	Adequate Precision	11.9921

The standard deviation is the root square of the error mean square. The quantity "R-Squared" measures the proportion of total variability in the data explained by the analysis of variance model (Montgomery, 2001) and can be calculated as;

R- Squared = $SS_{model} \div SS_{total} = 22.29798 \div 28.99289 = 0.769084$

The value 0.769084 in Table 4.15 explains about 76.91 % of the variability obtained in cation exchange capacity.

The coefficient of variation (C.V) measures the unexplained or residual variability in the data as a percentage of the mean of the response variable (cation exchange capacity). The adjusted R- squared (R^2_{Adj}) static, defined as; a statistic that is adjusted for the size of the model or the number of factors in the model (Montgomery, 2001). If non-significant terms are "forced" into the model this can decrease to very small values. It is represented by the equation below;

$R^2 \text{ Adj} = 1 - [(SSE/dfE) \div (SS_{Total}/df_{Total})]$

For the case of this design, the Adjusted R-squared in Table 4.14 can be calculated as;

$R^2 \text{ Adj} = 1 - [(2.3945/16) \div (28.99289/31)] = 0.713665$

In most cases, the adjusted R^2 decreases if nonsignifiant terms are added to a model.

The Predicted Error Sum of Squares (PRESS) is a measure of how well the model will predict responses in a new experiment. A model with a small value of PRESS indicates that

the model is likely to be a good predictor (Montgomery, 2001). Alternatively, The predicted R-squared (R^2_{Pred}) can be calculated based on PRESS as follows;

$$R^2_{Pred} = 1 - [(PRESS/SS_{Total})]$$

For this study, the

$$R^2_{Pred} = 1 - [(10.96894/28.99289)] = 0.621668$$

The "Predicted R-Squared" of 0.6217 (Table 4.15), which indicates that the model would be expected to explain about 62 % of the variability in the new data, is in reasonable agreement with the "Adj R-Squared" of 0.7137.

The "Adequate Precision" is computed by dividing the difference between the maximum predicted response and the minimum predicted response by averageing standard deviation of all predicted responses. It measures the signal to noise ratio and acts as a good indicator of whether the Response Surface Methods (RSM) are applicable (Montgomery, 2001). Large values are desirable and values greater than 4 give a good indication that the model will give reasonable performance in prediction. For this design, the ratio of 11.992 (Table 4.15) indicates an adequate signal. This model can be used to navigate the design space as show in the next Sections.

The next portion of the output presents the regression coefficient for each model term and the standard error of each coefficient which is defined as;

Standard error = $\sqrt{MSe / n2k} = \sqrt{0.149656 / (2)\,32} = 0.09148$

Where MSe = Mean Square error

The 95 % confidence intervals on each regression coefficient (Montgomery, 2001) are computed from

$$\text{Effect} - t_{0.025,\,N-p}\text{se (effect)} \leq \text{Confidence intervals (CI)} \geq \text{Effect} + t_{0.025,\,N-p}\text{se (effect)}$$

The degree of freedom on t is the number of degrees of freedom for error.

Where;

se = standard error

t = t value

N = the total number of runs in the experiment (32)

P = the number of model parameters (6)

CI = Confidence interval

Table 4-16: Regression Model for the Process.

Factor	Coefficient Estimate	df	Standard Error	95% CI Low	95% CI High	VIF
Intercept	3.061875	1	0.09148	2.873468	3.250282	
A-NaOH/SiO2	0.098125	1	0.09148	-0.09028	0.286532	1
B-Ageing temperature	-0.54875	1	0.09148	-0.73716	-0.36034	1
C-Hydrothermal treatment time	-0.22	1	0.09148	-0.40841	-0.03159	1
D-Hydrothermal treatment temperature	0.49625	1	0.09148	0.307843	0.684657	1
AB	-0.18625	1	0.09148	-0.37466	0.002157	1
BD	-0.23813	1	0.09148	-0.42653	-0.04972	1

The Variation of Inflation Factor (VIF) in Figure 4.16 measures how much the variance of the model is inflated by the lack of orthogonality in the design. The value of 1 obtained in this model implies that the factors are orthogonal and hence they are not too correlated meaning that they are independent (Design-Expert 7.1 user's guide).

It is normally useful to fit a response curve to the levels of a quantitative factor so that the experimenter has an equation that relates the response to the factor (R. Mead, 1991). Design expert software was used to generate the regression models. The equations generated can be used for extrapolation or predict the response at factor levels between those actually used in the experiment. In this case, the regression equations generated by this model are as follows;

Final Equation in Terms of Coded Factors:

CEC = + 3.06 + 0.098 * A -0.55 * B -0.22 * C + 0.50 * D-0.19 * A * B -0.24 * B * D

Final Equation in Terms of Actual Factors:

CEC = -18.29486 + 5.20139 * $NaOH/SiO_2$ + 0.33334 * Ageing temperature -0.018333 * Hydrothermal treatment time + 0.15678 * Hydrothermal treatment temperature -0.10347 * $NaOH/SiO_2$ * Ageing temperature -2.38125E-003 * Ageing temperature * Hydrothermal treatment temperature

4.2.2.4 Residuals and diagnostic checking

Before the conclusions from the analysis of variance could be adopted, the adequacy of the underlying model was checked. Corrections of diagnostic problems require re-analysing the dataset (re-doing the ANOVA module), either because outliers were deleted or the model was transformed (Mead, 1991). After this re-analysis, the complete diagnostics checking steps were repeated to check whether deleting some outliers caused other outliers to be identified. The chosen transformation was also checked to asses if it corrected normality or unequal variance. Figures 4.28 – 34 serve to confirm the adequacy of the selected factorial model.

Ideally the normal plot of residuals should be a straight line, indicating no abnormalities (Design-Expert 7.1 user's guide, 2001). In this study, the plot (Figure 4.28) largely followed the ideal case. It is desired that there be no apparent pattern in the observed data in the residual versus run (Montgomery, 2001) and this expectation is actualised as can be seen in Figure 4.29.

In the residual versus predicted plot, the spread of the studentized residuals (quotient resulting from division of a residual by an estimate of its standard deviation) should be approximately the same across all levels of the predicted values (Design-Expert 7.1 user's guide, 2001). This was confirmed as seen in Figure 4.30. For a good model, there should be

no apparent pattern in the observed data in the outlier analysis given by plot of Predicted vs. Actual (Montgomery 2001). This is confirmed as seen in Figure 4.31 since there is no pattern established in the observed data

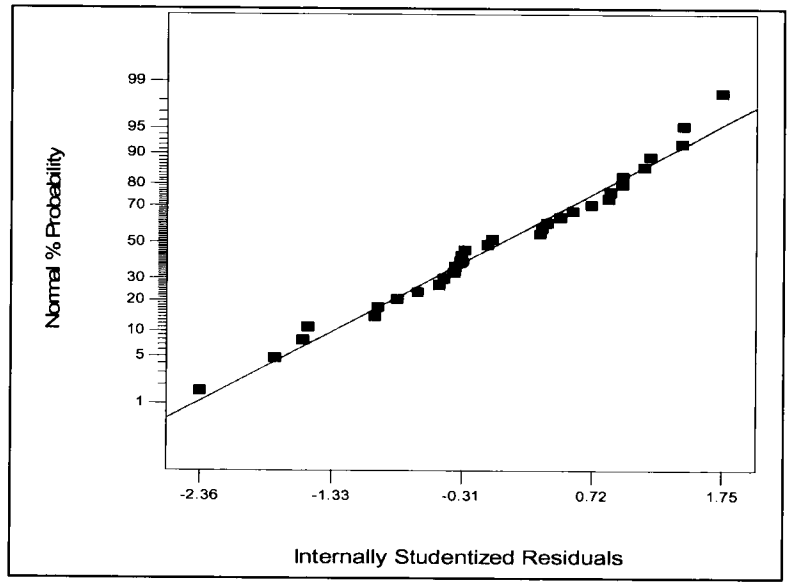

Figure 4-28: Normal plot of residuals.

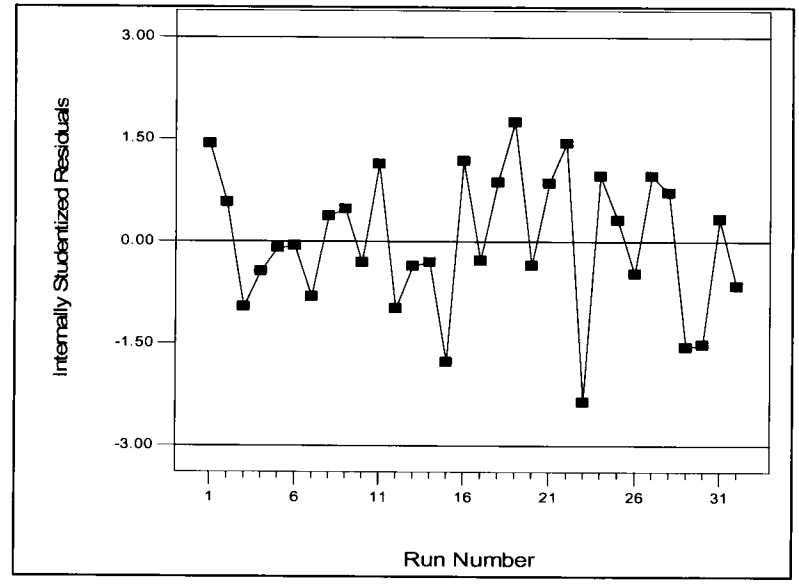

Figure 4-29: Plot of Residuals versus runs.

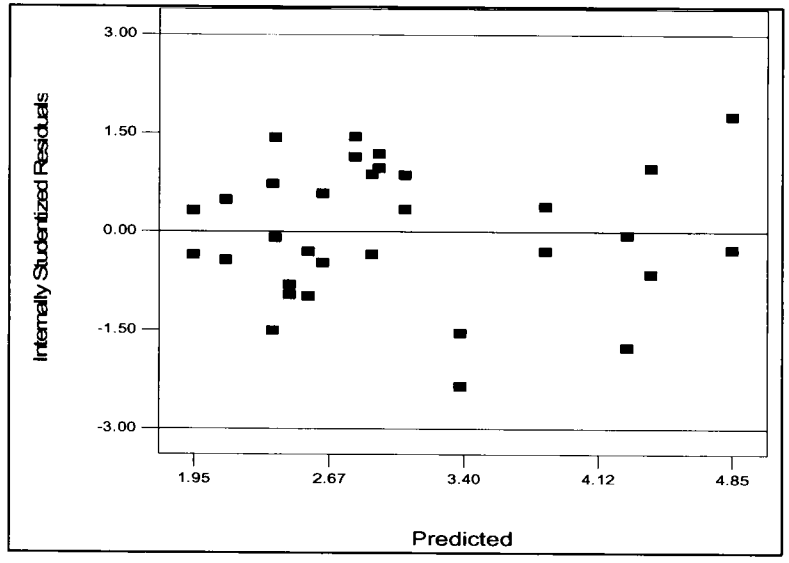

Figure 4-30: Plot of residuals versus predicted

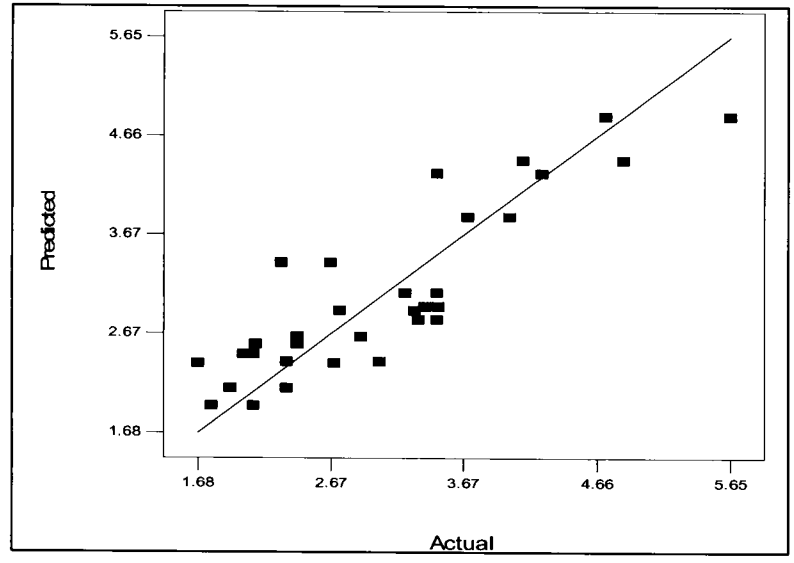

Figure 4-31: Plot of predicted versus actual.

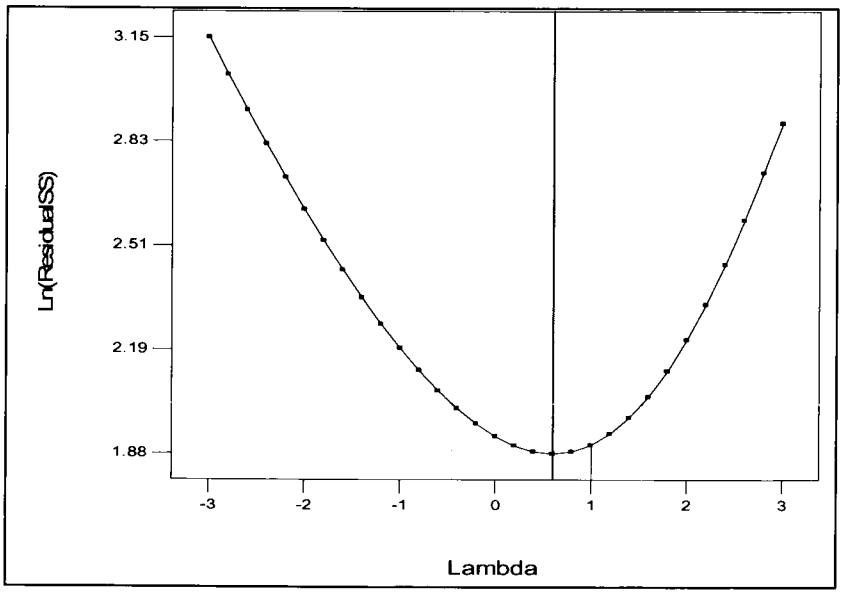

Figure 4-32: Box-Cox plot for power transforms.

Box-Cox plot for power transforms was developed to calculate the best power law transformation (Montgomery, 2001). Figure 4.32 indicates that there no need of the transformation. The green line indicates the best lambda values, while the red lines indicate 95% confidence interval surrounding it. If this 95% confidence interval includes 1, then no transformation is recommended.

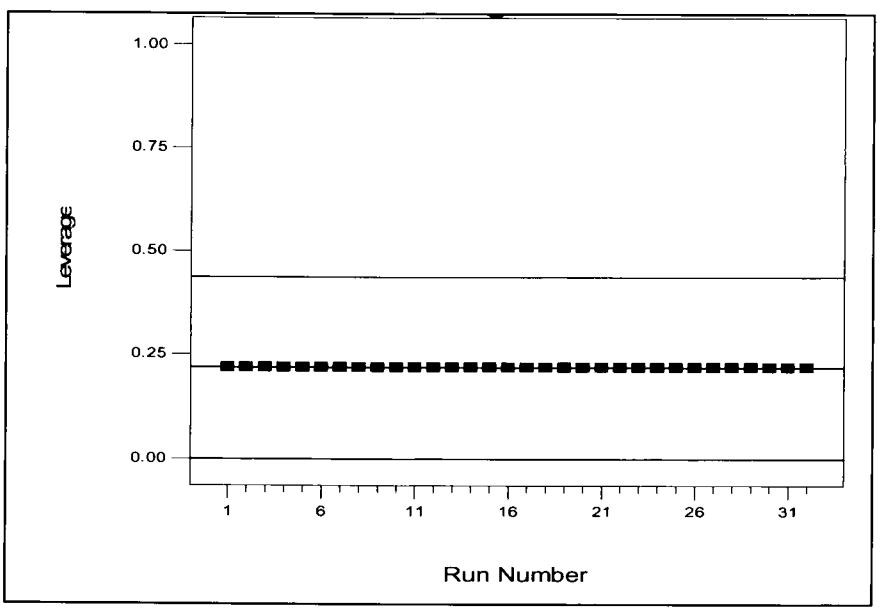

Figure 4-33: Plot of leverage versus run.

Leverage points are those observations, if any, made at extreme or outlying values of the independent variables such that the lack of neighbouring observations means that the fitted regression model will pass close to that particular observation (Everitt, 2002). Ideally, it is expected that there should be a strong clustering of points near the zero point and this was confirmed as shown in Figure 4.33.

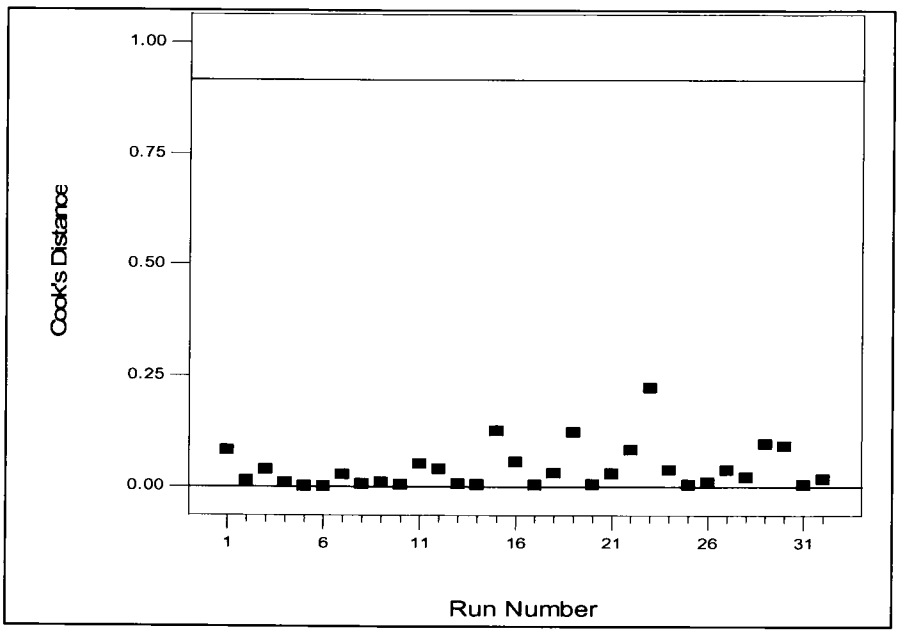

Figure 4-34: Plot of Cook's distance.

Cook's distance is used to measure the effect of deleting a given observation. In cases where there are data points with large residuals or outliers there may be distortion of the outcome and accuracy of a regression is not guaranteed. For points with a Cook's distance of 1 or more, they are considered to be a cause for alarm and calls for closer examination in the analysis (Montgomery, 2001). It is desired that there be strong clustering near the zero point which is actually verified in Figure 4.34 which shows that no point was deleted accidentally while entering the data in the software and hence the accuracy of regression can be trusted.

Having checked for outliers and confirmed that the residual checks were according to the expectations, the model was confirmed to be valid and could be used with confidence to interpret the results.

4.2.2.5 Interpretation of results

When an experiment involves levels of a quantitative factor, it is essential to examine the pattern response of the observed variable to the changing stimulus of the factor.

Interpretation of main effects and interactions

Principles of interpretation of main and interactive effects are based on the guidelines suggested by Mead (1991). The main factors should be examined first, then the two-factor interactions, then three-factor interactions and so on. Interactions essentially represent modification of the main effects, and have no sensible interpretation without consideration, at the same time, of the corresponding main effects.

In cases where the two-factor effects, and the higher order interactions appear negligible, then the results of the experiment should be interpreted in terms of the main effect mean responses only ignoring the mean responses of the combinations of levels. Like wise, if a two factor interaction is clearly important, then the interpretation of the effects of these two factors should normally be based on the mean responses for the combination of levels for those two factors (Mead, 1991).

i. Main effect

As can be seen from the analysis of variance (Table 4.13) and also plot of normal probability (Figure 4.27), factor B (ageing temperature) had a significant negative main effect on the cation exchange and the same effect can be confirmed by data shown in Figure 4.36. The same effect applies to factor A ($NaOH/SiO_2$ molar ratio) shown in Figure 4.35 and also factor C (hydrothermal treatment time) which is shown in Figure 4.37, although the significance of these two effects was minimal. Referring to the third stage of analysing the statistical data (use of normal probability plots), factor A was merely (Table 4.13 and Figure 4.27) incorporated in the model to make it hierarchical even though its influence was not all that significant.

Scrutinising the effect of factor D (hydrothermal treatment temperature) in Figure 4.38, it can be noted that it had a positive main effect on the value of cation exchange capacity,

which is to say that the CEC value increased with increasing hydrothermal treatment temperature. It is necessary to be careful when making conclusions for factor A, B and D because the calculations performed by the software signalled a warning that the factor was involved in an interaction. Therefore, basing final conclusions only on the main effects alone, especially the ones with a warning on top of the plot (Figure 4.35, 36 and 38), could provide misleading information although it is important to note their effect before investigations of their interaction effects (Design-Expert 7.1 user's guide).

.

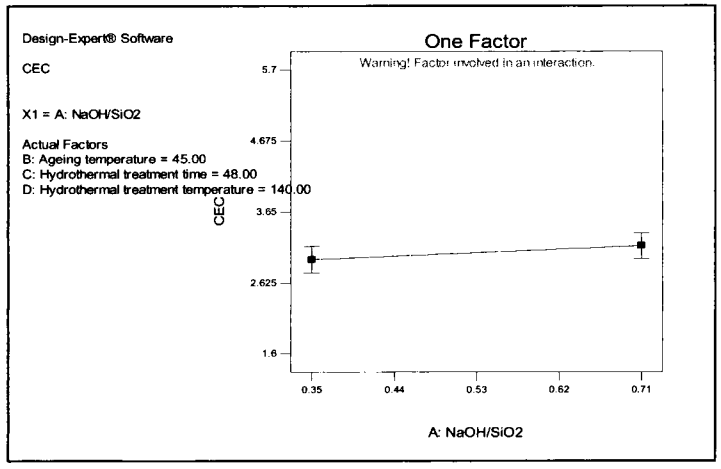

Figure 4-35: Main effect of $NaOH/SiO_2$ molar ratio.

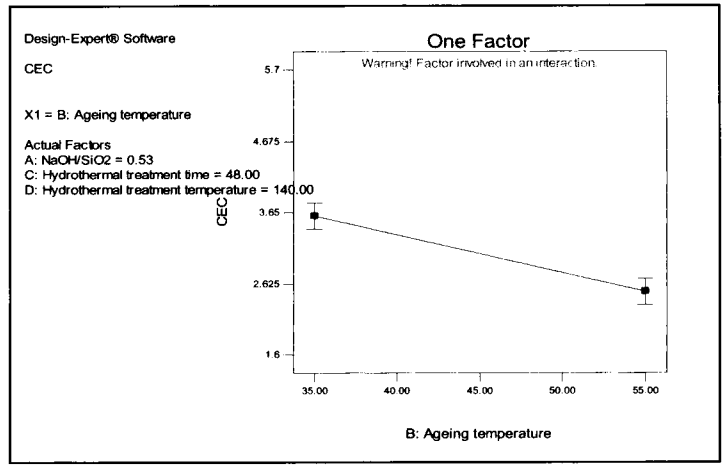

Figure 4-36: Main effect of ageing temperature.

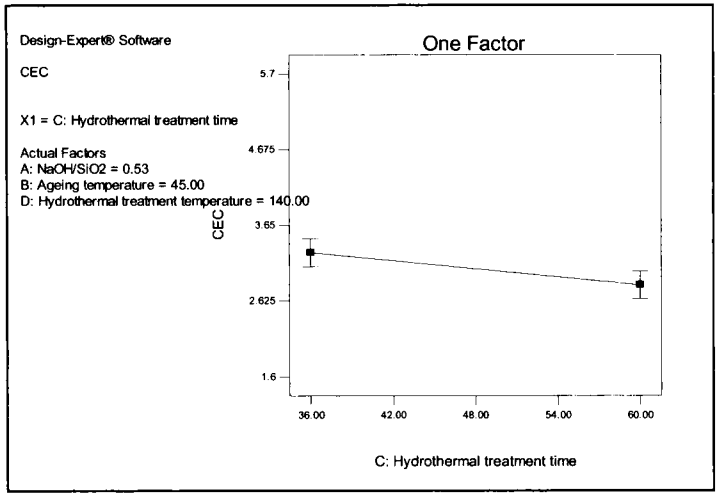

Figure 4-37: Main effect of hydrothermal treatment temperature.

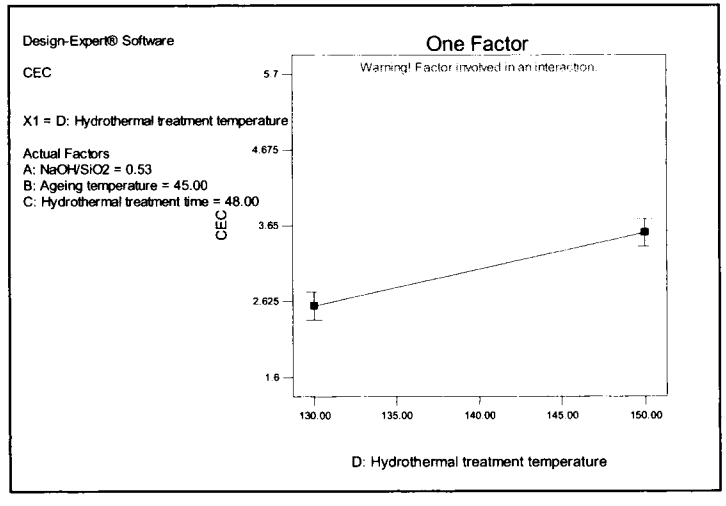

Figure 4-38: Main effect of hydrothermal treatment time.

ii. Interactions

A factor interaction is the variation among the differences between means for different levels of one factor over different levels of the other factor. Apart from using normal probability plots and analysis of variance to explain data, visual inspection of the data using line graphs is another way of looking for evidence of an interaction (Mead, 1991).

Changes in the main effect of one variable over levels of the other are most easily seen in the graph of the interaction. If the lines describing the simple main effects are not parallel, then a possibility of an interaction exists (Design-Expert 7.1 user's guide, 2001). As can be seen from Figure 4.39 and 4.40, the possibility of a significant interaction exists between ageing temperature and $NaOH/SiO_2$ molar ratio because the lines between the levels applied are not parallel. Indeed this could be expected because the glassy Si rich phase in the ash would require the mineralizing effect of the hydroxide to fully dissolve and become available as feedstock.

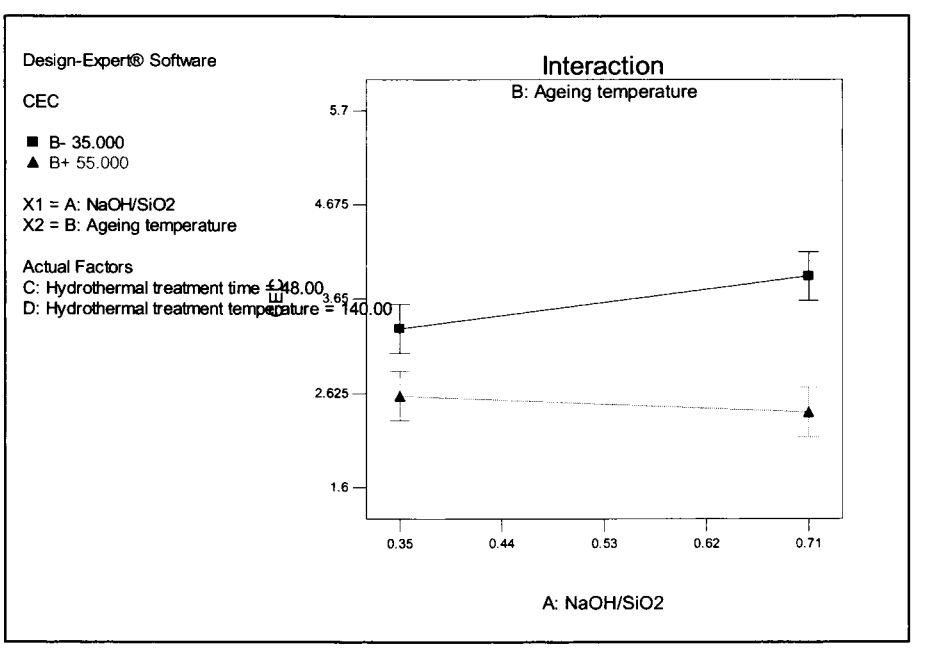

Figure 4-39: Interaction between ageing temperature and $NaOH/SiO_2$ molar ratio.

The magnitude of the difference of cation exchange capacity with different ageing temperature and $NaOH/SiO_2$ molar ratios is more pronounced at high values of ageing

temperature and $NaOH/SiO_2$ molar ratio. The Design Expert software had indicated a warning that the main effect of ageing temperature could be misleading since it was involved in this interaction. From the two-way interaction, it reaffirms the need for this warning since during the interaction between these two variables an increase in CEC value was observed as response in the product when the ageing temperature was high. This contradicted the conclusions that could be derived if one was to base the significance of the effect on its main influence alone.

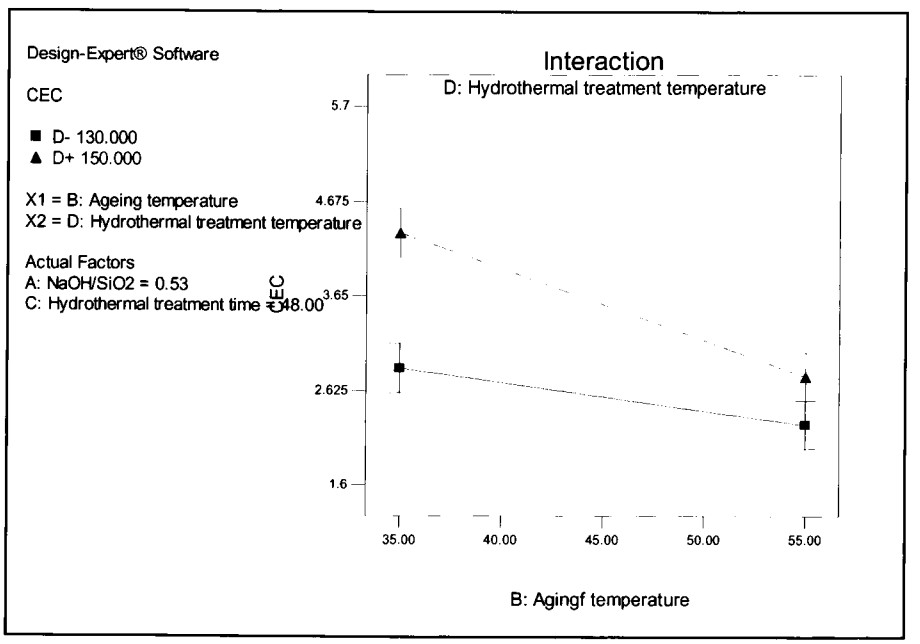

Figure 4-40: Interaction between ageing and hydrothermal treatment temperature.

Another significant two-way interaction was observed as can be seen in Figure 4.40. It was found that the interaction between the two variables, namely ageing temperature and hydrothermal treatment temperature, and their combined effect on the CEC of the product was much more pronounced at low values of ageing temperature and high values of hydrothermal treatment temperature. The interlocking of the error bars at the high values of ageing temperature indicates that the interaction at these levels was negligible.

i. Response surface analysis

Response surface methodology (RSM) refers to a collection of mathematical and statistical techniques that are useful for modelling and analysis of problems in which a response of interest is influenced by several variables and the objective is to optimise this response (Montgomery, 2001). The RSM is usually represented graphically.

In this study, the overall objective was to determine a region in space in which combination of the different variables yield a product with a high cation exchange capacity. It is important to highlight that the 2^k structures do not allow estimation of quadratic terms in the second-degree polynomial because with only two levels of a factor, there can be no information on the change of slope. Therefore, 2^k structures will provide information only on the gradient of the surface in all possible directions.

Figure 4.41 and 4.42 represent the response surface and contour plots of the relationship between ageing temperature and $NaOH/SiO_2$ molar ratio. The two plots provide essentially the same information.

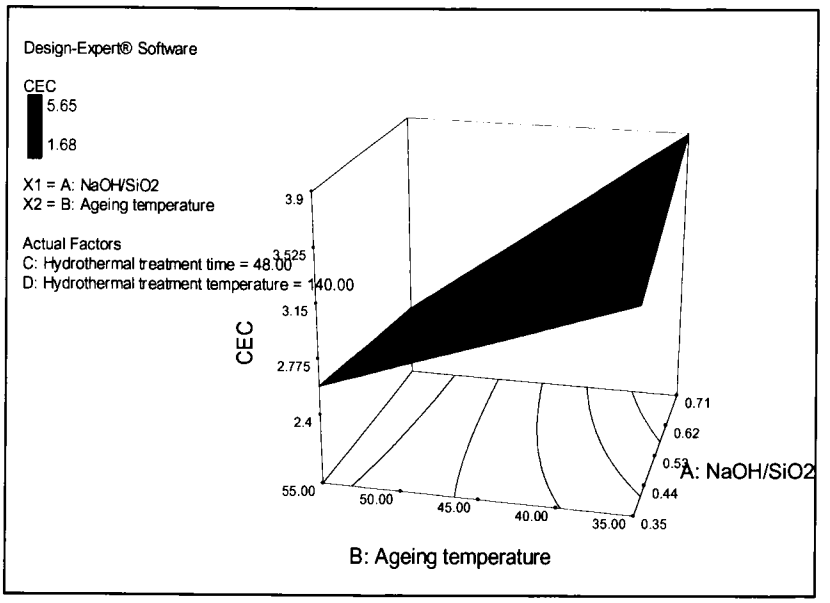

Figure 4-41: Three-dimensional response surface (relationship between ageing temperature and $NaOH/SiO_2$ molar ratio)

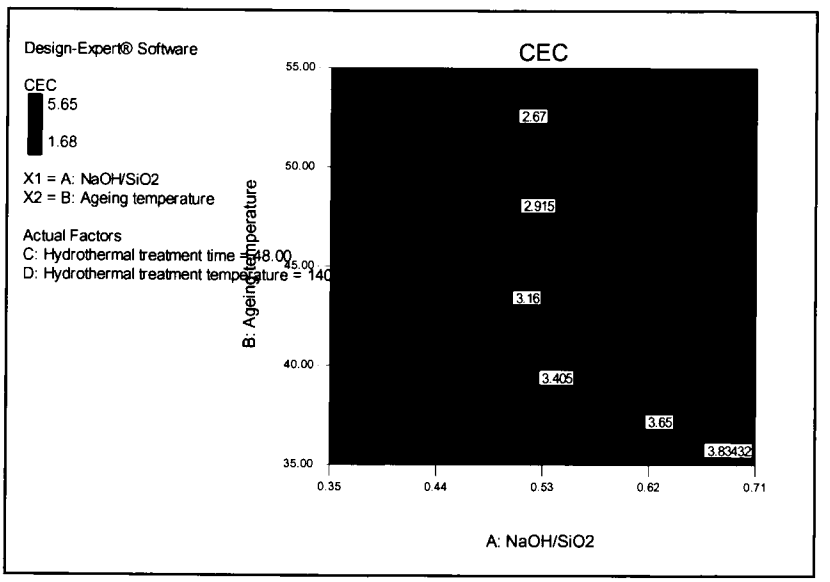

Figure 4-42: Two-dimensional contour plot (relationship between ageing temperature and $NaOH/SiO_2$ molar ratio).

.

Examination of the plots given in Figure 4.41 and Figure 4.42 show that the maximum cation exchange capacity is achieved at low values of ageing temperature (35 ^{o}C) and high values of $NaOH/SiO_2$ molar ratio (0.71. It can also be confirmed that there are interactions at high values of the $NaOH/SiO_2$ molar ratio since the contour lines are curved and the response surface is a 'twisted' plane (Montgomery, 2001).

Figures 4.43 and 4.44 present the three-dimensional response surface plots of the cation exchange capacity and the contour plot of the relationship between ageing and hydrothermal treatment temperature respectively. Because the model is first order (that is, it contains only the main effects), the fitted response surface shown in Figure 4.43 is a plane.

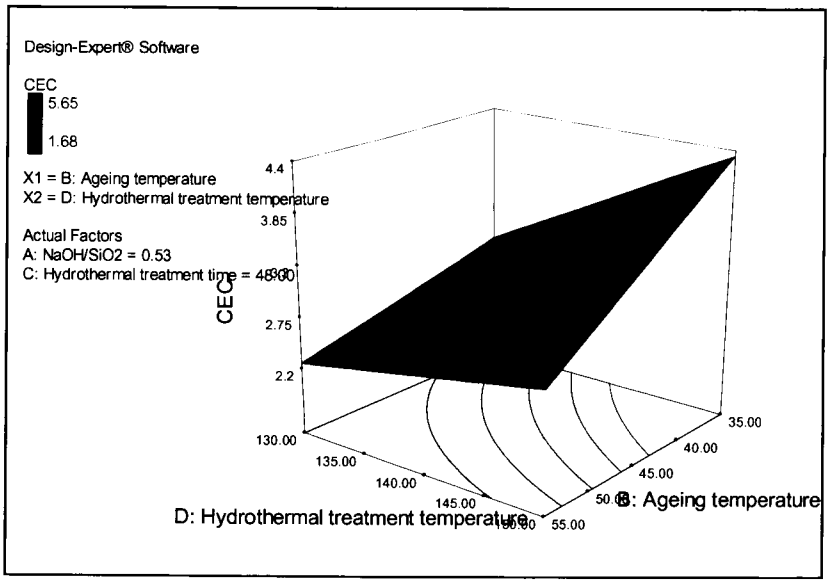

Figure 4-43: Three-dimensional response surface (relationship between ageing and hydrothermal treatment temperature).

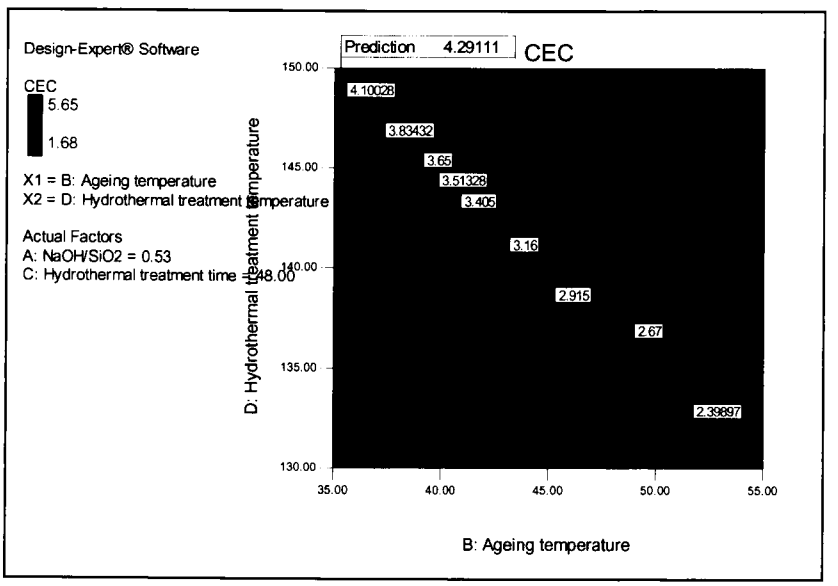

Figure 4-44: Two-dimensional contour plots (relationship between ageing and hydrothermal treatment temperature).

It can be observed that there are interactions of the hydrothermal treatment temperature and ageing temperature since the contour plots are curved and the response surface is 'twisted'. The best cation exchange capacity was obtained when the ageing and hydrothermal treatment temperature were held at 36 °C and 160 °C respectively.

Cube plots analysis

Cube plots are often useful visual displays of experimental results and in most cases they are used to find the direction of potential improvement for a process.

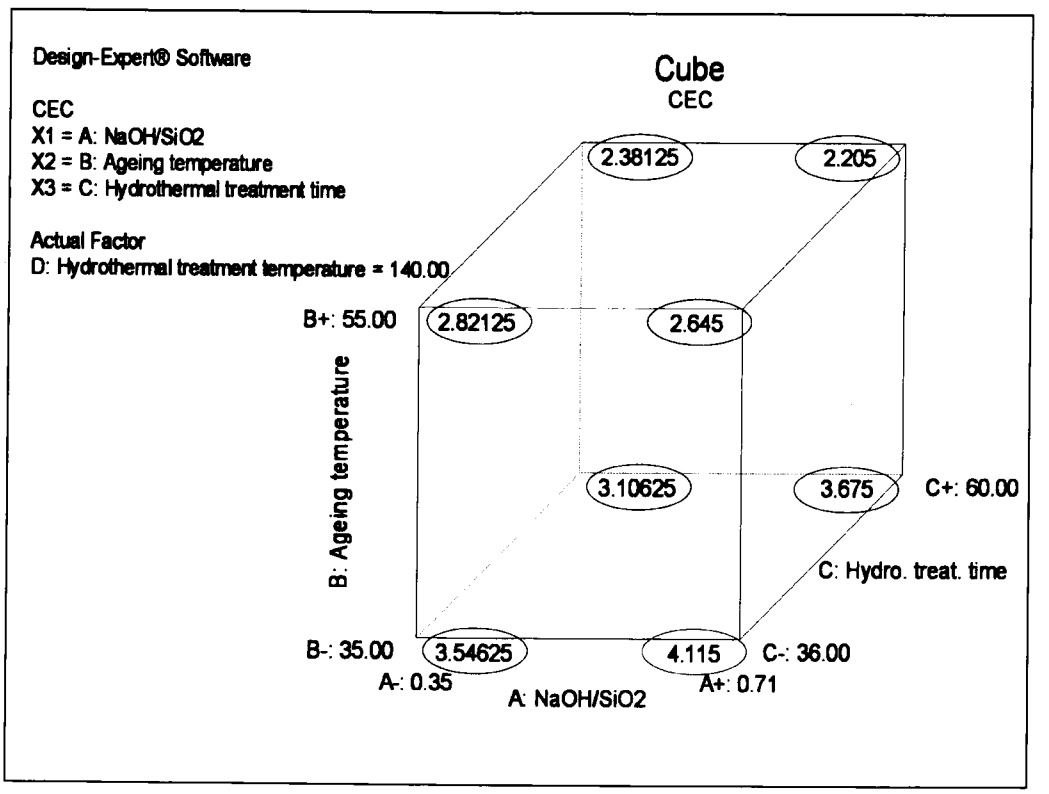

Figure 4-45: Cube plot for designed experiments.

Cube plots values are predicted values (circled values) and show how three factors combine to affect the cation exchange capacity response (Design-Expert 7.1 user's guide, 2001). Examining the cube plot in Figure 4.45, it is clearly evident that when the hydrothermal treatment temperature is held at 140 °C, the cation exchange capacity increases when ageing

temperature decreases, $NaOH/SiO_2$ molar ratio increases and when hydrothermal treatment time is at its lowest value.

Section summary

The approach presented in the previous sections, which is based on the theory of experimental designing, was a simple and economical way of detailed investigation on how the cation exchange capacity and phase composition of a zeolite depends on the conditions of zeolite Na-P1 synthesis. The information obtained is much richer than that which can be obtained through single-factorial studies given the same time and labour expenditure.

It is important to point out that results obtained when using the experimental plans should be interpreted carefully because their statistical verification can be arbitrary to a certain extent. Some effects being estimated as significant or insignificant might quite often on the significance limit in fact, and their estimation can be different when changing some statistical assumptions, such as the random error of measurements or the significance level.

4.3 PART C: Use of brine solution during the synthesis and its treatment

4.3.1 Mineralogy of zeolitic materials synthesized by use of brine solution

It would be useful to substitute costly deionized water with waste brine effluents that are readily available in close proximity to ash dumps especially in coalfields of South Africa's Mpumalanga province. Emalahleni brine solutions were used as a substitute. The conditions for synthesis were the ones obtained for optimised synthesis pure phase zeolite Na-P1 from Arnot fly ash using ultra pure water. These synthesis conditions were; molar ratio of 1 SiO_2 : 0.42 Al_2O_3 : 0.59 NaOH : 0.49 H_2O, ageing temperature and time of 47 °C and 48 hours respectively, and hydrothermal treatment temperature and time at 140 °C and 48 hours respectively. Figures 4.46 shows the XRD results of products obtained when Arnot, Hendrina and Duhva fly ashes were used as feedstock for preparing synthesis gel as was described in experimental section 3.1.2.

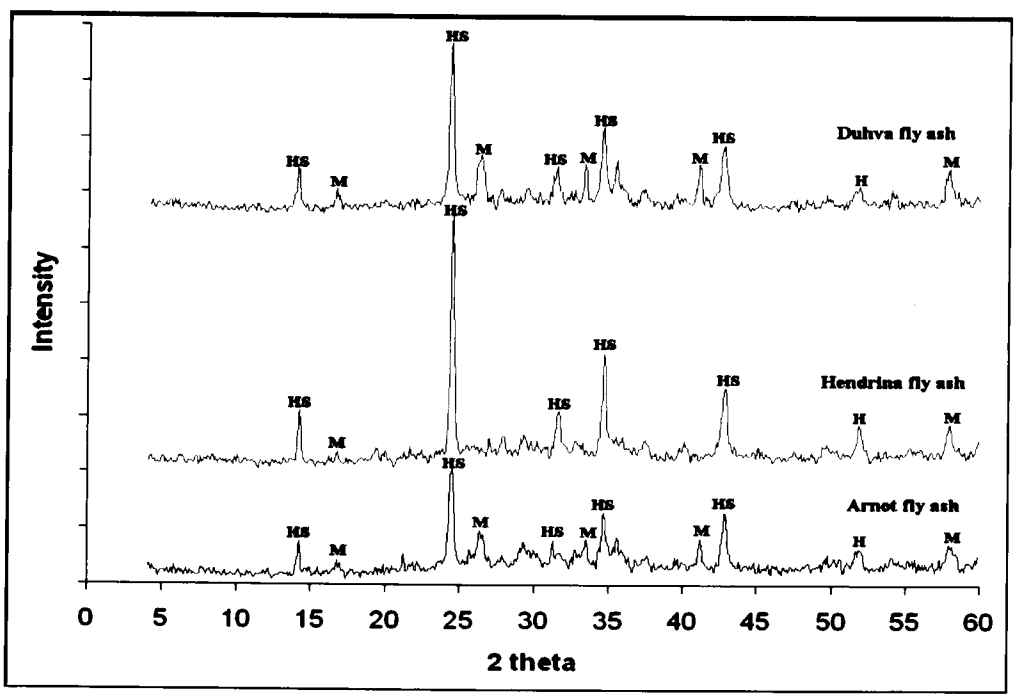

Figure 4-46: XRD comparison for zeolitic material synthesized using brine solution (HS = Hydroxy-sodalite, M = Mullite, H = Hematite).

The major phase obtained in Figure 4.46 was hydroxyl-sodalite. Presence of non digested mullite and hematite was also confirmed. Hydroxy-sodalite belongs to the group of clathrasils; it is made of a cubic array of cages and has the same framework structure as sodalite (Khajavi et al., 2007).

4.3.2 Elemental analysis of product synthesized using brine

It was important to check the composition of synthesis product for incorporation of toxic elements since the presence of these elements could affect its ultimate usage. Table 4.17 lists the mass % of the component elements of the mineral products obtained when Emalahleni brine was used as replacement for ultra pure water during synthesis using Arnot, Duhva and Hendrina fly ash as feedstock.

Table 4-17: Elemental analysis of zeolitic materials synthesized using brine solution.

Major oxide %	**From Arnot fly ash**	**From Duhva flay ash**	**From Hendrina fly ash**
SiO_2	34.094	32.182	34.249
TiO_2	1.516	1.834	1.231
Al_2O_3	23.026	28.179	20.770
Fe_2O_3	3.256	3.152	2.785
MnO	0.066	0.045	0.046
MgO	2.762	1.716	2.019
CaO	6.560	4.521	5.355
Na_2O	10.271	9.593	12.734
K_2O	0.748	0.729	0.899
P_2O_5	0.047	0.073	0.055
SO_3	3.495	3.316	4.547
Cr_2O_3	0.038	0.031	0.030
NiO	0.021	0.024	0.022
H_2O^-	2.834	4.015	3.440
LOI	10.805	9.581	11.031
Total	99.540	98.990	99.214

From Table 4.17 the SiO_2/Al_2O_3 for the synthesis product from Arnot, Duhva and Hendrina fly ash was 1.48, 1.14 and 1.65 respectively. These ratios were low when compared with synthesis products obtained when ultra pure water was used (see Tables 4.2 and 4.4). The presence of elements such as Ti, Fe, Mn, Ti, Ca, Cr, Ni and K, may be due to the presence of these elements in brine or dissolution of these elements from fly ash under the alkaline synthesis conditions.

Some of these elements may be incorporated into the framework structure during the hydrothermal treatment. Comparing the percentage composition of the zeolitic material synthesized using Arnot fly ash (see Table 4.2) when using ultra pure water with the products obtained when using brine solution, it is clear that the brine used as a solvent instead of ultra pure water contributed to the elevated amounts some elements found in the product. For example, the elements that showed elevated concentrations were; Na, Fe, Mg, Ca, and K.

4.3.3 Elemental analysis of post synthesis filtrate

Hydrothermal treatment process reduces the major and trace element concentration from initial concentration present in the fly ash as demonstrated in section 4.1.3. The consequence of this phenomenon is the accumulation of these elements in the aqueous phase as shown in Table 4.17. Even though some elements are released in to the aqueous phase, Nairn *et al* (2001) reported that some of these elements are locked into the unreacted armorphous and crystalline phases of the fly ash.

Table 4-18: Analysis of post synthesis supernatant for zeolites synthesized using brine.

Element	Arnot	Duvha	Hendrina
	Concentration in ppm		
Si	416.99	673.27	278.16
P	122.15	190.65	161.75
K	118.24	112.46	101.06
Al	40.77	40.53	27.65
V	9.78	7.00	9.60
B	5.01	2.48	3.21
	Concentration in ppb		
As	925.35	1420.00	986.60
Pb	601.60	1055.50	513.60
Fe	548.60	1502.00	235.85
Mo	417.35	577.40	431.25
Zn	231.50	151.55	318.80
Se	193.25	133.10	139.90
Sr	110.65	109.55	118.85
Ca	98.61	166.81	133.83
Ba	98.55	164.30	292.45
Cu	60.53	41.19	15.83
Mn	31.11	24.39	18.97
Cr	25.34	11.23	13.06
Be	6.02	3.70	10.15
Cd	2.64	2.75	1.35
Ni	1.77	1.98	0.71
Co	1.50	1.63	0.74

When using brine during synthesis, a significantly higher amount of the Si feedstock was not incorporated into the product than when ultrapure water was used whereas more Al was generally utilized. Even though trace elements in the zeolite products synthesized using brine solution were not analyzed, it is evident from Table 4.17 that trace elements such as V, B,

As, Pb, Fe, Mo, Zn, Se, Sr and Ba were mainly found in the post synthesis supernatant. The levels were relatively similar in both cases but generally, less Cr was released into the supernatant from the ash feedstock when using brine than ultrapure water.

4.3.4 Preliminary brine treatment experiments

Research has established that the presence of heavy metals in the environment even in moderate concentrations is responsible for illnesses related to respiratory, dermal damage and even several kinds of cancers (Barceloux, 1999). It is therefore, important to remove toxic metal contaminants from waste water prior to discharge as they are considered persistent and bio-accumulative.

Different treatment technologies have been developed to remove metal species from waste waters. Some of the methods applied are:

i. Precipitation of metal hydroxides followed by filtration for treatment of highly concentrated waste water streams.
ii. Use of zeolites, clays or ion resins when the range of concentration is low,
iii. Bioremediation (use of micro algae and bacteria)

It has been reported that zeolites synthesized from fly ash can be used to take toxic elements out of acid mine drainage (Petrik *et al.*, 2007) and brine (Sonqishe, 2008) but the zeolite used in these studies was impure since it had undissolved phases such as mullite, hematite and quartz that had remained during the synthesis process.

This preliminary study in section deals with application of the pure phase zeolite Na-P1 synthesized from Arnot fly ash to remove the toxic elements from brine collected from Emalahleni water reclamation plant.

4.3.4.1 Brine composition

The initial composition of the brine, prior to the contact with adsorbent (zeolte Na-P1) is provided in Table 4.19. The initial pH and EC of brine was 7.8 and 15.83 mS/cm, respectively.

Table 4-19: Elemental composition of Emalahleni brine (stage 3).

Trace cations	
Element	Concentration (ppb)
Al	48.38
V	9.92
Cr	10.14
Mn	11.19
Fe	22.81
Co	13.53
Ni	67.85
Cu	5.48
Zn	35.46
As	25.77
Se	45.9
Sr	9,932
Mo	8.87
Cd	0.2
Ba	300.83
Pb	20.45
Major cations	
Element	Concentration (ppm)
Ca	477.49
K	1390.91
Mg	252.73
Na	5337.87

4.3.4.2 Percentage removal of toxic elements from brine

The preliminary brine treatment experiments were carried out as outlined in section 3.3.1. The percentage removal of toxic elements from brine (Figure 4.47) were calculated using equation:

$$\% \text{ removal} = (C_i - C_e)/C_i * 100$$

Where C_i and C_e are the initial and final concentrations of the metal ion in the solution.

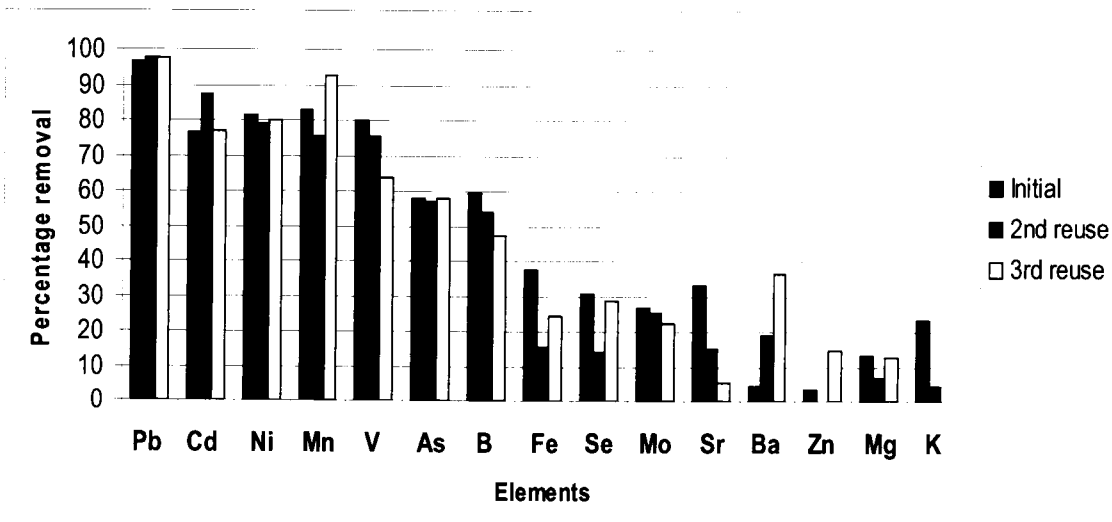

Figure 4-47: Percentage removal of trace elements from brine using zeolite Na-P1.

The % removal of Pb, Cd, Ni, Mn, V, As, B, Fe, Se, Mo Sr, Ba and Zn from raw Emalahleni water reclamation plant brine onto the zeolite was dependent on the nature of the metal ion. It is clearly shown in Figure 4.47 that most of the toxic elements in Emalahleni (stage 3) brine were significantly reduced after contact with the zeolite adsorbent. It should be noted that the zeolite Na-P1 could be reused three times in fresh batches of brine, while maintaining an almost similar capability for removal of toxic elements from brine for many of the elements. It would be necessary to continue these reuse experiments to see at which point the zeolite material was saturated, and breakthrough occurs.

It is important to point out the conclusion by Hendricks (2005) who reported that even though cation exchange capacity is an important characteristic quality during the removal of undesired species from polluted effluents; it is not the only deciding factor in determining the

zeolite's performance during ion exchange, since there are other factors to be considered such as sorption. According to Hendricks (2005), the characteristic difference between sorption and ion exchange is that ion exchange is a stoichiometric process in which every ion that is removed from the solution is replaced by an equivalent amount of another species, whereas sorption indicates that a solute is taken up without being replaced by another species.

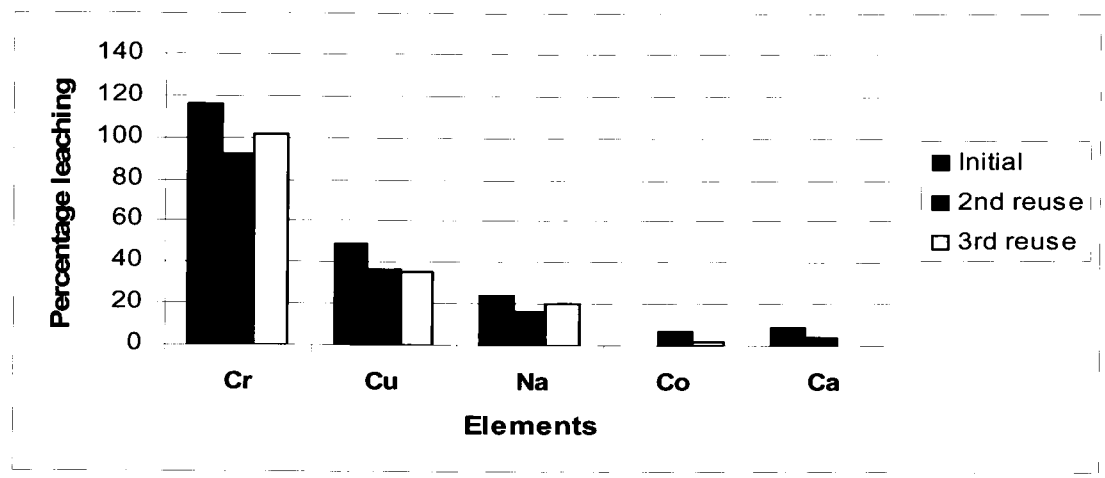

Figure 4-48: Percentage increase of trace elements concentration (in brine) relative to initial brine composition after treatment using zeolite Na-P1.

As shown in Figure 4.48, the concentration of Cr, Cu, Na, Co and Ca increased in the brine after treatment using zeolite Na-P1. The percentage values implied that the concentration of these elements after treatment using zeolite Na-P1 were elevated from their original trace levels in the brine. For example, there was more Cr than its initial concentration (10.14 ppb) in the brine that leached out from zeolite Na-P1 upon contact with the brine. The amount of Cu and Co leached was about 50 % of their individual original concentration in brine.

Because of the high cation exchange capacity reported previously as well as the significant Na content of the zeolite product, it was expected that ionexchange would be the dominant mode of removal of the toxic elements and thus it was expected to see the Na level increase in the brine after contact with the zeolite. The high concentration of Cr and lower amounts of Cu and Co may be due to competitive desorption. It has been reported that unlike mono- and

divalent metal ion, chromium removal behavior is more complex and is strongly influenced by the pH in aqueous solution (Deyi *et al.,* 2008).

Toxic element leachability is an important factor as the zeolite should not contaminate the water being treated. Experiments that were conducted by Petrik et al., 2007 using the dosage (50 g/ml) of impure phase zeolite P showed that some toxic elements such as Pb, Cd, Mn, Mo and Sr leached out from the impure phase zeolite P into the treated water solution. The same elements in this study are found to be adsorbed by the pure phase zeolite Na-P1 which implies that that the improved purity of the zeolite correlated very well with the efficiency of removal of toxic elements. But Cr, Cu and Co were not removed from the brine when using zeolite Na-P1.

Chapter 5

This chapter takes as its starting point a summary of the major issues addressed in this thesis. This is followed by a consideration of possible directions for future work and a summary of the main contributions made in this thesis.

5 GENERAL CONCLUSIONS

The study has shown that pure phase zeolite Na-P1 can be prepared from South African Class F fly ashes because of their compositional dominance of aluminosilicate and silicate phases. Fly ashes sourced from Arnot and Hendrina coal-fired power plants were found to produce the same high purity zeolite Na-P1 under the same conditions identified in this study. Fly ash sourced from Duvha coal-fired power plant was found to be different in terms of elemental and mineralogical composition hence required further optimisation of synthesis conditions.

The results in this study highlight the fact that by simple adjustment of reactant composition and presynthesis or synthesis parameters, the zeolite Na-P1 product showed a great improvement in phase purity and cation exchange capacity (4.11 meq/g) hence an improved potential for application of zeolites prepared from waste fly ash in the treatment of effluent water.

The optimum synthesis conditions for preparing pure phase zeolite Na-P1 were achieved when the molar regime was 1 SiO_2 : 0.36 Al_2O_3 : 0.59 NaOH : 0.49 H_2O and at synthesis conditions such that ageing was done at 47 °C for 48 hours. The hydrothermal treatment time and temperature was 48 hours and 140 °C respectively.

It was interesting to note that the water content added after the ageing step, expressed as H_2O/SiO_2 molar ratio, played an important role in the hydrothermal conversion of fly ash to zeolites. By varying the water content after ageing between H_2O/SiO_2 molar ratios of 0 – 0.49, it was found that the best purity obtained was when the molar ratio value was 0.49, which was confirmed by XRD and CEC studies.

The systematic approach, incorporating statistical design of experiments, developed in this study has resulted in a better understanding regarding transformations and relationship of synthesis parameters in the formation of zeolites from fly ash. The application of the statistical experimental designs was found to yield the following benefits:

i. It became possible to reduce the number of experiments, enabling higher throughout and also reduced the cost. It proved possible to independently separate the individual effects and the interaction of the initial parameters of the reaction mixture.

ii. It enabled the evaluation all effects in terms of value and direction and to verify them statistically; due to coding of the parameters, it also became possible to compare all effects, provided that the experimental and instrumental conditions were the same;

The preliminary experiments done in this study using higher purity zeolite Na-P1 synthesized from Arnot fly ash showed a better removal efficiency of toxic elements from brine solution. The point of interest in this preliminary experiments was the proof that a higher removal efficiency of some toxic element from brine is possible and is expected to show much improvement when the brine treatment procedure is optimized.

5.1 RECOMMENDATION AND FUTURE WORK

The broad scope of this thesis means there is a plethora of further work that can be done.

Having investigated and confirmed the possibility of synthesizing of zeolite Na-P1 from three South African fly ashes (Arnot, Duvha and Hendrina), similar investigations should be extended for the other sources of fly ashes in South Africa. This should be conducted to ascertain whether they can be used to synthesize zeolite Na-P1 using the optimised conditions achieved in this study. If they do not produce the same zeolite Na-P1 at these conditions, the synthesis conditions should be optimised to get the right conditions.

Pilot scale zeolite synthesis of zeolite Na-P1 from South African fly ash should be attempted to replicate the conditions applied at the bench scale.

The use of ultrasonication should be investigated to see whether it would be possible to reduce the ageing time and temperature. This will enable reduction of cost of production especially when the synthesis procedure is scaled up.

A complete optimisation study should be done to achieve the right conditions for toxic element removal from brine solutions. Column experiments on the adsorption of toxic elements should also be done to confirm the removal efficiency and also regeneration of the zeolite product.

In future studies, the long term stability of immobilized metals of the used zeolite Na-P1 should be conducted to determine if they can leach out or not.

Mass balances should be done in future studies to determine the actual synthesis efficiency and mobility and fate of trace elements the during the synthesis process.

REFERENCES

A´lvarez-Ayuso E., Querol X., Plana F., Alastuey A., Moreno N., Izquierdo M., Font O., Moreno T., Diez S., V´azquez E., Barra M. (2008). "Environmental, physical and structural characterisation of geopolymer matrixes synthesised from coal (co-) combustion fly ashes" Journal of Hazardous Materials. 154: 175–183.

Adriano, D.C., Page, A.L., Elseewi, A.A., Chang, A.C., and Straughan I. (1980). "Utilization and disposal of fly ash and other coal residues in terrestrial ecosystems" A review Journal of Enviromental Quality. 9: 333-344.

Albert, B.R., Cheetham, A.K., Stuart, J.A. & Adams, C.J. (1998). "Investigations on P zeolites: synthesis, characterisation, and structure of highly crystalline low-silica NaP", Microporous and Mesoporous Materials. 21: (1-3) 133-142.

Alain C. Pierre and Gérard M. Pajonk (2002). "Chemistry of Aerogels and their applications" Chemical reviews 102: 4243 – 4265.

Amrhein, C., Gaghnia, G.H., Kim, T.S., Mosher, P.A., Gagajena, R.C., Amanios, T. and Torre, I.D.L. (1996). "Synthesis and properties of zeolites from coal fly ash" Environmental Science & Technology. 30 (3): 735 - 742.

ASTM C618-92a. (1994). "Standard Specification for Fly Ash and Raw or Calcined Natural Pozzolan for Use as Mineral Admixture in Portland Cement Concrete," American Society for Testing and Materials, Annual Book of ASTM Standards, Volume 04.02, West Conshohocken, Pennsylvania.

Baerlocher C. and McCusker L.B., (2008) "Database of Zeolite Structures" available at http://www.iza-structure.org/databases/ [accessed on 12th June 2008]

Baerlocker, C.H, McCuster, L.B., Oslon, D.H., (2007) "Atlas of zeolite framework types" 6th edition. Elsevier.

Bailey, S.E., Olin, T.J., Bricka, R.M. & Adrian, D.D. (1999). "A review of potentially low-cost sorbents for heavy metals", Water Research. 33 (11): 2469-2479.

Barceloux, D.G (1999). "Copper" Journal of Toxicology, Clinical Toxicology. 37: 217-230.

Barnwell, William L., P. E and Tapp, Kenny (2001). "Ponded bottom ash, one man's treasure" International ash utilization symposium, center for applied energy research, University of Kentucky, paper # 89.

Barrer, R. M. (1982). "Hydrothermal chemistry of zeolites" Academic press, London.

Bayati, B., Babaluo, A.A and Karimi, R. (2008). "Hydrothermal synthesis of nanostructure NaA zeolite: The effect of synthesis parameters on zeolite seed size and crystallinity" Journal of the European Ceramic Society. 28: 2653–2657.

Bekkum, Van H., Flanigen, E. M., Jansen, J.C. (1991). "Introduction to zeolite science and practice" Elsevier Science, Amsterdam, Netherlands.

Berkgaut, V. and Singer, A. (1996). "High capacity cation exchanger by hydrothermal zeolitization of coal fly ash" Applied Clay Science. 10 (5): 369-378.

Betti, C., Fois E., Mazzucato, E., Medici, C., Quartieri, S., Tabacchi, G., Vezzalini, G. and Dmitriev, V. (2007). "Gismondine under HP: Deformation mechanism and re-organization of the extra-framework species" Microporous and Mesoporous Materials. 103: 190–209.

Bhanarkar, A.D., Gavane, A.G., Tajne, D.S., Tamhane, S.M., Nema, P. (2008). "Composition and size distribution of particules emissions from a coal-fired power plant in India" Fuel. 87: 2095–2101.

Breck, D. W. (1974). "Zeolite molecular sieves" John Wiley & Sons, New York.

Caputo Domenico and Pepe Francesco (2007). "Experiments and data processing of ion exchange equilibria involving Italian natural zeolites: a review" Microporous and Mesoporous Materials. 105: 222–23.

Casci, John L. (2005). "Zeolite molecular sieve: Preparation and scale up" Microporous and mesoporous Material. 82: 217-226.

Catalfamo, P., Corigliano, F., Primerano, P. and Pasquale, S. D. (1993). "Study of the pre-crystallisation stage of hydrothermally treated amorphous aluminosilicates through the composition of the aqueous phase" Journal of the chemical Society, Faraday Transactions. 89 (1): 171 – 175.

Catalfamo, P., Pasquale, S. D., Corigliano, F. and Mavilia, L. (1997). "Influence of the calcium content on the coal fly ash features in some innovative applications" Resources, Conservation and Recycling. 20: 119 – 125.

Chang, H.L. and Shih, W.H. (1998). "A general method for the conversion of fly ash in to zeolites as ion exchangers for cesium" Industrial & Engineering Chemistry Research. 37:7178.

Chareonpanich, M., Namto, T., Kongkachuichay, P., Limtrakul, J. (2004). "Synthesis of ZSM-5 zeolite from lignite fly ash and rice husk ash" Fuel Processing Technology. 85: 1623–1634.

Chun-Feng Wang, Jian- Sheng Li, lian-Jun Wang and Xiu-Yun Sun (2008). "Influence of NaOH concentrations on synthesis of pure-form zeolite A from fly ash using two-stage method" Journal of Hazardous Materials. 155: 58 – 64.

Ciccu, R., Ghiani, M., Muntoni, Serci, A., Perreti, R., Zucca, A., Orsenigo and Quattroni G. (1999). International Ash Utilisation symbosium, Center for applied Energy Research, University of Kentucky, Paper # 84. (www.flyash.info).

Colella, C. & Gualtieri, A.F. (2007). "Cronstedt's zeolite", Microporous and Mesoporous Materials. 105 (3): 213-221.

Colella, C., in: I. Kiricsi, G. Pa'l-Borbe'ly, J.B. Nagy, H.G. Karge (Eds.), (1999). "Porous Materials in Environmental Friendly Processes, Studies in Surface Science and Catalysis" 125, Elsevier, Amsterdam, page 641.

Colthup, N.B., Daly, L.H. and Wiberley, S.E. (1964). "Introduction to infrared and Raman spectroscopy" Academic Press, New York.

Crawley, Michael J. (2005). "Statistics; An introduction using R" John Wiley and sons.

Criado, M. (2007) "Alkali activation of fly ash: Effect of the SiO2/Na2O ratio Part I: FTIR study" Microporous and Mesoporous Materials.106: 180–191.

Czurdo, K. A. and Haus, R. (2002). "Reactive barriers with fly ash zeolites for in situ ground water remediation" Applied Clay Science. 21: 13 – 20.

Derkowski, A., Franus, W., Beran, E. & Czímerová, A. (2006). "Properties and potential applications of zeolitic materials produced from fly ash using simple method of synthesis" Powder Technology. 166 (1): 47-54.

Design-Expert 7.1 user's guide, "Two –level factorial tutorial – part 1" DX7 - 03A – Two level - P1 Revised on 15th April 2007.

Deyi Wu, Yanming Sui, Shengbing He, Xinze Wang, Chunjie Li and Hainan Kong (2008). "Removal of trivalent chromium from aqueous solution by zeolite synthesized from coal fly ash" Journal of Hazardous Materials 155 (3):415-423

Dyer, A. (1988). "An introduction to Zeolite Molecular Sieves" John Wiley, London.

Eary, L. E, Rai, D., Mattigold, S.V and Ainsworth, (1990). "Geochemical factors controlling the mobilization of inorganic constituents from fossil fuel combustion residues: II. Review of the minor elements" Journal of Environmental Quality. 19: 202 – 214.

Elliot, A.D. PhD Thesis (2006). "An investigation in to the hydrothermal processing of coal fly ash to produce zeolite for controlled release fertilizer applications", School of engineering, Curtin University of Technology, Perth.

Eskom Holdings Limited (2009)" available at http://www.eskom.co.za; [accessed on 12th May, 2009]

Everitt, B.S. (2002). Cambridge Dictionary of Statistics. CUP. ISBN 0-521-81099.

Fansuri Hamzah, Pritchard Debora and Zhang Dong-ke (2008). "Manufacture of low-grade zeolites from fly ash for fertilizer applications" Research report 91 for Cooperative research Centre for coal in sustainable development, Australia.

Farmer, V. C. (1988). "The infrared spectra of minerals" Mineralogical Society Monogram 4, London.

Feijen, E.J.P., Martens, J.A., Jacobs, P.A., in: Weitkamp J., Karge H.G., Pfeifer H., Hölderich W. (Eds.), (1994). "Zeolites and Related Microporous Materials", vol. 84A, Elsevier, Amsterdam, page 3.

Fernández-Jiménez A. and Palomo A. (2005). "Mid-infrared spectroscopic studies of alkali-activated fly ash structure" Microporous and Mesoporous Materials. (86): 207-214

Flanigien, E. M (1991). "Zeolite and molecular sieves: A historical perspective. In Van Bekkum H. Flanigen E.M and Jansen J.C (eds) Introduction to zeolite science and practice. Elsevier , Amsterdam.

Frost and Sullivan. (2001). "Zeolites: Industry trends and worldwide markets in 2010" A report from Technical Insights.

Gitari, M., Petrik Leslie, Key D., Etchebers O. and Okujeni C. (2005). "Mineralogy and Trace Element Partitioning in Coal Fly Ash/Acid Mine Drainage Co-Disposed Solid Residues" http://whocares.caer.uky.edu/wasp/AshSymposium/AshLibraryAgenda.asp (accessed on 24th March, 2009).

Gitari, W.M. (2006). "Evaluation of the Leachate Chemistry and Contaminants Attenuation in Acid Mine Drainage by Fly Ash and its derivatives" Unpublished PhD Thesis, University of the Western Cape, South Africa.

Goodarzi, F. (2002). "Mineralogical, elemental composition and modes of occurrence of elements in canadian feed coals" Fuel. 81: 1199–213.

Gottardi, G. and Galli, E. (1985). "Natural Zeolites" Springer-Verlag, Heidelberg.

Guang Xiong, Yi Yu, Zhao-chi Feng, Qin Xin, Feng-Shou Xiao and Can Li (2001). "UV Raman spectroscopic study on the synthesis mechanism of zeolite X" Microporous and Mesoporous Materials. 42 (2-3): 317-323.

Gutierrez B, Pazos C, Coca J. (1993) "Characterization and leaching of fly ash" Waste Manage and Research. 11: 279–86.

Helble, J. J. (1994). "Trace element behavior during coal combustion: results of a laboratory study" Fuel Process Technology. 39: 159– 172.

Hendricks, N.R (2005). "The applications of high capacity ion exchange adsorbent material synthesized from fly ash and acid mine drainage, for the removal of heavy and trace metals from secondary co-disposed process waters" Unpublished master's thesis, University of the Western Cape.

Hirai Takashi and Yoshizuka Kazuharu "Preparation of zeolitic adsorbents for environmental improvement from coal fly ash using alkali fusion method" proceedings of the 3rd Japan – Taiwan joint international symposium on environmental science and technology. December 1-2, 2008. Kitakyushu, Japan.

Holler, H. and Wirsching, U. (1985). "Zeolite formation from fly ash" Fortschritte der Mineralogie. 63 (1): 21 – 43.

Hollman, G.G., Steenbruggen, G. & Janssen-Jurkovicová, M. (1999). "A two-step process for the synthesis of zeolites from fly ash" Fuel. 78 (10): 1225-1230.

Hower James C., Robertson J. David, Gerald A. Thomas, Wang Amy S., William Schram H., Graham Uschi M., Rathbone Robert F. and Robl Thomas L. (1996). "Characterization of fly ash from Kentucky power plants" Fuel. 75 (4): 403-411.

Hui, K. S, Chao, C. Y. H. (2005). "Effects of step-change of synthesis temperature on synthesis of zeolie 4A from fly ash" Microporous Mesoporous Materials. 88: 145–151.

Hurley, John P. and Schobert Harold H. (1991). "Ash Formation during Pulverized Subbituminous Coal Combustion. 1. Characterization of Coals, and Inorganic Transformations during Early Stages of Burnout" Energy & Fuels. 6: 47-58.

Inada Miki, Tsujimoto Hidenobu, Eguchi Yukari, Enomoto Naoya, Hojo Junichi (2005). "Microwave assisted zeolite synthesis from fly ash in hydrothermal process" Fuel. 84: 1482 – 1486.

Jansen J.C., Stöcker M., Karge H.G. and Weitkamp J. (eds) (1994). "Advanced zeolite science and applications: volume 85 – Studies in surface science and catalysis" Elservier, Amsterdam. Page 1 – 30.

Kim, D.S., Chang, J., Hwang, J., Park, S. & Kim, J.M. (2004). "Synthesis of zeolite beta in fluoride media under microwave irradiation" Microporous and Mesoporous Materials. 68 (1-3): 77-82.

Klink, M. J. (2003). The potential use of South African coal as a neutralisation treatment option for acid mine drainage. Unpublished MSc Thesis, University of the Western Cape, South Africa.

Knight, C.L, Williamson, M.A and Bodnar, R.J. (1989). "Raman spectroscopy of zeolites: Characterization of natural zeolites with laser raman microscopy" P.E. Russell., Ed., Microbeam Analysis.

Koukouzas, N., Hämäläinen, J., Papanikolaou, D., Tourunen, A. & Jäntti, T. (2007). "Mineralogical and elemental composition of fly ash from pilot scale fluidised bed combustion of lignite, bituminous coal, wood chips and their blends" Fuel. 86 (14): 2186-2193.

Koukouzas, Nikolaos K., Zeng Rongshu, Perdikatsis Vassilis, Xu Wendong, Kakaras, Emmanuel K. (2006). "Mineralogy and geochemistry of Greek and Chinese coal fly ash" Fuel. 85: 2301–2309.

Krevelen, D. W. (1993). "Coal: Topology, chemistry, physics, constitution" 3rd edition. Elsevier, Amsterdam p. 979.

Krüger, Japie E. (2003). "South African fly ash: a cement extender South African Coal Ash Association" Monograph publication on behalf of South African Coal Ash Association (SACAA).

Kruger, Richard A. (1997). "Fly ash beneficiation in South Africa: creating new opportunities in the market-place" Fuel. 76 (8): 777-779.

Khajavi Sheida, Kapteijn Freek, Jansen, Jacobus C. (2007). "Synthesis of thin defect-free hydroxy sodalite membranes: New candidate for activated water permeation" Journal of Membrane Science 299: 63–72

Lawrence A. Ruth (1998). "Energy from municipal solid waste: A comparison with coal combustion technology" Progress in Energy and Combustion Science. 24: 545-564.

Lee, D.B., Matsue, N. and Henmi, T. (2001). "Influence of NaOH concentrations dissolved in sea water and hydrothermal temperature on the synthesis of artificial zeolite from coal fly ash" Clay science. 11: 451 – 463.

Lin, C.F and His, H.C. (1995) "Resource recovery of waste fly ash: synthesis of zeolite-like materials", Environmental Science and Technology. 29 (4) 1109 – 1117.

Liu G, Zhang H, Gao L, Zheng L, Peng Z. (2004). "Petrological and mineralogical characterizations and chemical composition of coal ashes from power plants in Yanzhou mining district, China" Fuel Process Technology. 85: 1635–46.

Lowell, S., Joan, E. S., Martin, A. T. and Matthias, T. (2006). "Characterization of porous solids and powder: surface area, pore size and density" Spinger, Netherlands. pg. 123.

McLennan, A. R., Bryant G. W., Stanmore B. R. and Wall T. F. (2000). "Ash Formation Mechanisms during pf Combustion in Reducing Conditions" Energy & Fuels. 14: 150-159.

Mead, R. (1991). "The design of experiments; statistical principles for practical applications" Cambridge University press, New York.

Meier, W.M., Olson D.H., and Baerlocher, C. (1996). "Atlas of Zeolite Structure Types" 4th revised edition, Structure Commission of the International Zeolite Association.

Molina, A. & Poole, C. (2004). "A comparative study using two methods to produce zeolites from fly ash" Minerals Engineering. 17 (2): 167-173.

Mollah, M. Y. A., Promreuk S., Schennach R., Cocke D. L. and Güler R. (1999). "Cristobalite formation from thermal treatment of Texas lignite fly ash" Fuel. 78 (11): 1277-1282.

Montgomery, D.C. (2001). "Design and Analysis of Experiments" (5th ed.), John Wiley, New York.

Mosca, Alexandra's thesis (2006). "Structured zeolite adsorbents" Lule'a University of Technology.

Mouhtaris T., Charistos D., Kantiranis N., Filippidis A., Kssoli-Fournaraki A. and Tsirambidis A. (2003). "GIS-type zeolite synthesis from Greek lignite sulphocalcic fly ashes promoted by NaOH solutions" Microporous and Mesoporous Materials. 61 (1-3): 57-67.

Mumpton, F. A., (1999). "La roca magica, Uses of natural zeolites in agriculture and industry" Proceeding of National. Academy of Science. 96: 3463–3470.

Murayama, N., Yamamoto H., Shibata J. (2002). "Mechanism of zeolite synthesis from fly ash by alkali hydrothermal reaction" International Journal Mineral Processing. 64 (1): 1–17.

Murphy Thomas E., Phyllis, Christensen A., Behrns, Roger J. and Jaquier, Douglas R. (1984). "Fly ash analysis by complementary atomic absorption spectrometry and energy dispersive X-ray spectrometry" Analytical Chemistry. 56: 2534-2537.

Nagy, J.B., Bodart, P., Hannus, I. & Kiricsi, I. (1998). "Synthesis, Characterization and Use of Zeolitic Microporous Materials" Deca Gen Ltd, Szeged, Hungary.

Nairn J., Blackburn D. and Wilson M. (2001). Research and development for fly ash: opportunity or alchemy. 18th annual international Pittsburgh coal conference, Newcastle.

Nisnevich Mark., Sirotin Gregory., Schlesinger Tuvia and Eshel Ya'akov. (2008). "Radiological safety aspect of utilizing coal ashes for production of light weight concrete. Fuel. 87: 1610-1616.

Park, M., Choi, C.L., Lim, W.T., Kim, M.C., Choi, J. & Heo, N.H. (2000). "Molten-salt method for the synthesis of zeolitic materials: I. Zeolite formation in alkaline molten-salt system" Microporous and Mesoporous Materials. 37 (1-2): 81-89.

Petrik, L. Hendricks, N. Ellendt, A. and Burgers C. (2007). "Toxic element removal from water using zeolite adsorbents made from solid waste residues" Water Research Commission Report No. 15446/1/07.

Petrik, L., White, R., Klink, M., Somerset, V., Key, D.L. Iwuoha, E., Burgers C. and Fey, M.V. (2005). "Utilization of Fly Ash for Acid Mine Drainage remediation" Water Research Commission Report No. 1242/1/05.

Petrik, Leslie F., White, Richard A., Klink, Michael J., Somerset, Vernon S., Burgers, Colleen L. and Fey, Martin V. "Utilisation of South African fly ash to treat acid coal mine drainage and production of high quality zeolites from the residual solids. International Ash Utilisation symposium, October 20-22, 2003, Lexington, Kentucky, USA.

Querol, X., Fern'andez-Turiel, J.L., and Lopez-soler, A. (1995). "Trace elements in coal and their behaviour during combustion in a large power station" Fuel. 74 (3): 331-343.

Querol, X., Moreno, N., Alastuey, A., Juan, R., Andres, J.M., Lopez-Soler, A., Ayora, C., Medinaceli A. and Valero A. (2007). "Synthesis of high ion exchange zeolites from coal fly ash" Geologica Acta. 5 (1): 49-57.

Querol, X., Moreno, N., Umaña, J.C., Alastuey, A., Hernández, E., López-Soler, A. & Plana, F. (2002). "Synthesis of zeolites from fly ash: an overview" International Journal of Coal Geology. 50 (1-4): 413-423.

Querol, X., Plana, F., Alastuey, A. & López-Soler, A. (1997). "Synthesis of Na-zeolites from fly ash" Fuel. 76 (8): 793-799.

Querol, X., Umana, F., Plana, F., Alastuey, A., López-soler, A., Medinaceli, A., Valero, A., Domingo, M.J., garcia-rojo, E. (2001). "Synthesis of zeolites from fly ash at pilot scale. Example of potential applications" Fuel. 80: 857-865.

Radojević, M. and Bashkin, V.N. (1999). "Practical Environmental Analysis" The Royal Society of Chemistry, Cambridge.

Rayalu, S.S., Udhoji, J.S., Munshi, K.N. & Hasan, M.Z. (2001). "Highly crystalline zeolite — a from flyash of bituminous and lignite coal combustion" Journal of Hazardous Materials. 88 (1): 107-121.

Reto Gieré, Carleton, Loran E. and Lumpkin, Gregory R. (2003). "Micro- and nanochemistry of fly ash from a coal-fired power plant" Mineralogical Society of America. 88 (11-12): 1853-1865.

Reynold Kelley, Kruger Richard and Rethman Norman. (1999). "The manufacture and evaluation of an artificial soil (SLASH) prepared from fly ash and sewage sludge" International Ash Utilization Symposium, Center for Applied Energy Research, University of Kentucky , paper #1.

Ríos, C.A. and Williams, C. D. (2008). "Synthesis of zeolitic materials from natural clinker: A new alternative for recycling coal combustion by-products" Fuel. 87 (12): 2482-2492.

Scheetz, B. E. and Earle, R. (1998). "Utilisation of fly ash" Current opinion in solid state and material science. 3: 510-520.

Scott, J., Guang, D., Naeramitmarnsuk, K., Thabout, M. and Amal, R. (2001). "Zeolite synthesis from coal fly ash for the removal of lead ions from aqueous solution" Journal of chemical Technology and Biotechnology. 77 (1): 63 – 69.

Shao, J., Z. Wang, H., Li, H. and Shao, X. (1997). "Fly ash as an adsorbent for wastewater treatment" Proceedings 14th International Pittsburgh Coal Conference, Taiyan, Shanxi, China.

Shigemoto, N., Hayashi, H. and Miyama, K. (1993). "Selective formation of Na-X zeolite from coal fly ash by fusion with sodium hydroxide prior to hydrothermal reaction" Journal of materials science. 28 (17): 4781 – 4786.

Singer, A. and Berkgaut, V. (1995). "Cation exchange properties of hydrothermally treated coal fly ash" Environmental Scienece and Technology. 29 (27): 1748 – 1753.

Sloss, L.L., Smith, I.M. and Adams, D.M. B. (1996). "Pulverised coal ash – requirements for utilisation". IEA Coal research. IEACR/88. London.

Smith Kevin R., Veranth John M., Lighty JoAnn S. and Aust Ann E. (1998). "Mobilization of Iron from Fly ash Was Dependent upon the Particle Size and the Source of Coal" Chemical Research in Toxicology. 11: 1494-1500.

Somerset, V., Petrik, L. and Iwuoha, E. (2008). "Alkaline hydrothermal conversion of fly ash precipitates into zeolites 3: The removal of mercury and lead ions from wastewater" Journal of Environmental Management. 87 (1): 125-131.

Somerset, V.S., Petrik, L.F., White, R.A., Klink, M.J., Key, D. & Iwuoha, E. (2004). "The use of X-ray fluorescence (XRF) analysis in predicting the alkaline hydrothermal conversion of fly ash precipitates into zeolites" Talanta. 64 (1):109-114.

Sonqishe, T. M. (2008). "Treatment of brines using commercial zeolites and zeolites from ash derivative" Unpublished MSc thesis, University of the Western Cape.

Szostak, R, (1989). "Molecular Sieves, Principles of synthesis and Identification" Van Nostrand Reinhold, New York.

Treacy, M. M. J., and Higgins, J.B. (2007). "Collection of simulated XRD powder patterns for zeolites" 5th edition, Elsevier, Amsterdam, Netherlands.

Truter, Wayne F., Rethman, Norman F.G., Reynolds, Kelley A. and Kruger, Richard A. (2001). "The use of a soil ameriolant based on fly ash and sewage sludge" International Ash Utilization Symposium, Center for Applied Energy Research, university of Kentucky, paper #80.

Vathaluru, H.B., French D. (2008). "Ash chemistry and mineralogy of an Indonesian coal during combustion: part two – pilot scale observations" Fuel processing technology. 89: 608 – 621.

Vaughan, D. E. W. (1991). Catalysis and Adsorption by zeolites (Eds: G. Öhlmann, H. Pfeifer, R. Frickle), Elsevier science, Amsterdam, Page 275.

Vories Kimery C. and Throgmorton Daine (2002). Proceedings of coal combustion by-products and western coal mines: a technical interactive forum held from April 16-18, 2002 at Denver Marriot west hotel, Golden, Colorado.

Walek, Tomasz T., Saito Fumio and Zhang Qiwu (2008). "The effects of low solid / liquid ratio on hydrothermal synthesis of zeolites from fly ash" Fuel. 87: 3194 – 3199.

Wang, C., Li, J., Wang, L. and Sun, X. (2008). "Influence of NaOH concentrations on synthesis of pure-form zeolite A from fly ash using two-stage method", Journal of Hazardous Materials. 155 (1-2): 58-64.

Wang, S. & Wu, H. (2006). "Environmental-benign utilisation of fly ash as low-cost adsorbents" Journal of Hazardous Materials. 136 (3): 482-501.

Weitkamp, J. and Puppe, L. (eds.). (1999). "Catalysis and zeolites: fundamentals and applications" Springer, German.

Willis, J.P. (1987). "Variations in the composition of South African fly ash. Ash - a valuable resource" Council for Science and Industrial Research. 3: 2-6

Woolard, C. D., Petrus, K. and Van der Horst, M. (2000). "The use of modified fly ash as a sorbent for lead" Water SA. 26 (4).

World Coal Institute (2009). "The Coal Resource: A Comprehensive Overview of Coal" available online at; http://www.worldcoal.org [accessed on 8th April 6, 2009].

Yaping Ye, Xiaogiang Zeng, Weilan Qian and Mingwen. (2008) "Synthesis of pure zeolites from supersaturated silicon and aluminium alkali extracts from fused fly ash" Fuel. 87: 1800 – 1886.

Zholobenko, Vladimir L., Dwyer John, Zhang Renping, Chapple, Andy P., Rhodes, Nigel P. and Stuart, John A. (1998). "Structural transitions in zeolite P An in situ FTIR study" Journal of Chemical Society. 94 (12): 1779-1781.

APPENDIX

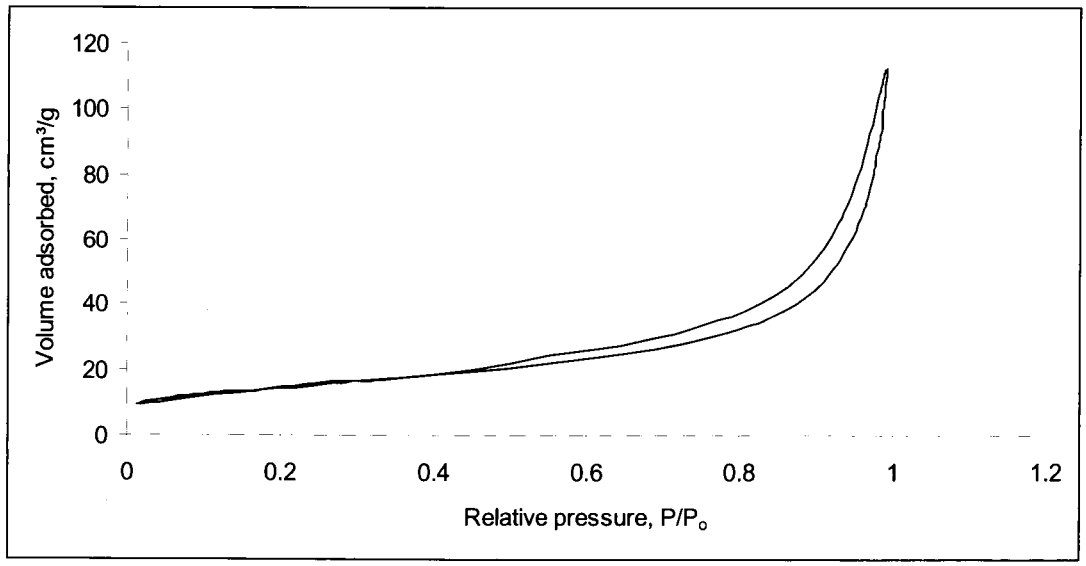

Figure A1: N_2 adsorption – adsorption isotherm for zeolite Na-P1 synthesized at 140°C for 48 hours.

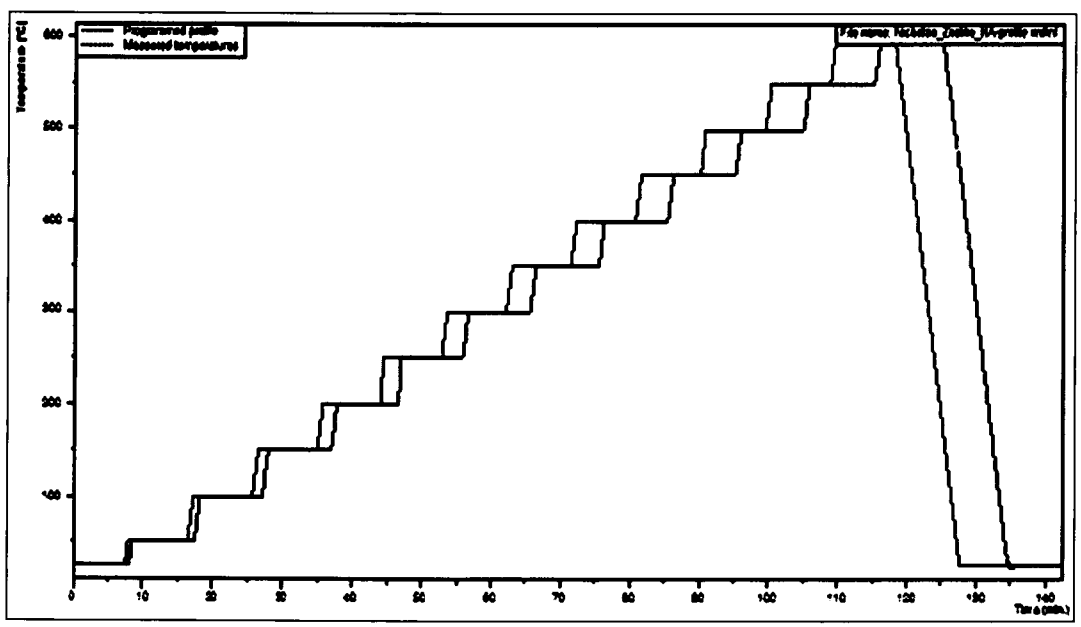

Figure A2: Heating profile for temperature programmed XRD study of zeolite Na-P1 synthesized at 140°C for 48 hours.

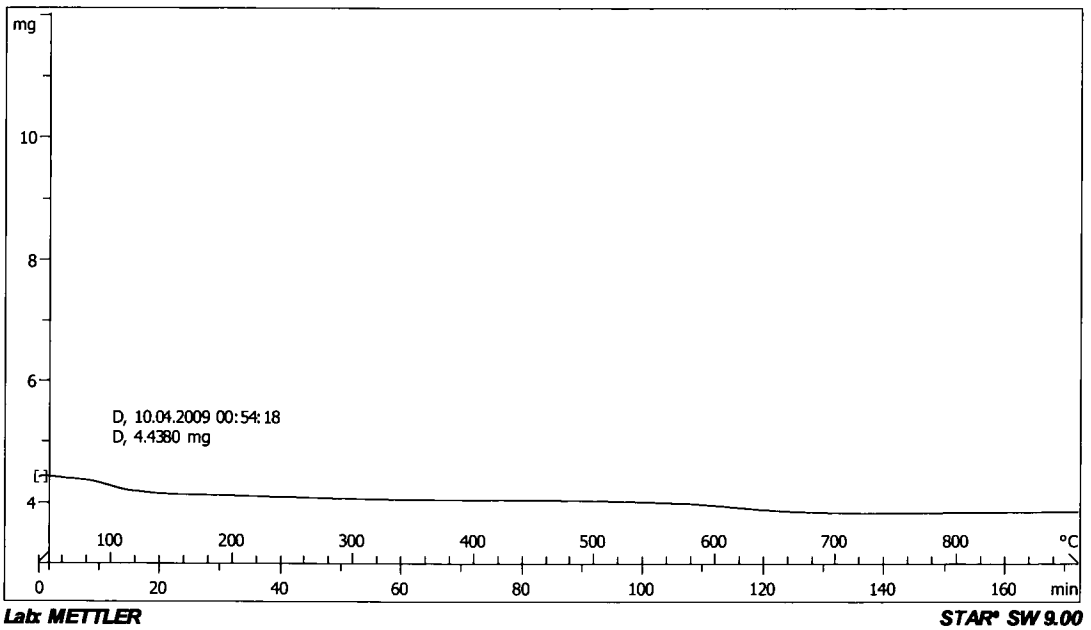

Figure A3a: Weight-temperature behaviour of zeolite Na-P1 from Duhva ash by TGA.

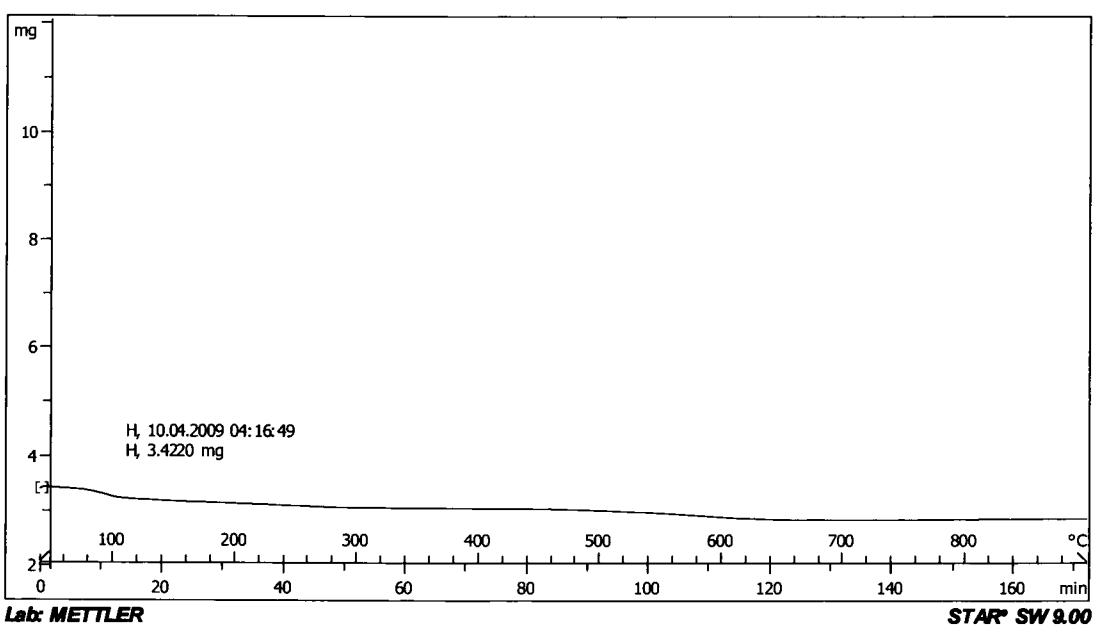

Figure A3b: Weight-temperature behaviour of zeolite Na-P1 from Hendrina ash by TGA.